Proteomic analysis of the Rad18 interaction network in DT40 – a chicken B cell line

Thesis submitted for the degree of Doctor of Natural Sciences
at the Faculty of Biology,
Ludwig-Maximilians-University Munich

15th January, 2009

Submitted by
Sushmita Gowri Sreekumar
Chennai, India

Completed at the Helmholtz Zentrum München
German Research Center for Environmental Health
Institute of Clinical Molecular Biology and Tumor Genetics, Munich

Examiners: *PD Dr. Berit Jungnickel*

Prof. Heinrich Leonhardt

Prof. Friederike Eckardt-Schupp

Prof. Harry MacWilliams

Date of Examination: *16th June 2009*

To my Parents,

Sister, Brother

& Rajesh

Table of Contents

1. SUMMARY **1**

2. INTRODUCTION **2**

2.1. MECHANISMS OF DNA REPAIR 3

2.2. ADAPTIVE GENETIC ALTERATIONS – AN ADVANTAGE 5

2.3. THE PRIMARY IG DIVERSIFICATION DURING EARLY B CELL DEVELOPMENT 6

2.4. THE SECONDARY IG DIVERSIFICATION PROCESSES IN THE GERMINAL CENTER 7

2.4.1. Processing of AID induced DNA lesions during adaptive immunity 9

2.5. TARGETING OF SOMATIC HYPERMUTATION TO THE IG LOCI 10

2.6. ROLE OF THE RAD6 PATHWAY IN IG DIVERSIFICATION PROCESSES 12

2.7. THE RAD6 PATHWAY 12

2.7.1. Translesion Synthesis *13*

2.7.2. Error free bypass *14*

2.7.3. Interactions of components of the Rad6 pathway *15*

2.8. MOLECULAR INTERPLAY BETWEEN THE RAD6 PATHWAY AND CHECKPOINT SIGNALLING COMPONENTS 15

2.9. OTHER FUNCTIONS OF COMPONENTS OF THE RAD6 PATHWAY 16

2.10. FUNCTIONAL CHARACTERISATION OF RAD18 PROTEIN DOMAINS 17

2.11. BIOCHEMICAL AND GENETIC APPROACHES TO STUDY CELLULAR NETWORKS 18

2.11.1. The tandem affinity purification (TAP) technique *19*

2.11.2. The DT40 system *21*

2.12. OBJECTIVES 21

3. RESULTS **23**

3.1. ESTABLISHMENT OF TAP IN THE DT40 CELL LINE USING AID-TAP FUSIONS 23

3.1.1. Expression of the AID-TAP fusion proteins in the DT40 cell line *24*

3.1.2. Tandem affinity purification in DT40 cells using the AID-TAP fusions *28*

3.1.2.1. Western blot analysis of the TAP fractions in DT40 cells 28

3.1.2.2. Silver Stain Analysis of the TAP fractions 30

3.1.3. Trypsin Digestion and nano-Liquid Chromatography of the final eluates *30*

3.1.4. MALDI TOF-TOF analysis of the peptides of the AID fusion eluates *32*

3.1.5. Generation of an NCBI Gallus database and MASCOT analysis for AID-TAP fusions *32*

3.2. STUDY OF THE RAD18 INTERACTION NETWORK IN DT40 CELLS 35

Table of Contents

3.2.1. Exogenous expression of Rad18-HA-TAP fusions in rad18$^{-/-}$ DT40 cells *35*
3.2.2. Native PAGE of Rad18 fusion protein complexes *36*
3.2.3. Cellular localization of Rad18 fusion proteins *36*
3.2.4. Functional Characterization of Rad18-HA-TAP fusions *38*
3.2.5. Isolation of Rad18-HA-TAP fusion complexes by the TAP method *39*
3.2.6. Silver Stain analysis of the Rad18 TAP fractions *40*
3.2.7. LC-MALDI analysis of Rad18 TAP samples *41*
3.2.8. MASCOT analysis for Rad18 fusions *41*
3.2.9. Immunoprecipitation attempts for confirmation of some potential Rad18 interaction partners *44*
3.2.10. Functional Link of Rad18 to the JNK pathway *46*

4. DISCUSSION **50**
5. MATERIALS **64**
5.1. CHEMICALS AND REAGENTS 64
5.2. EQUIPMENTS 64
5.3. KITS 65
5.4. BACTERIA 65
5.5. ENZYMES 65
5.6. ANTIBODIES 66
5.7. OLIGONUCLEOTIDES 67
5.8. PLASMIDS 68
5.9. CELL LINES 68
5.10. SOFTWARES 69

6. METHODS **70**
6.1. STANDARD METHODS 70
6.2. CLONING OF THE RAD18-HA-TAP FUSIONS 70
6.3. CLONING OF RAD18-HA (R18-HA1) 70
6.4. RNA ISOLATION AND CDNA SYNTHESIS 71
6.5. SDS PAGE & WESTERN BLOT ANALYSIS 71
6.6. NATIVE PAGE & BLOTTING 71
6.7. TAP EXTRACTION OF GOI-TAP FUSIONS 72
6.8. TANDEM AFFINITY PURIFICATION 72
6.9. TCA PROTEIN PRECIPITATION 73
6.10. SILVER STAIN ANALYSIS 73

6.11. IN-GEL TRYPSIN DIGEST 74
6.12. REVERSE PHASE NANO-LIQUID CHROMATOGRAPHY 74
6.13. MALDI TOF-TOF 75
6.14. CO-IMMUNOPRECIPITATION IN THE RAD18-HA-TAP DT40 CELLS 77
6.15. ENDOGENOUS CO-IMMUNOPRECIPITATION IN RAJI CELLS 77
6.16. CELL CULTURE 77
6.17. TRANSFECTION OF DT40 CELLS 78
6.18. COLONY SURVIVAL ASSAY FOR DT40 USING CHEMICAL AGENTS 79
6.19. NUCLEAR/CYTOPLASMIC FRACTIONATION 79
6.20. DNA DAMAGE INDUCED ACTIVATION OF THE JNK/AP1 PATHWAY 79

REFERENCES **80**
APPENDIX **92**
ABBREVIATIONS **110**
INDEX OF FIGURES **113**
INDEX OF TABLES **114**
ACKNOWLEDGEMENTS **115**
EHRENWÖRTLICHE ERKLÄRUNG **117**
DECLARATION **117**
CURRICULUM VITAE **118**

1. Summary

Cells have developed many mechanisms to repair alterations of the DNA, but in the adaptive immune system, the immunoglobulin (Ig) gene diversification processes of the B lymphocytes require drastic genetic changes. Activation induced cytidine deaminase (AID) is the key enzyme involved in the secondary diversification of the Ig genes by somatic hypermutation (SHM) or class switch recombination (CSR). Recently, it was found that AID acts in a genome wide manner and the ultimate distribution of mutations is achieved by locus specific regulation of error-prone and error-free DNA repair.

The Rad6 pathway is known to be the molecular switch between error-prone and error-free DNA repair during replication. Rad18 is a key mediator of the Rad6 pathway and also plays a role in SHM and in the ubiquitination of the 9-1-1 checkpoint DNA clamp. These emerging evidences of Rad18 as a central player of DNA damage recognition, response and repair makes it an interesting candidate to explore its interaction network.

The aim of this work was to study the Rad18 interaction network in DT40 cells by combination of a contemporary biochemical tool – tandem affinity purification (TAP) with the versatile DT40 cell system, followed by mass spectrometric analysis.

The approach was established successfully using AID-TAP fusion constructs as a model system and was subsequently transferred to the study of the Rad18 interaction network. The Rad18-HA-TAP tagged constructs were expressed in rad18$^{-/-}$ DT40 cells and the fusions were characterised for expression, localisation, complex formation and functionality. Subsequently, the TAP technique was employed to isolate the Rad18 interaction complex, which was then analysed by LC-MALDI analysis. The bait protein and known interaction partners were identified in the analysis. There were also interesting new interactions identified, some of which were known to be linked to the JNK pathway. Functional analyses were carried out to test the activation of JNK pathway upon MMS induced DNA damage in different sets of Rad18 proficient and deficient DT40 cells. These assays revealed a novel function of Rad18 in the activation of JNK pathway upon DNA damage induced stalled replication and also implied that this function of Rad18 does not require the RING domain of RAD18 and the ubiquitination of PCNA.

This novel function of Rad18 in the JNK pathway may imply a possible mechanism of regulation of cell fate towards survival or apoptosis. Future studies would be focussed on characterising this novel function by mutational analysis of Rad18 and a more sensitive proteomic approach to pinpoint the interaction partner(s) that may be involved in this function of Rad18.

2. Introduction

The genome of a cell is often subject to alterations by exogenous challenges such as ultraviolet or ionizing radiation and certain chemicals that damage DNA. Endogenous processes also contribute to DNA damage, such as base oxidation and strand breaks induced by reactive oxygen species, the spontaneous depurination/ depyrimidination of DNA by hydrolysis, replication defects resulting in mismatches, and the collapse of replication forks leading to strand breaks. DNA damage can be broadly classified into four types based on the type of modification of the DNA, namely 1) base modifications such as alkylation, deamination etc, 2) mismatches of bases on opposite strands, 3) single and double strand breaks and 4) interstrand and intrastrand crosslinks. These damages are often deleterious to the cell when they are left unrepaired, since they may result in blockage of transcription and replication, mutagenesis and/or cytotoxicity (Friedberg 1995). In humans, defective repair of DNA damage is associated with a variety of hereditary disorders, aging and carcinogenesis (Finkel and Holbrook 2000; Hoeijmakers 2001; Peltomaki 2001). Under normal conditions, the DNA damage is repaired by various mechanisms depending on the type of damage, and in proliferating cells, the repair is carried out in concert with cell cycle regulation.

When damage to the genome is recognized, DNA damage checkpoints are activated by the ATM (ataxia telangiectasia, mutated) and/or ATR (ATM and Rad3 related) protein kinases (Abraham 2001; Shiloh 2003) by primarily protein phosphorylation events from the factors detecting the damage to the cell cycle targets downstream. The cell cycle progression is halted at the G1/S transition, intra-S phase and the G2/M transition checkpoints and is coordinated with several biochemical pathways that respond to the damage and repair the DNA structure (Bartek and Lukas 2007). The checkpoints delay DNA replication and mitosis for the repair of the damage. All these processes are coordinated to achieve faithful maintenance, replication and segregation of the genetic material.

Figure 1 represents an instance of such a regulation starting with the processing of DNA adducts in the G1 phase. The various mechanisms of repair that are engaged to process the different types of damaged structures are also depicted. The failure to repair adducts before the G1/S checkpoint could trigger p53 induced apoptosis (Lowe et al. 2004). On the other hand, the subsequent entry of damaged DNA into the S-phase would lead to stalling of replication forks. The intra-S-phase checkpoint halts the cell cycle at this point and the enzymes of the Rad6 pathway are recruited to the stalled fork (Broomfield et al. 2001). This pathway is the molecular switch between bypass of the damage either by error-prone translesion synthesis (TLS) or by error-free bypass of the lesion by a template switch

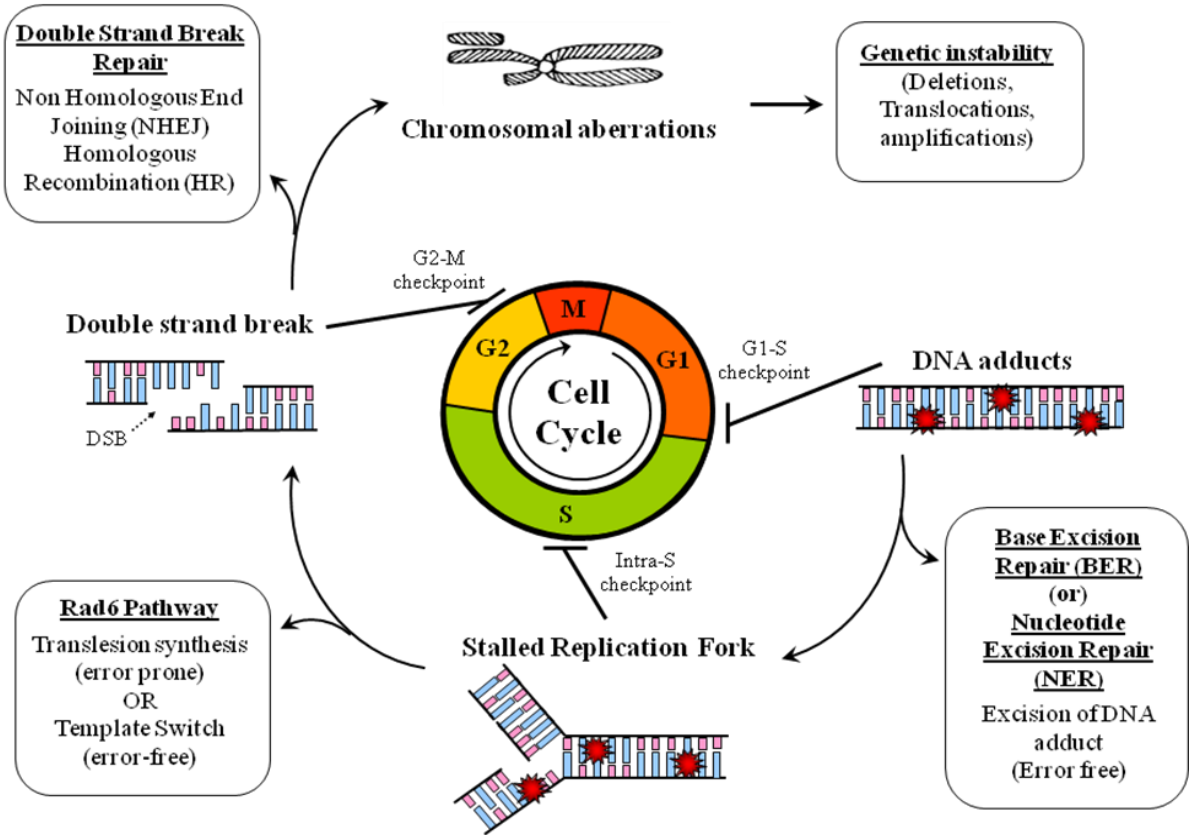

***Figure 1*: Coordination of the cell cycle checkpoints with DNA damage processing**
The figure depicts a generalised representation of the processing of various forms of DNA damage (starting from DNA adducts in the G1 phase) by different repair mechanisms in concert with the cell cycle regulation by cell cycle checkpoints. See details in text. Abbreviations: G1 – Gap1, S – Synthetic, G2 – Gap2 and M – Mitotic phases of the cell cycle; DSB – double strand break.

mechanism (Broomfield et al. 2001). In the event of persistent damage, the stalled replication fork may collapse during repair, giving rise to strand breaks. Strand breaks may also arise when cells are exposed to ionizing radiation, free radicals and certain genotoxic chemicals. The double strand breaks (DSB) may be repaired by non-homologous end joining (NHEJ) or by homologous recombination (HR). Aberrant DSB repair could lead to chromosomal translocations. While the persistence of damage from one cell cycle phase to the next can lead to the generation of secondary damaged structures, it must be noted that the types of DNA damage are not strictly confined to a particular cell cycle phase.

2.1. Mechanisms of DNA repair

The repair of the DNA damage generally involves recognition, isolation and removal of the damage, followed by DNA synthesis and ligation. The direct reversal of base damage, base excision repair (BER), nucleotide excision repair (NER) and mismatch repair (MMR) are simple yet very important DNA repair mechanisms. Besides these mechanisms, there are also

certain intricate repair pathways, i.e. the replication associated repair and the DSB repair pathways.

The direct reversal of base damage is the simplest of the human DNA repair pathways involving the direct reversal of the highly mutagenic alkylation lesion O6-methylguanine (O6-mG) adduct via the action of the enzyme O6-methylguanine DNA methyltransferase (MGMT) (Margison and Santibanez-Koref 2002). The O6-mG adduct is generated at low levels by the reaction of cellular catabolites with guanine residues in the DNA (Sedgwick 1997). The base is corrected by the direct transfer of the alkyl group from the guanine base to the cysteine residue in the active site of MGMT, which is then degraded by an ATP-dependent proteolytic pathway (Srivenugopal et al. 1996), requiring a new molecule of the MGMT protein for every methyl group.

BER is a multi-step process that restores non-bulky base damages resulting from methylation, oxidation, deamination, or spontaneous loss of the DNA base itself (Memisoglu and Samson 2000). Although these alterations are simple in nature, they are highly mutagenic and hence represent a significant threat to genome fidelity and stability (Friedberg 1995). The action of DNA glycosylases removes the damaged base (Lindahl 1974) followed by incision of the abasic site by apurinic/apyrimidinic (AP) endonuclease. The gap is then filled by DNA synthesis by either a short patch repair if the gap is single nucleotide (Matsumoto et al. 1999) or by a long patch repair if the gap is 2-8 nucleotides in size (Pascucci et al. 1999). The short patch repair involves the synthesis of a single nucleotide into the abasic site and is carried out by Polβ and represents the major route of BER (Fortini et al. 1998). The long-patch repair is the back-up pathway of BER and is employed when a modified base resistant to the AP lyase activity of the Polβ is present in the DNA (Matsumoto et al. 1994). The long patch base excision repair is mediated by Polδ and Polε (Stucki et al. 1998). Subsequently the strand nick is ligated by a DNA ligase, thereby restoring the integrity of the DNA.

NER is capable of acting on diverse DNA lesions and the pyrimidine dimers caused by UV are the most significant of these lesions. Bulky chemical adducts, intrastrand crosslinks and some forms of oxidative damage are other forms of lesions that are substrates of NER. The common features of the lesions recognized by NER are that they cause distortion of the DNA helix and a modification of the DNA chemistry (Hess et al. 1997). During NER, the damage is removed along with several nucleotides flanking it and the gap is filled by normal DNA synthesis and ligation (de Laat et al. 1999). NER is executed either as a global repair which repairs lesions over the entire genome, or also as transcription coupled repair that processes transcription-blocking lesions present in transcribed DNA strands (de Laat et al.

1999). Xeroderma Pigmentosum is a rare inherited disease caused by mutations in any one of the several genes involved in NER (Cleaver 1968). Defects in two of the genes involved in the transcription coupled NER are implicated in an inherited disorder called Cockayne's syndrome (Mullenders et al. 1988).

The MMR pathway plays an essential role in the correction of replication errors such as mispaired bases or helix distorting insertion/deletion loops in the DNA duplex that result from misincorporation of nucleotides and template slippage, respectively. The repair is carried out by exonuclease digestion of the damaged strand, followed by DNA repair synthesis and re-ligation (Marti et al. 2002). Mutations in several human MMR genes cause a predisposition to hereditary nonpolyposis colorectal cancer, as well as a variety of sporadic tumors that display microsatellite instability (Peltomaki 2001). BER, NER and MMR are error-free repair mechanisms, as the newly synthesized bases are added complementary to the opposite strand.

In normal vertebrate cells, 6-4 photoproducts are efficiently repaired by NER, but nearly 50% of cyclobutane pyrimidine dimers remain unrepaired even at 24h after UV irradiation (Mitchell and Nairn 1989). In such cases, the DNA replication machinery often encounters errors during S-phase and stalls the replication fork, resulting in a gap opposite the site of damage in the newly synthesized strand. The Rad6 pathway is engaged when the replication fork stalls to fill this gap and is mediated via bypassing the lesion by TLS or recombination to resolve the stalled replication fork (Broomfield et al. 2001). This pathway will be described in detail in section 2.7 of this thesis.

Cells have evolved two distinct pathways to repair DSBs, namely HR and NHEJ. It appears that the choice between these pathways is largely influenced by the stage within the cell cycle at the time of damage acquisition (Takata et al. 1998). The HR-directed repair takes place in late S and G2 phases of the cell cycle when an undamaged sister chromatid is available for use as homologous template from which the genetic information is retrieved for an error-free repair. After the identification of the homologous DNA, the damaged DNA strand is synthesized from the information in the undamaged homologue. In contrast to HR, NHEJ does not require a homologous template for DSB repair and the strand break is usually corrected by a direct ligation of broken ends in a potentially error-prone mechanism as sometimes loss of some DNA at the ends may occur.

2.2. Adaptive genetic alterations – an advantage

DNA repair mechanisms are able to mend most genetic changes before they become permanent mutations. Further mutations that are deleterious are often eliminated by natural selection. Yet, a basal level of mutations accumulate in the genome with a frequency of about

10^{-9}mutations/bp/generation that may contribute to single nucleotide polymorphisms (SNPs), variations in the gene pool, new phenotypes and ultimately evolution whenever the mutations occur in the germline. Therefore, in order to help the organism to adapt to a changing environment, genetic alterations may be often tolerated to a certain extent or even may be a prerequisite. These are adaptive genetic changes that are advantageous to the survival of the organism. The lymphocytes of the adaptive immune system present a classic instance when mutations and genetic alterations are adaptive. The genes that code for antibodies (or Ig) have an unusual architecture that facilitates the generation of a diverse set of polypeptide products comparable to the diversity of existing antigens.

2.3. The primary Ig diversification during early B cell development

The B cell development occurs through several stages, throughout which genetic alterations occur during the following important events: V(D)J recombination, Ig gene conversion in some organisms, SHM and CSR (Figure 2). The Ig genes expressed by B cells comprising heavy and light chains with both constant (C) and variable (V) regions are encoded by the heavy chain gene on chromosome 14 (M. J. Hobart 1981) and the light chains kappa (κ) and lambda (λ) genes located on chromosome 2 and chromosome 22 (McBride et al. 1982), respectively, in humans.

In humans and mice, genes for the variable region of the Ig are encoded in the genome by three distinct types of segments, namely variable (V), diversity (D) and joining (J) segments. The preimmune repertoire is established early in the B-cell development in the bone marrow by germline rearrangements of each one of the numerous V, D and J gene segments of Ig genes for heavy chain and the V and J segments for the light chains to produce B cells each of which expresses an unique B cell receptor (Figure 2). The critical lymphocyte specific enzymes, called recombination activating gene-1 and -2 (RAG1 and RAG2) are involved in the initial steps of V(D)J recombination (Janeway 2004). These enzymes associate with each other to recognize the recombination signal sequences that flank the V, D and J gene segments and induce DNA cleavage at these sequences. The resultant V regions encode the antigen binding sites of antibodies that are then expressed with the constant region on the surface of the B cells and its clonal progeny and define the future fate of the naïve B cells.

In some organisms such as rabbits, cows, pigs, horse and chicken, the primary antibody diversification is achieved through Ig gene conversion of the V region. The Ig loci of chicken, for instance, consist of a single V and J segment, and in case of the heavy chain locus, about 15 D segments (Reynaud et al. 1989). Therefore, the combinatorial Ig diversification that

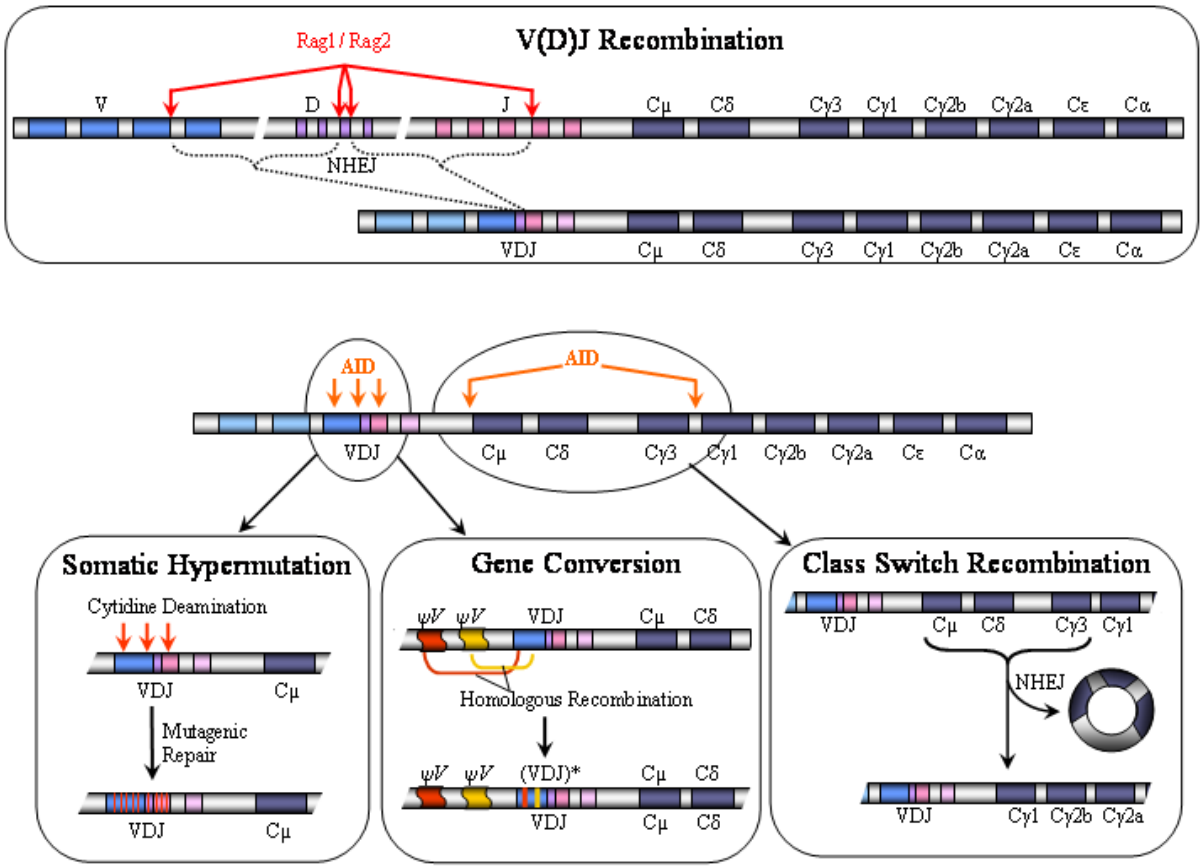

***Figure 2*: Adaptive genetic alterations in the Ig heavy chain locus.** *See text for details.*
Abbreviations: Ig – immunoglobulin; AID – Activation induced cytidine deaminase; RAG – Recombination activating gene; NHEJ – Non-homologous end joining; V – exons of the variable segments; D – exons of the diversity segments; J – exons of the joining segments; Cμ, Cδ, Cγ1, Cγ2a, Cγ2b, Cγ3, Cε and Cα – different exons of the constant segments; ψV – pseudo-V genes

occurs in humans and mice is not possible. Instead, there are pseudogenes for the V segment at the region 5' of the V segment at both the light- and heavy- chain Ig loci. They lack functional promoters and V(D)J recombination signal sequences and are often truncated (Reynaud et al. 1987; McCormack and Thompson 1990). These pseudoV genes (ψV) are used as templates in the Ig gene conversion process in the bursa of Fabricius, during which sequence information is incorporated by homologous recombination into the single active V gene (Reynaud et al. 1987; Carlson et al. 1990) (Figure 2). The naïve B cells circulate in the blood and lymph and are carried to the secondary lymphoid organs, the spleen and lymph nodes (Janis Kuby 2003).

2.4. The secondary Ig diversification processes in the germinal center

Following specific antigen recognition by its cognate B cell receptor and co-stimulation by T cells, the naïve B cells are activated and move to the center of the secondary lymphoid follicle together with some T helper cells, thereby forming a germinal center. The activated B

cells undergo intense proliferation and appear in the germinal centers as a well defined dark zone that is distinct from the region that also contains the follicular dendritic cells called the light zone (Hanna 1964; Jacob et al. 1991).

In mice, the B cells in lymph node germinal centers have been directly visualised by two-photon laser-scanning microscopy, revealing that nearly all antigen-specific B cells participating in a germinal center reaction were motile within the germinal center and migrated bi-directionally between dark and light zones (Schwickert et al. 2007). The B cells encounter the antigens trapped on follicular dendritic cells in the germinal centers triggering the second wave of antibody diversification through several rounds of SHM and affinity maturation during which process the competition for T cells plays a dominant role in the selection of B cells with high affinity B cell receptors (Allen et al. 2007). SHM of the Ig loci in germinal center B cells introduces random, single base substitutions and rarely insertions or deletions (Figure 2). The process is initiated by the deamination of cytosine by AID and completed by error-prone processing of the resulting uracils by MMR and BER.

In the germinal center, CSR, an intrachromosomal recombinatorial event, also ensures that the antigen binding site can be expressed in combination with any one of the constant (C) region genes to achieve many different effector functions and be distributed throughout the body, while the antigen specificity remains unchanged (Rajewsky 1996). During this process, the functional V(D)J segment is brought into proximity with the exons of downstream Ig constant regions (Cγ2b, Cγ2a, etc), while the exons of the IgM constant region is removed by recombinational deletion (Figure 2). Thus, the IgM antibody coding genes, specific for a given antigen, are transformed into genes encoding high-affinity antibodies such as an IgG, IgA, or IgE isotype.

SHM and CSR are the secondary Ig diversification processes in mice and humans while in birds, Ig gene conversion and SHM seems to act cooperatively in the germinal center (Arakawa et al. 1996; Arakawa et al. 1998), Ig gene conversion being the predominant process (Li et al. 2004). CSR is also known to occur in the germinal center of chicken (Yasuda et al. 2003). V(D)J rearrangements, Ig gene conversion and CSR generate changes by combinations of existing gene segments, whereas SHM is a unique process that generates changes in the sequence by point mutations (Figure 2). AID has been identified as a major enzyme involved in of all the three processes – SHM, Ig gene conversion and CSR (Honjo et al. 2004). While all the three processes are initiated by AID, the processing of the AID induced lesions are different for each process.

2.4.1. Processing of AID induced DNA lesions during adaptive immunity

Initially, AID was thought to be an RNA-editing enzyme, owing to the homology of its active site to the catalytic site of other RNA editing enzymes such as APOBEC1 (Muramatsu et al. 1999; Muramatsu et al. 2000). However subsequent studies revealed that AID is a DNA editing enzyme (Pasqualucci et al. 2001; Bransteitter et al. 2003; Pham et al. 2003; Li et al. 2004). The role of AID as the initiating factor in SHM and CSR was confirmed by studies showing that AID knockout mice were unable to carry out SHM and CSR similar to the patients with type II hyper-IgM immunodeficiency syndrome (Revy et al. 2000; Honjo et al. 2004). The role of AID in Ig gene conversion has also been established (Arakawa et al. 2002). The AID protein has been well characterized and it has been suggested that the function of AID in SHM and CSR requires the interaction of AID with specific cofactors at distinct domains of AID (Shinkura et al. 2004).

AID deaminates dC:dG pairs in the vicinity of either the IgV or Ig switch regions generating dU:dG lesions in the DNA (Rada et al. 2004). Figure 3 shows a schematic representation of the model for the processing of AID induced lesions. The dU:dG mismatch generated by AID may be further processed in three different ways. The mispair may be simply replicated over, leading to transition mutations at dC:dG pairs which may be grouped as phase 1A of SHM. The dU:dG mismatch may also be recognized by the mismatch repair enzymes MSH2/MSH6, generating dA:dT by mutagenic patch repair of the dU:dG lesion (or of derivatives thereof). These dA:dT biased mutations contribute to the phase 2 of the SHM model. The dU:dG mispair may also be subjected to uracil excision by uracil N-glycosylase (UNG), leading further to BER mediated repair of the abasic site thus generated. However, the UNG mediated base excision pathway is just one of the repair pathways following UNG action. Replication over the abasic site would yield both transitions and transversions at dC:dG (phase 1B). The pattern of gene diversification in UNG-deficient mice revealed that uracil excision by UNG played a dominant role in generating abasic sites upon which phase 1B mutations were templated (Rada et al. 2004). When the activity of UNG was blocked, it resulted in blockage of Ig gene conversion in DT40 cells and a disconcerted SHM (Di Noia and Neuberger 2002; Di Noia and Neuberger 2004; Li et al. 2004; Saribasak et al. 2006). The abasic sites generated by UNG can also be subject to apurinic/apyrimidinic endonuclease (AP-endonuclease) cleavage that leads to a SSB, eventually leading to DSBs as the initial substrates for CSR, Ig gene conversion and deletions.

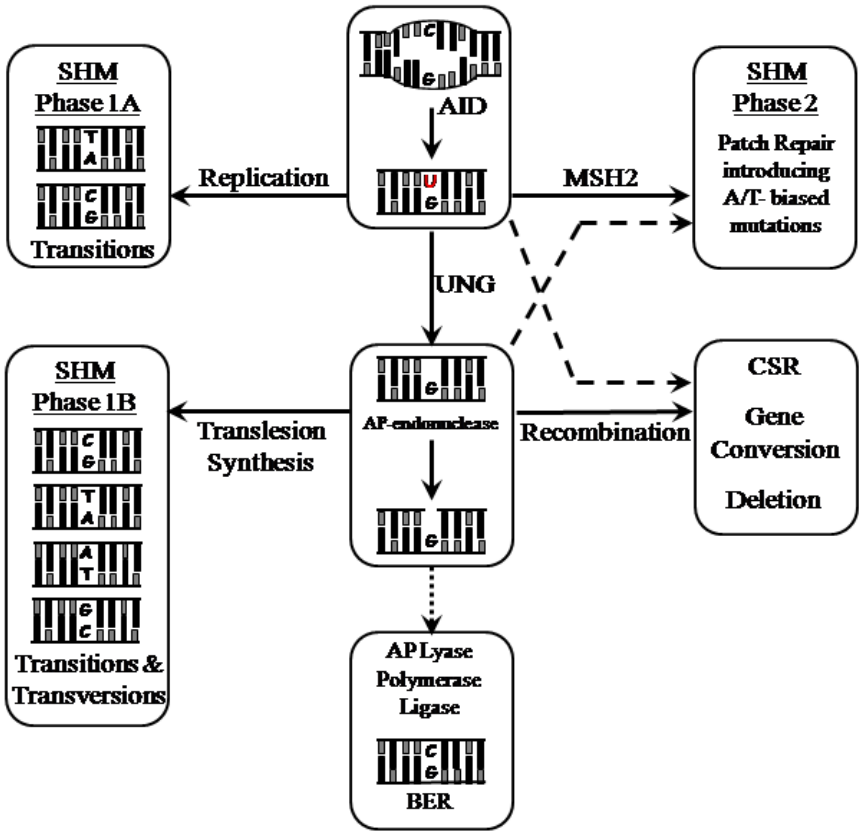

***Figure 3*: Model for repair of AID-induced lesions by somatic hypermutation, class switch recombination and Ig gene conversion (Rada et.al. 2004).** *See details in text.*
Abbreviations: AID – Activation induced cytidine deaminase; UNG – Uracil-N glycosylase; AP-endonuclease – apurinic/apyrimidinic endonuclease; SHM – somatic hypermutation; CSR – class switch recombination; BER – base excision repair

2.5. Targeting of somatic hypermutation to the Ig loci

Earlier, most studies on the targeting of SHM conceptually centered on the targeting of AID by many factors, including transcription-coupled regulation and Ig enhancers (Bachl et al. 2001). The transcriptional machinery may regulate SHM either through interactions of various factors with the RNA polymerase complex or by alterations in the chromatin structure that may provide more access to potential mutator factor binding sites in the DNA. The Ig enhancers may regulate hypermutation by providing transcriptional activation of Ig loci and/or by containing cis-element(s) to target the AID mutator system. However, since most of the mutations in the V regions of the Ig genes are dependent on error prone repair, the recruitment of error-prone processing of the AID induced dU:dG mispair would also have to be regulated in addition to the targeting of AID to transcribed genes. Recently the non-Ig genes of the murine Peyer's patch B-cells of wild-type and AID-deficient mice littermates

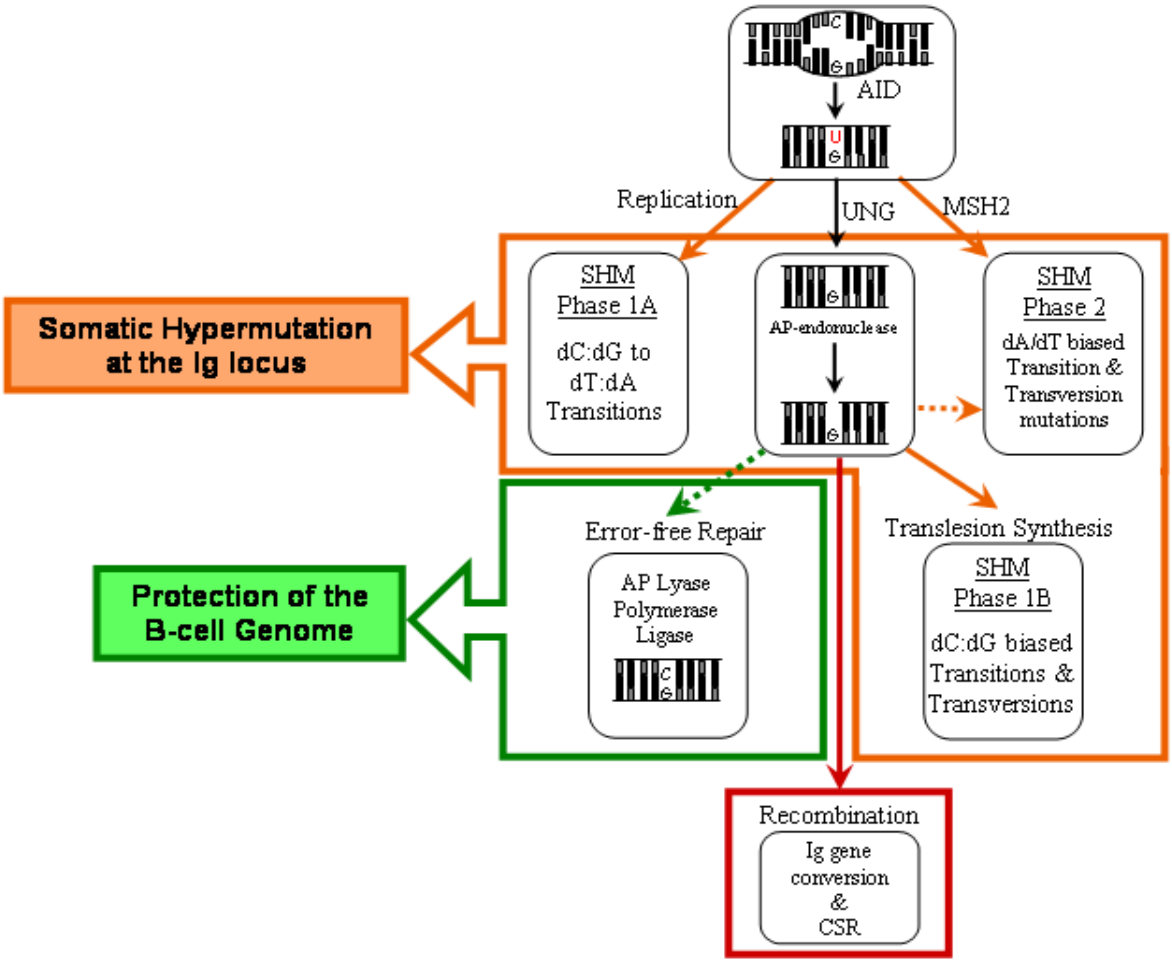

***Figure 4*: Targeting of somatic hypermutation by locus-specific differential processing of AID-induced lesions**. *The Phases 1A, 1B and 2 of SHM are depicted as proposed by the SHM model of Rada et al 2004. SHM involves error-prone BER and MMR mechanisms that may be preferentially targeted to the Ig loci. The error-free BER might contribute to the protection of the genome. The translesion synthesis to achieve SHM phase 1B and recruitment of Polη during dA/dT mutagenesis are regulated by the Rad6 pathway. Thus the Rad6 pathway may be the molecular regulator of the ultimate distribution of AID induced mutations in the B cell genome.*
Abbreviations: AID – Activation Induced Cytidine deaminase; UNG – Uracil-N glycosylase; AP-endonuclease – Apurinic/Apyrimidinic Endonuclease; SHM – Somatic Hypermutation; CSR – class switch recombination; BER – base excision repair; MMR – mismatch repair

were extensively sequenced (Liu et al. 2008). The mutational analysis showed that AID acts broadly on the transcribed genes in the mouse genome.The sequence analysis also showed that numerous genes linked to B-cell tumorigenesis, including Myc, Pim1, Pax5, Ocab, H2afx, Rhoh and Ebf1, are deaminated by AID but did not acquire mutations, apparently by the combined action of BER and MMR. The genome is thus protected by two distinct mechanisms, namely selective targeting of AID to transcribed genes and gene-specific, high-fidelity repair of AID-generated uracils. However, approximately 25% of expressed genes analyzed were not fully protected by either mechanisms and accumulated mutations in

germinal centre B cells. These results indicated that the ultimate distribution of the AID induced mutations is determined by differential processing of AID induced lesions by a balance between high-fidelity DNA repair and error-prone DNA repairs. This observation in the context of the SHM model for the processing of AID mutations is summarized in figure 4. It is known that the Rad6 pathway is a molecular regulator of the switch between error-prone and error-free repair and is thus an interesting field of study.

2.6. Role of the Rad6 pathway in Ig diversification processes

The Rad6 pathway involves a heterogeneous group of enzymes that mediate error-prone and error-free repair of stalled replication forks, mediated by ubiquitination of PCNA (Lawrence 1994; Hoege et al. 2002). Nearly half of the known genes of the Rad6 epistasis group are enzymes of the ubiquitin system, and the remaining others mainly belong to the family of TLS polymerases (Jentsch et al. 1987; Ulrich and Jentsch 2000; Hoege et al. 2002). Many of the components of the Rad6 pathway have been found to be involved in one or more Ig diversification processes. The error-prone TLS polymerase, Polη is known to be an A:T mutator in SHM (Zeng et al. 2001). Another TLS polymerase encoded by *REV3* and *REV7*, Polζ is able to elongate mismatched base insertions and this property of Polζ is also utilized during SHM (Zan et al. 2001). Recently the key mediator of the Rad6 pathway – Rad18, was found to play a role in SHM (Bachl et al. 2006). The role of PCNA ubiquitination in SHM has also been substantiated in DT40 chicken B-cells (Arakawa et al. 2006). Also in mice, the A:T mutagenesis of SHM was shown to be strongly dependent on monoubiquitinated PCNA ($PCNA^{(ubi)}$), since the $PCNA^{K164R/K164R}$ mutant mice showed an altered SHM phenotype similar to Polη and MMR deficient B-cells, although the B cells could proliferate and perform CSR normally (Langerak et al. 2007). While Mms2, a ubiquitin conjugating enzyme that is involved in the error-free bypass of DNA lesion during the Rad6 pathway, is not required for efficient Ig gene conversion (Simpson and Sale 2005), a role of Rad18 in homologous recombination hints to a potential role of Rad18 in Ig gene conversion in DT40 chicken B-cells (Szuts et al. 2006). Therefore, a role of the Rad6 pathway in templated and non-templated Ig diversification is evident.

2.7. The Rad6 Pathway

The Rad6 pathway has been extensively characterized in yeast. Figure 5 shows an overview of the Rad6 pathway in yeast. Depending on the type of ubiquitination of PCNA, there are two subpathways, the TLS pathway and the error-free template switch repair. The monoubiquitination of PCNA triggers the TLS pathway while the polyubiquitination of

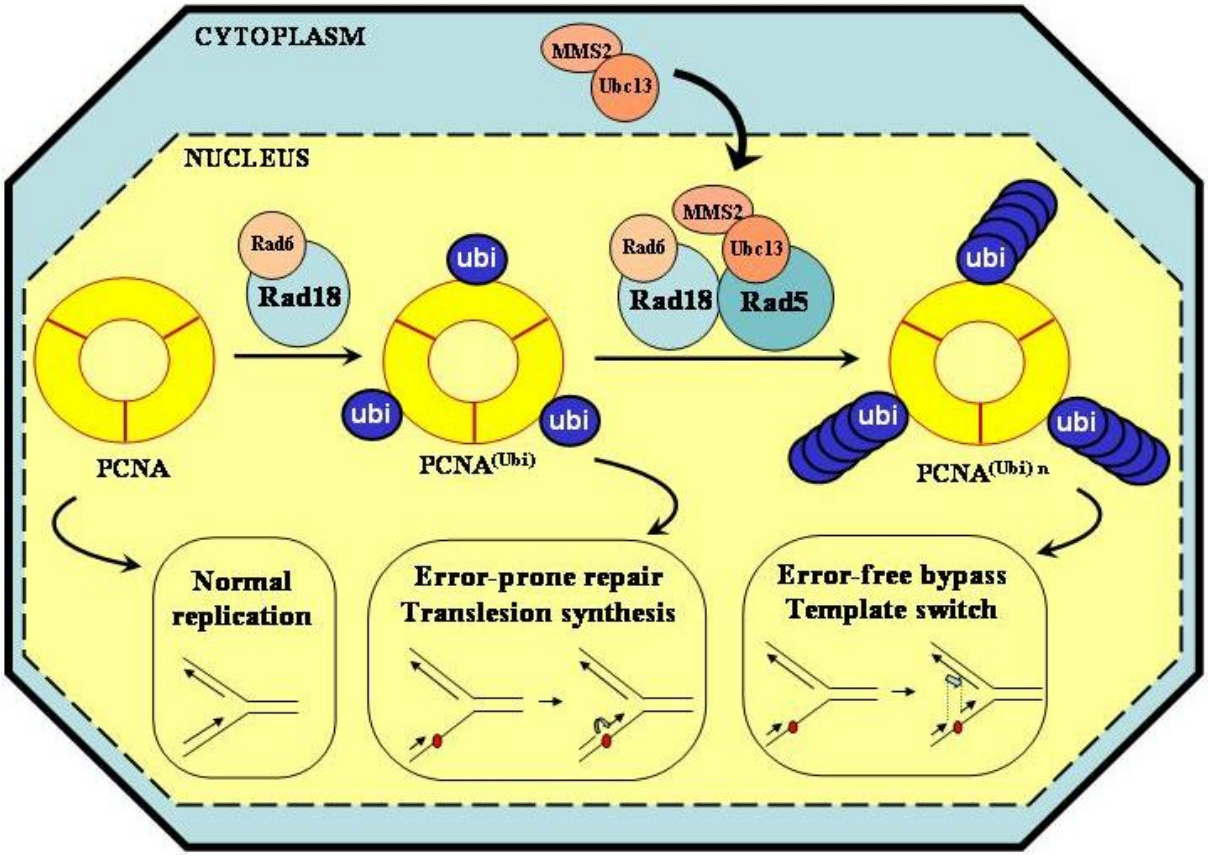

***Figure 5*: The Rad6 Pathway in yeast.** *The ubiquitination status of PCNA serves as the molecular switch between error prone and error free DNA repair pathways. The unmodified PCNA is involved in normal replication. When replication stalls due to damage, PCNA is monoubiquitinated by Rad6/Rad18 to accomplish translesion synthesis. Polyubiquitination of PCNA involves Rad5/Ubc13 and MMS in addition to Rad6/Rad18 and this leads to error-free bypass of the damage by template switch to the undamaged sister chromatid.*
Abbreviations: Ubi – ubiquitin; PCNA – proliferating cell nuclear antigen; $PCNA^{(Ubi)}$ – mono-ubiquitinated PCNA; $PCNA^{(Ubi)\,n}$ – poly-ubiquitinated PCNA

PCNA activates the error-free repair. Apart from recognition and repair of stalled replication forks, the Rad6 pathway is also known to be involved in dsDNA gap repair and Rad5 is involved in the avoidance of NHEJ during DSBR in yeast (Ahne et al. 1997; Moertl et al. 2008).

2.7.1. Translesion Synthesis

The monoubiquitination of PCNA at lysine164 (K164) involves the Rad6/Rad18 complex (Hoege et al. 2002). The Rad6 is an E2 ubiquitin conjugating enzyme (UBC) and Rad18 is an E3 ubiquitin ligase. The Rad18 protein forms a tight complex with Rad6 and associates with itself through the RING finger domain, forming a dimer of the Rad6/Rad18 heterodimer (Bailly et al. 1994; Xin et al. 2000; Miyase et al. 2005). Rad18 recruits the ubiquitinating

system to the DNA and TLS is carried out by $PCNA^{(ubi)}$ that recruits the error-prone polymerases such as Polη and Polζ.

The mechanism of TLS involves the $PCNA^{(ubi)}$ possibly by multiple polymerase switching events which include a TLS polymerase that inserts a base opposite to the damage and subsequently another specific TLS polymerase that extends the insertion by few additional nucleotides past the lesion (Friedberg et al. 2005). The interaction of $PCNA^{(ubi)}$ and Polη has already been demonstrated (Kannouche et al. 2004; Watanabe et al. 2004). Polη is able to first insert a base independently of the information on the template strand (Johnson et al. 1999). The extension of the inserted base is performed by another polymerase such as Polζ encoded by *REV3* and *REV7* (Nelson et al. 1996), which is able to extend the insertion only for a few base pairs further owing to its low processivity. Similarly Polκ, another member of the TLS polymerases, is efficient in the insertion of the correct cytidine opposite of a benzo(a)pyrene adducted guanine base and is recruited by Rad18 to $PCNA^{(ubi)}$ (Ohmori et al. 2004). Thus depending on the type of lesion many TLS polymerases are involved that are able to synthesize DNA past a lesion with low fidelity.

2.7.2. Error free bypass

In addition to Rad6 and Rad18, polyubiquitination of PCNA requires another ubiquitin conjugating heterodimer, Ubc13-Mms2 (Hofmann and Pickart 1999) recruited by the E3 ubiquitin ligase – Rad5 (Ulrich and Jentsch 2000). The Ubc13-Mms2 and Rad5 cooperate with the Rad6-Rad18 heterodimer to generate polyubiquitinated PCNA ($PCNA^{(ubi)n}$) using K63 linked polyubiquitin chains and activate the error-free template switch that is important for the completion of replication during replication stress (Broomfield et al. 1998; Hofmann and Pickart 1999; Ulrich and Jentsch 2000; Hoege et al. 2002; Branzei et al. 2004). The proteins modified with K63 polyubiquitin chains are involved in many cellular processes including DNA repair and are different from those modified with K48 linked ubiquitin chains that are subject to proteosomal degradation (Hofmann and Pickart 1999).

The mechanism of activation of the error free bypass by $PCNA^{(ubi)n}$ remains speculative. The template switch to the undamaged sister chromatid may be achieved by fork regression resulting in the formation of a four-way junction intermediate called “chicken foot” structure. This requires the unwinding of the leading and lagging strands of the replication fork and Rad5 is able to fulfill this requirement by its helicase activity (Blastyak et al. 2007). The DNA synthesis then occurs based on the information on the undamaged sister chromatid, thus achieving error-free bypass of the lesion.

2.7.3. Interactions of components of the Rad6 pathway

The components of the Rad6 pathway and their interactions are highly conserved and the vertebrate homologs for all the known components of the Rad6 pathway have already been identified. In fact two proteins have been identified as the vertebrate homologues of Rad5, namely SHPRH and HLTF (Motegi et al. 2006; Unk et al. 2006; Motegi et al. 2008; Unk et al. 2008).

The interaction complexes of the Rad6 pathway have been described in yeast. There is substantial evidence for the assembly of two distinct UBC complexes mediated by Rad18 and Rad5, each for the error-prone and error-free pathways (Ulrich and Jentsch 2000). The homodimeric self association of Rad18 promotes the assembly of Rad6 to the complex that is involved in TLS, while the heteromeric association of Rad18 with Rad5 results in two distinct UBCs – Rad6 and Ubc13/Mms2 which activate the error-free bypass. It is postulated that the homodimerization and heterodimerization complexes are mutually exclusive and may not form supramolecular complexes owing to the weak interactions between Rad18, Rad5 and Ubc13 (Ulrich and Jentsch 2000).

2.8. Molecular interplay between the Rad6 pathway and checkpoint signalling components

There are evidences that indicate an important role of the Rad6 pathway in other signaling pathways affecting cell cycle, DNA repair and apoptosis. For instance, there are molecular crosstalks between components of the checkpoint signaling and the Rad6 pathway, resulting in the regulation of both pathways.

The ssDNA binding protein - Replication Protein A (RPA) plays a central role in recruiting DNA repair proteins to the DNA damage. Recently, the direct interaction of RPA and Rad18 and the function of the RPA complex to recruit Rad18 to ssDNA *in vitro* was demonstrated (Davies et al. 2008). The recruitment of the Rad18-Rad6 complex to stalled replication forks by the ability of this complex to recognize forked and ssDNA structures is also known (Tsuji et al. 2008). Taking these two findings together, it may be postulated that the Rad18/Rad6 complex is able to recognize the damage and it is recruited to the DNA by RPA. Further, RPA is indeed known to be required for efficient PCNA ubiquitination (Davies et al. 2008).

On the other hand, the ATR-ATRIP kinase complex and the 9-1-1 checkpoint clamp are also recruited separately to single-stranded (ss)DNA, by the interactions of ATRIP and the 9-1-1 specific clamp-loader with the RPA complex (Zou and Elledge 2003; Zou et al. 2003).

These two complexes are activated by stalled replication forks, resulting in the initiation of the checkpoint signaling cascade during S-phase.

A clear role of checkpoint signaling in the regulation of the Rad6 pathway has also been observed. The inhibition of RPA/ATR-Chk1 mediated S-phase checkpoint signaling partially inhibited PCNA ubiquitination and also prevented interactions between PCNA and Polκ (Bi et al. 2006). Another study revealed that while the ATR-Chk1 pathway is important for coping with intrinsic replication stress, Chk1 together with Claspin and Timeless regulate efficient ubiquitination of PCNA independently of ATR (Yang et al. 2008).

While the influence of checkpoint signaling components on the Rad6 pathway is known, there is also recent evidence of the role of Rad6 pathway and/or its components on checkpoint signaling itself. For instance, in addition to ubiquitination of PCNA, the Rad6-Rad18 complex is also involved in the ubiquitination of the Rad17 (Rad1 in mammals) subunit of the 9-1-1 checkpoint DNA clamp, thus promoting DNA damage-dependent transcriptional induction and checkpoint functions (Fu et al. 2008). The 9-1-1 DNA clamp is also known to be required for Ig gene conversion (Saberi et al. 2008). Although these data indicate a definite molecular crosstalk between the DNA damage response signaling components and the Rad6 pathway, the biological consequences of this communication are worth further study.

2.9. Other functions of components of the Rad6 pathway

Besides the role of the Rad6 pathway in DNA repair, Ig diversification and its interplay with the checkpoint signaling, the enzymes of this pathway are able to function with other unconventional substrates, or are themselves substrates to enzymes not involved in the pathway. For instance, there is evidence for an alternative PCNA ubiquitinating enzyme in DT40 (Szuts et al. 2006) and recently the E3 ligase RNF8 was found to be able to ubiquitinate PCNA, although the E2 conjugating enzyme involved in this reaction is yet to be identified (Zhang et al. 2008). Similarly, a Rad18 function independent of PCNA monoubiquitination has also been identified in S-phase specific SSB repair (Shiomi et al. 2007). Rad18 is also involved in HR in DT40 cells (Szuts et al. 2006) and plays a role in meiosis and sperm maintenance (van der Laan et al. 2004). Ubc13-Mms2 also interacts with the heterodimeric RING E3 BRCA1-BARD1 to polyubiquitinate BRCA1 (Christensen et al. 2007). Ubc13 is the only known E2 conjugating enzyme that performs K63 linkage of Ubiquitins. Rad6 is not only involved in DNA repair via the Rad6 pathway, but also in sporulation (Cox and Parry 1968), retrotransposition (Picologlou et al. 1990), silencing (Huang et al. 1997) and in protein degradation (Sung et al. 1990; Dohmen et al. 1991).

2.10. Functional characterisation of Rad18 protein domains

The components of Rad6 pathway are involved in many cellular processes besides their role in DNA repair at the stalled replication forks. Therefore it would be interesting to study the molecular interaction network of Rad18, the critical component of the Rad6 pathway that is involved in many other cellular processes. Rad18 exists in association with Rad6 and is usually present as a dimer of the Rad6/Rad18 heterodimer (Ulrich and Jentsch 2000; Miyase et al. 2005; Notenboom et al. 2007). The functional domains of Rad18 have been well characterized. Figure 6 shows a schematic representation of the functional domains of Rad18 according to Notenboom et al. 2007.

Rad18 is a multidomain E3 ligase, equipped with functional domains for DNA binding, PCNA modification and for interaction with Rad6, PCNA and Polη. At the N-terminus, Rad18 carries a RING domain (25 – 63 amino acid residues) that interacts with its cognate E2 enzyme, Rad6. A second region between 340 – 395 residues in the C-terminus are also involved in this interaction (Bailly et al. 1997; Ulrich and Jentsch 2000; Back et al. 2002). The amino acid residues 401 – 445 in the C-terminus is also involved in binding to Polη (Watanabe et al. 2004). The C2HC Zinc-finger (ZnF) domain (201 – 255) was initially postulated to have a DNA binding potential (Jones et al. 1988; Bailly et al. 1994). Mutations of this domain disrupted self-association of Rad18, indicating that this potential DNA binding domain is essential for dimerisation (Tateishi et al. 2000; Ulrich and Jentsch 2000; Miyase et al. 2005). The ZnF domain is also important for auto-monoubiquitination and localisation of Rad18 to cyclobutane pyrimidine dimer damages of DNA (Nakajima et al. 2006), but in a later study it was found to be the binding domain for ubiquitin and rather not involved in DNA recognition (Notenboom et al. 2007). The SAP domain (248 – 282 residues), named after the three proteins in which the domain was first identified as a DNA interacting domain (Aravind and Koonin 2000), is capable of DNA recognition in vitro (Notenboom et al. 2007) and was also found to be responsible for the localisation of Rad18 to DNA foci containing Polη (Nakajima et al. 2006).

While evidences for the role of Rad6 pathway in Ig gene diversification and its interplay with DNA damage checkpoint signaling are mounting, there are also substantial findings about the influence of other processes on regulation of the different events of the Rad6 pathway. At this juncture, a robust biochemical and genetic approach is needed to unravel the hidden links of this crosstalk among different pathways to provide a more integrated perspective to the molecular network of the Rad6 pathway.

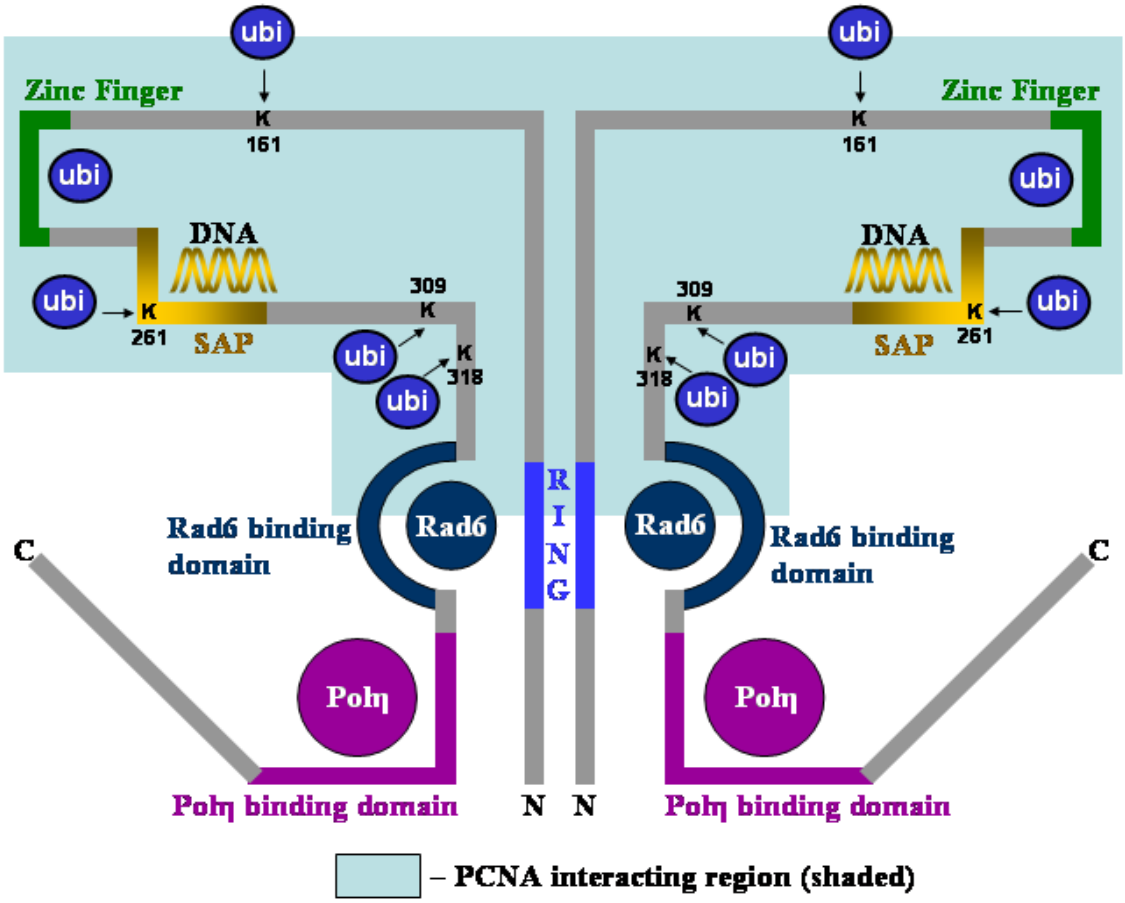

***Figure 6*: Schematic representation of the functional domains and ligand-interacting regions of human Rad18 Source: Notenboom et al. 2007.** *The N terminus of the human Rad18 protein contains the RING domain (25-63) which along with the Rad6 binding domain (340-395) is essential for Rad6 interaction. The Zinc finger domain (201-225 residues) binds Ubiquitin while the SAP domain (243-282 residues) is required for DNA binding. Between 401-445 residues is the Polη binding region. The PCNA-interacting region that is contained within residues 16–366 (shaded). K161, K261, K309 and K318 are four sites of autoubiquitination of Rad18 which are conserved between murine and human Rad18. The ubiquitination sites of the protein are also conserved in chicken Rad18 protein except the K161 site of ubiquitination.*
Abbreviations: Ubi – ubiquitin; PCNA – proliferating cell nuclear antigen; K – Lysine residue; Pol – Polymerase

2.11. Biochemical and genetic approaches to study cellular networks

The recent sequencing of the genomes of many organisms has steered reverse genetic approaches into a major focus of investigation. The study of cellular networks is important to understand the higher order molecular organization of cellular processes. Protein-protein interactions are intrinsic to cellular networks. There are many techniques to study protein interactions such as immunoprecipitation, affinity chromatography, library-based methods like the two-hybrid system and phage display, mutational analysis etc. The isolation and characterization of the complexes of the protein of interest followed by analysis of its

constituents is one of the best approaches to study protein interactions. This would provide a better understanding of cellular networks than identifying one to one interactions, since proteins are often involved in more than one process or pathway that may or may not be interlinked.

The information about protein interaction alone is not sufficient unless the functional significance of the interaction is elucidated. Protein interactions can have many different measurable effects on the level of its function (for a review see Phizicky and Fields 1995). One such measurable effect is in terms of alterations in the kinetic properties of the interacting proteins by altered catalysis, binding of substrates or allosteric properties of the complex. For instance, the ubiquitination status of PCNA alters its binding to different types of polymerases, while the binding also alters the processivity of a polymerase such as that of Polδ (Prelich et al. 1987). The other measurable effects of protein interactions are that the interaction may lead to new binding sites, allow for substrate channeling, inactivate or activate one of the interactors, and/or change the specificity of the protein for its substrate (Phizicky and Fields 1995). Thus, the functional analysis of different interactions is crucial to understand the impact of an interaction on cellular processes and ultimately interaction networks. Functional analysis can be carried out by analyzing the effects of genetic manipulation such as gene knockout or knockdown approaches, overexpression, silencing, etc and complementation of the phenotype. A combination of interaction studies and functional studies is therefore important to unravel cellular networks.

2.11.1. The tandem affinity purification (TAP) technique

While many methods of isolation of protein complexes are available, tandem affinity purification (TAP) is one of the few techniques that allows isolation of native protein complexes in even the lowest concentrations of protein complexes recovered (Rigaut et al. 1999). The method does not require prior knowledge of the complex composition or function. In this method, the TAP tag is fused to the target protein of interest and expressed in the cell. The figure 7a represents the C-terminal and N-terminal TAP fusion constructs of a gene of interest (GOI). The TAP tag consists of two Ig binding proteinA domains of *Staphylococcus aureus* and a calmodulin binding peptide (CBP) separated by a Tobacco Etch Virus (TEV) protease cleavage site. The basic principle of TAP method is depicted in Figure 7B. The total cell extracts prepared from cells expressing the TAP tagged protein undergo two specific affinity purification/elution steps to recover the fusion protein along with its interaction partners. In the first affinity purification step, the Prot A binds tightly to an IgG matrix, requiring the use of the TEV protease to elute the bound material under native conditions.

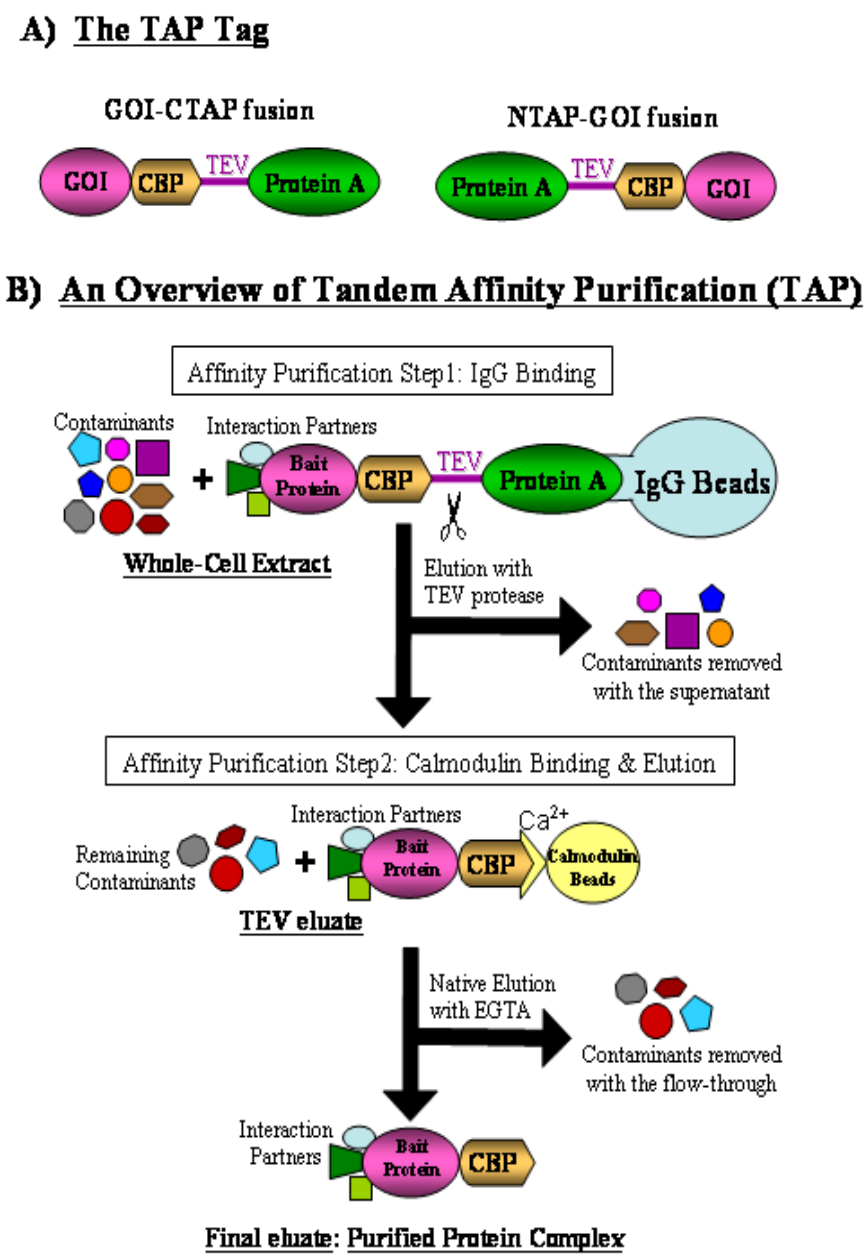

***Figure 7*: A) Schematic representation of the TAP Tag:** *The TAP tag consists of Protein-A moiety, TEV site and CBP fused to the protein either to its C- or N- terminus.*
B) An overview of Tandem Affinity Purification (TAP): *The TAP method involves two successive affinity purification steps. The first step exploits the tight binding of the Protein A moiety of the tag to IgG beads while the contaminants are removed with the supernatant. The bound protein is eluted by TEV protease cleavage. In the second purification step, the CBP of the TAP tag binds to the calmodulin coated beads in the presence of calcium ions. After removal of the contaminants with the flow-through, the complex is eluted in the presence of EGTA.*
Abbreviations: GOI – gene of interest; TEV – Tobacco Etch Virus; CBP – calmodulin binding peptide; CTAP/NTAP – C- or N- terminal TAP fusion; TAP – tandem affinity purification

In the second step, this eluate is incubated with calmodulin-coated beads in the presence of calcium. After washing away the contaminants and remnant TEV protease, the bound material is released under mild conditions with EGTA. For characterization of the protein complex thus recovered, the final eluate is concentrated before further analysis.

2.11.2. The DT40 system

The TAP tag is large (about 200 amino acid residues), so its fusion to the GOI may impair protein function and interactions. Consequently as a functional test, complementation of a knockout phenotype is an appropriate method to overcome this difficulty. The DT40 chicken B-cell line is an appropriate model system that allows easy manipulation of the genome in order to perform reverse genetic experiments and complementation studies. The cell line, derived from an avian leukosis virus (ALV)- transformed cells, is known for the ease of genetic manipulation for gene disruption experiments (Winding and Berchtold 2001) and it offers targeted to random DNA integration ratio far exceeding that of any mammalian cell line (Buerstedde and Takeda 1991; Winding and Berchtold 2001; Hudson et al. 2002). The Cre/loxP vector system is an ideal system to execute complementation of a knockout phenotype. While the disruption of multiple genes and complementation of phenotypes is limited by the number of available selectable markers, the recent development of mutant loxP vectors for conditional knockouts and selectable marker recycling in DT40 overcomes this limitation (Arakawa et al. 2001).

The combination of the TAP method with the DT40 system offers the possibility to assess the functionality of the fusion in the knockout cells and also the competition for interaction partners between the endogenous protein and the TAP tagged fusion protein could be avoided. Functional studies can also be performed directly in cells deficient for the GOI or a novel interaction partner. Thus the combination of the DT40 knockout approach with the TAP technique constitutes an immensely powerful tool to study protein interaction networks and to identify and characterize new interaction partners for the protein of interest. Ig gene conversion and SHM are constitutive in this cell line (Sale 2004) and hence the study of factors regulating these Ig diversification processes is also feasible in this cell line.

2.12. Objectives

Rad18 appears to be a central player in regulating the Rad6 pathway; Ig gene diversification processes and DNA damage checkpoint signaling. There are also evidences of the regulation of the Rad6 pathway by the components of the checkpoint signaling system. Ultimately, the function of Rad18 in DNA damage repair outside the Rad6 pathway is also

known. All these facts taken together suggests a role of Rad18 as a global mediator in DNA damage recognition, response, repair affecting genome maintenance as well as adaptive DNA alterations during Ig gene diversification processes.

Thus the aim of the current study was to identify new interaction partners of Rad18 which might lead to identification of 1) modulators of the Rad6 pathway, 2) factors that link the Rad6 pathway and SHM and possibly the mechanism of this interplay, and 3) factors linking the Rad6 pathway to other DNA repair pathways and/or cell cycle control. Following the identification of new interaction partners of Rad18, subsequent functional analysis for the new interactions would be performed if feasible, in order to achieve a better perspective on the Rad18 interaction network.

Since the combination of high throughput proteomic analysis with a reverse genetic system has been well established in yeast, but not for vertebrate systems, the establishment of the TAP method in the DT40 cells would therefore be the first of its kind for such studies in a vertebrate system. The success of the TAP method in DT40 would be tested using AID-TAP fusion constructs already available, followed by mass spectrometric analysis of the constituents of the complex purified thereby. Subsequently, this approach would be adapted to study the Rad18 interaction network, thereby establishing a system that in future could be extended to study protein interaction network of any protein of interest.

3. Results

The approach that was used to investigate the interaction network of the Protein of Interest (POI) in the DT40 chicken B cell line entailed the isolation of native complexes of the POI by the TAP method followed by mass spectrometric analysis (Figure 8). The GOI fused to the TAP tag comprising a protein A, TEV cleavage site and CBP was expressed in the GOI knockout DT40 cells and verified for functionality of the fusion. At expression levels comparable to the endogenous gene, the fusion interacts and forms complexes which were then purified by the TAP method. The proteins in the final eluates of this purification were concentrated and subjected to in-gel trypsin digestion. The mixture of peptides generated by the trypsin digest was resolved by nano-liquid chromatography (nano-LC) based on the hydrophobicity of each peptide. The nano-fractions eluting from the capillary of the LC system were mixed with the matrix, a-Cyano-4-hydroxycinnamic acid (CHCA), while being collected on a MALDI target by the automated Probot microfraction collector from Dionex Corporation. Subsequently, the peptide samples were subjected to mass spectrometric analysis by Matrix Assisted Laser Desorption Ionization/Time-of-flight (MALDI TOF/TOF) using the 4700 proteomics analyser from Applied Biosystems Inc. The data from the MS/MS analysis were processed with the GPS Explorer software using the MASCOT search engine and the NCBI *Gallus* database to generate a list of potential interaction partners of the bait protein. The cell clone expressing the TAP tag alone was used as an appropriate negative control. This approach was established in DT40 cells in this study using the AID-TAP fusion as a model system, since an equivalent purification was already successfully accomplished in the Raji human B cell line (Tobollik 2007). The approach was then adapted for the study of the Rad18 interaction network. Hence, the current study can be categorised into two parts, namely 1) the establishment of TAP in the DT40 cell line and 2) the study of the Rad18 interaction network in DT40 cells.

3.1. Establishment of TAP in the DT40 cell line using AID-TAP fusions

The AID-TAP tagged constructs were already available with the TAP tag fused to the human AID either at the C-terminus or at the N-terminus of the protein, designated as AID-CTAP and NTAP-AID, respectively. The functionality of the AID-TAP fusions was ascertained earlier and it was known that the AID-CTAP fusion was functional for SHM whereas the NTAP-AID fusion was non-functional (Tobollik 2007).

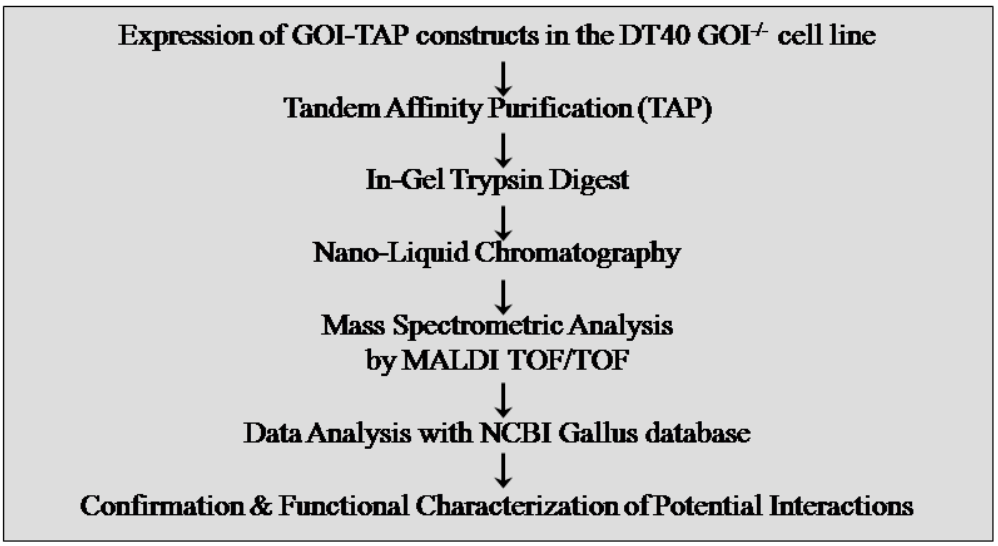

***Figure 8*: An overview of the approach to study protein interaction networks in DT40 cells.** *See text for details.*
Abbreviations: GOI-TAP – TAP tagged gene of interest; GOI$^{-/-}$ – knockout of gene of interest; MALDI – Matrix assisted LASER desorption ionisation; TOF – Time of flight

3.1.1. Expression of the AID-TAP fusion proteins in the DT40 cell line

There are two alternatives to express the TAP tagged fusion protein. One is to express the fusion from the endogenous locus by modifying the C-terminal or the N-terminal exons. The other option is to stably transfect exogenous vectors carrying the fusion protein with a suitable promoter into the GOI knockout DT40 cells. The NTAP-AID fusion in the pCAG vector and the AID-CTAP fusion in the pZome as well as a pCAG vector were readily available. Hence the exogenous expression of the TAP fusion was tested. The general features of the two vectors are depicted in Figure 9.

The 141pCAG-3SIP vector carries a composite CAG promoter that combines the human cytomegalovirus immediate-early enhancer (hCMVieE) and a modified chicken beta-actin promoter (Niwa et al. 1991). The CAG is known to drive a very strong expression of the downstream transgenes. The puromycin resistance gene is expressed from an Encephalomyocarditis internal ribosomal entry site (EMC IRES) element that is placed 3' of the GOI so that both the resistance gene and the GOI are driven by the CAG promoter. The pZome-1C vector is based on pBABE that carries Long Terminal Repeats (LTRs) to drive the expression of the fusion and a Simian Virus 40 (SV40) promoter to express the puromycin resistance gene. The vector is supplied by the company Cellzome, Heidelberg, Germany and was the original TAP tag vector.

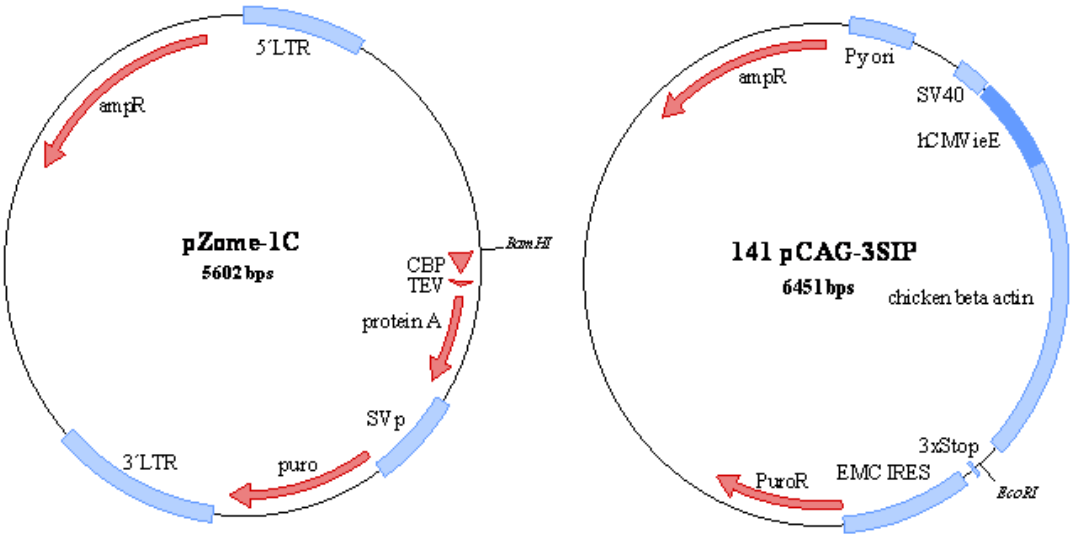

***Figure 9*: A Schematic depiction of the exogenous expression vectors tested**: *pZome-1C carrying a LTR promoter and SV40 driven puromycin resistance and pCAG-3SIP with a CAG promoter and puromycin resistance gene. The constructs were cloned in such a way that the PCR amplified GOI was cloned into the BamHI site. The GOI-TAP insert in this vector was then cleaved out using the EcoRI enzyme and cloned in to the pCAG-3SIP vector. The AID-TAP contructs were already available in these vectors from an earlier study (Tobollik 2007).*
Abbreviations: LTR – long terminal repeats; SVp – Simian Virus promoter; puro – puromycin resistance; ampR – ampicillin resistance; CBP – calmodulin binding peptide; TEV – tobacco etch virus protease cleavage site; SV40 – Simian virus 40 promoter; py ori – Polyoma origin of replication; hCMVieE – human cytomegalovirus immediate-early enhancer; EMC IRES – Encephalomyocarditis internal ribosomal entry site

The differences in the type of promoters, in the number of copies transfected per cell and in the site(s) of integration into the genome may result in clones with a wide range of exogenous expression levels. This allows the choice of the clone with an optimum expression level that is required for a successful proteomic approach and that is closest to the endogenous expression level.

The expression of the endogenous GOI and the exogenous TAP fusions from the expression vectors were assessed by quantitative Reverse Transcriptase - Polymerase Chain Reaction (qRT-PCR) and Western blotting for the mRNA and protein amounts, respectively. The estimation of the cDNA quantity was performed in a Light Cycler® by the Syber Green® method. The relative number of mRNA copies was estimated by normalising to the reference gene, Hypoxanthine phosphoribosyltransferase (*hprt*), which should be expressed constitutively on an identical level in all samples analysed. The relative amounts of mRNA for the endogenous GOI and its exogenous GOI-TAP fusions are summarised in Table1.

	Promoter	No. of mRNA copies per *hprt* copy
Endogenous expression levels of GOIs		
AID	Endogenous Promoter	1.89
Rad18		1.2
Exogenous expression levels of AID-TAP fusions		
pZome expressing AID-CTAP	LTR	0.26 to 13*
pCAG expressing NTAP-AID	CAG	79 to 360*

*** - a range obtained in different clones**

***Table 1*: An overview of exogenous and endogenous expression levels determined by qRT-PCR.**. *The mRNA was isolated from the cells and reverse transcribed. The cDNA thus obtained was used to assess the relative copy numbers of the exogenous AID-TAP fusions and the endogenous GOIs with respect to hprt as the house keeping gene. The qRT-PCR was performed in the Light Cycler by the Syber Green® method. The exogenous vectors pZome and pCAG controlled the gene expression from the LTR and CAG promoters, respectively. This was compared to the expression levels achieved by the endogenous promoters of the GOIs.*
Abbreviations: AID – Activation Induced Cytidine deaminase; LTR – Long terminal repeats; CAG – the CAG promoter; HPRT – Hypoxanthine phosphoribosyltransferase; GOI – gene of interest

The endogenous mRNA levels of AID and Rad18 were estimated to be 1.89 mRNA copies per *hprt* copy and 1.2 mRNA copies per *hprt* copy, respectively. For exogenous expression of AID-TAP fusions, the pZome and pCAG vectors carrying the AID-TAP fusions were stably transfected into $AID^{-/-}$ DT40 cells. The pCAG expressing AID-CTAP fusion did not yield any transfected clones even upon repeated attempts, whereas the transfection of pCAG expressing the NTAP-AID fusion and the pZome expressing the CTAP-AID fusion were successful. A reason for this might be that the functional AID-CTAP fusion, when expressed from a potential overexpression vector such as pCAG, could result in too high mutagenesis for the transfected DT40 cells to survive.

The mRNA levels of the AID-CTAP fusion expressed from the pZome vector were between 0.26 to 13.2 mRNA copies per *hprt* copy, i.e. ranging from nearly physiological expression levels to slight overexpression (Figure 10A). The pCAG vector expressed the NTAP-AID fusion at a much higher level, ranging from 79.09 to 360.13 mRNA copies per *hprt* copy (Figure 10A). Hence, this vector could serve as an overexpression vector if required.

The protein levels were determined by western blot analysis and were compared to the fusion protein amounts expressed in the human cell line Raji, which were already known to be sufficient for a successful TAP purification (Figure 10B). It was deduced that a protein level

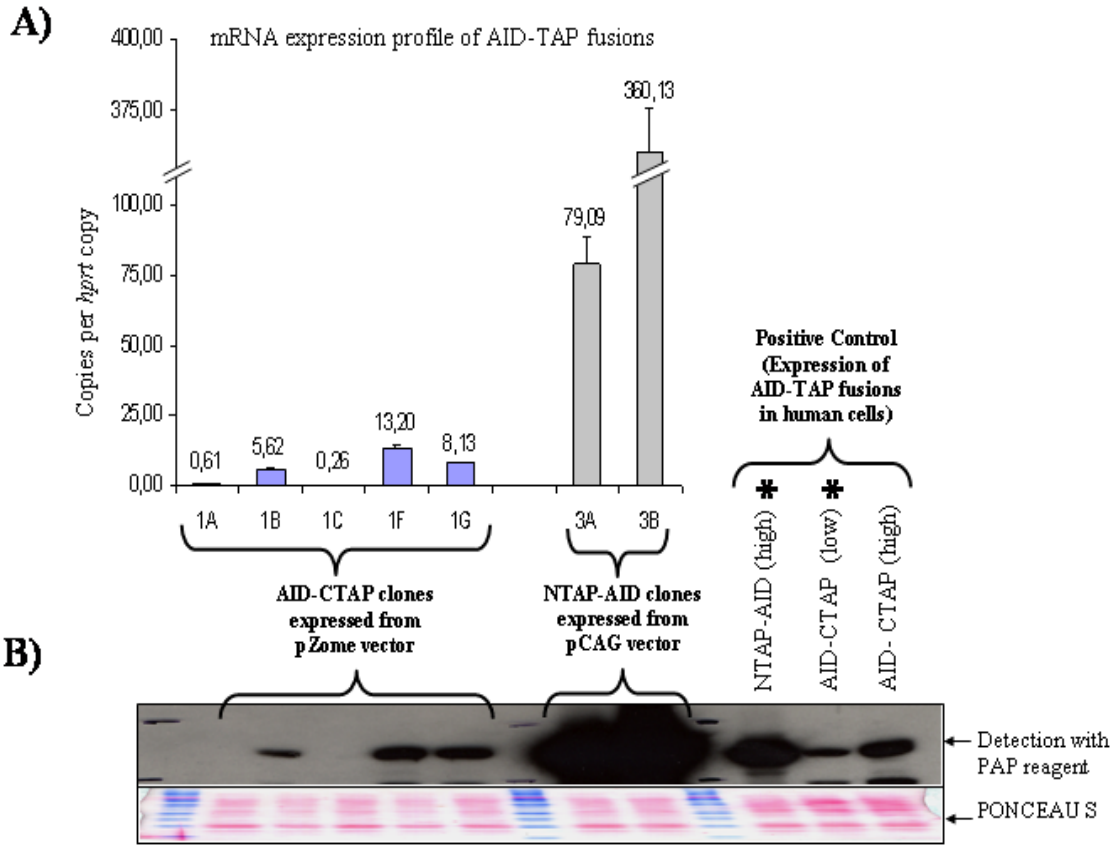

***Figure 10*: Expression levels of AID-TAP fusions in DT40 cells.**
A) qRT-PCR data for AID-TAP mRNA expression normalised to hprt expression. Values derived from AID-CTAP expressed from pZome are given in blue while those derived from AID-NTAP expressed from pCAG are given in grey. The mean and standard deviation of two independent quantifications are indicated.
B) Western blot analysis of AID-TAP expression. The fusion proteins were detected with a peroxidase antiperoxidase (PAP) reagent detecting the TAP tag. The DT40 clones expressing the AID-TAP fusions were loaded along with AID-TAP expressing human Raji clones that were previously used for a successful TAP method. The last lane shows the highest expression of AID-CTAP that was achieved in Raji cell line. Ponceau S staining is shown as a control of equal loading.
Abbreviations: AID – activation induced cytidine deaminase; hprt - Hypoxanthine phosphoribosyltransferase

corresponding to 5 to 10 copies of fusion protein mRNA per *hprt* copy should be sufficient to make a successful TAP procedure. The clone number 1B of the AID-CTAP clones with 5.62 mRNA copies per hprt copy and clone number 3B of the NTAP-AID clones with 360.13 mRNA copies per hprt copy were selected as representative of close to physiological and overexpression clones for further experiments. AID-CTAP fusion and TAPalone clones generated in ψ^- AID$^{-/-}$ cells (pST10-10B and pSK1-1A, respectively) were also used in the establishment of the approach.

3.1.2. Tandem affinity purification in DT40 cells using the AID-TAP fusions

Whole cell protein extracts were made from $5x10^8$ cells of CTAP- and NTAP-AID expressing clones. The pCAG vector expressing the TAP tag alone in DT40 cells (henceforth referred to as "TAPalone") served as an appropriate negative control. The extract was then subjected to TAP during which the fusion protein underwent two specific affinity purification steps to recover the bait protein along with its interaction partners. The technique will be described in detail in the methods (section: 5.2.7). 1/10th of the input and fractions of each step of the purification were collected for western blot and silver stain analyses. The aliquots of the calmodulin beads (CB) flow through and CB eluate were concentrated by Trichloroacetic acid (TCA) precipitation before performing further analysis.

3.1.2.1. Western blot analysis of the TAP fractions in DT40 cells

The western blot of the TAP was analysed with the anti-AID (5G9) antibody for the purification of the AID-TAP fusions (Figure 11a). The 1^{st}, 2^{nd} and the 3^{rd} lanes were loaded with $1/1600^{th}$ of the original volume of the whole cell protein extract (input), IgG beads supernatant and IgB before TEV cleavage, respectively. These three lanes represent the success of IgG binding of the fusion proteins to the beads. This step was successful with a variation of 50% to 90% binding in different experiments.

The next three lanes were loaded with $1/80^{th}$ of the original volume of the IgG beads before TEV cleavage, IgG beads after TEV cleavage and the TEV eluate to analyse the efficiency of the TEV cleavage step. As expected, after TEV cleavage, the electrophoretic mobility of the AID-CBP protein was detected at a lower molecular weight of about 30kDa. This step was successful with a variability of 60% to 90% between different purification experiments and samples. The final recovery of the TEV-cleaved fusion in the TEV eluate was nearly 95-100%.

The last three lanes represent the final steps of the TAP method, the calmodulin binding and elution steps. These lanes were loaded with $1/40^{th}$ of the original volume of the CB Flow through, CB-E and the calmodulin binding beads after elution. The western blot analysis showed that detectable amounts of the fusion protein were recovered in the final eluate, although a substantial amount of the fusion was lost in the flow through and some of the fusion remained bound to the beads. The amount of protein finally eluted was about 3-5% of the amount contained in the TEV eluate. The range of loss and recovery of the fusion protein in the different steps of the purification was within the known experimental feasibility of the method (Rigaut et al. 1999).

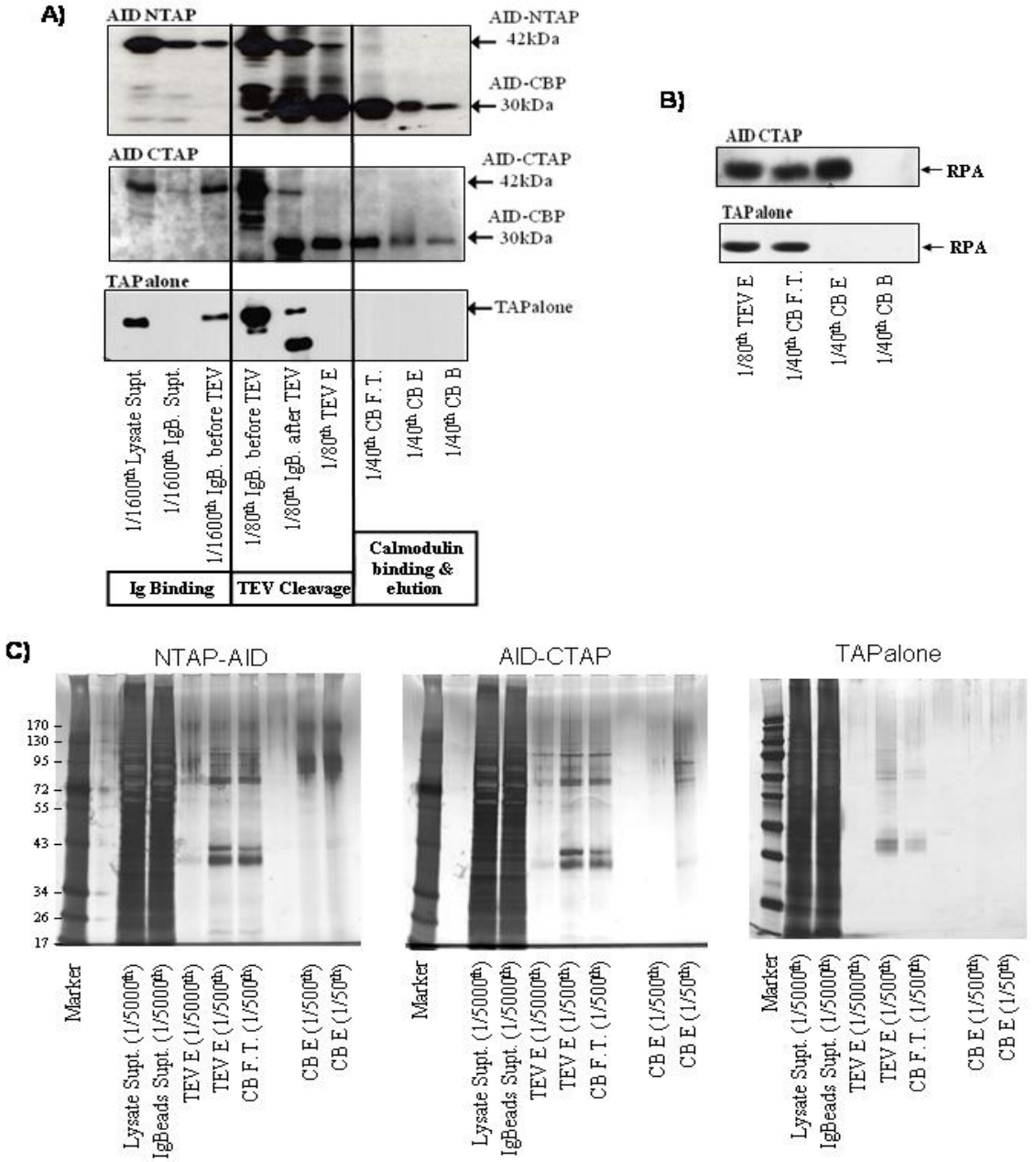

<u>Figure 11</u>: Analysis of tandem affinity purifications of AID-TAP fusions.

A) Western blot analysis of tandem affinity purifications of NTAP-AID (Tf2/3B) and AID-CTAP (pST10-10B) fusions and TAPalone (pSK1-1A). The Ig binding (lanes 1 to 3), the TEV protease cleavage step (lanes 4 to 6) and the calmodulin binding and elution (lanes 7 to 9) are shown. The fusions were detected with anti-AID (5G9) antibody and the TAPalone control was detected with PAP reagent.

B) Copurification of Replication protein A (RPA). The CB-E of the AID-CTAP (Tf5/1-1B) shows copurification of RPA while the TAPalone control lost the RPA in the CB F.T.

C) Silver-stain analysis of the TAP purification for AID-TAP fusions, Tf2/3B, pST10-10B and TAPalone, pSK1-1A. Specific bands for the fusions and protein depletion could be seen. The fraction of the volume of sample at each step that was loaded in the gel is shown in parentheses.

Abbreviations: IgB Supt. – Ig beads Supernatant; IgB before TEV – Ig beads before TEV; IgB after TEV – Ig beads after TEV protease cleavage ; TEV E – TEV protease eluate; CB F.T. – Calmodulin binding flow through; CB E – calmodulin binding eluate; CB B – calmodulin binding beads

The TAPalone control used in the purification was analysed with peroxidase anti-peroxidase (PAP) reagent that detects the protein A moeity of the TAP tag. Since the protein A is cleaved off after the TEV cleavage step, the western blot analysis for the TAP alone could be assessed only for the Ig binding step.

The co-purification of a known AID interaction partner, RPA (Chaudhuri et al. 2004), along with the bait protein in the final step of the TAP purification was verified by western blot analysis. Figure 11B shows the co-purification of RPA in the final eluate of the AID-CTAP fusion, while it was lost in the CB flow through for the TAPalone, indicating the importance of the second step of the TAP purification. It was not possible to verify the same for the NTAP fusion since the mobility of the CBP-AID cleaved from the NTAP fusion was the same as that of RPA on the SDS PAGE.

3.1.2.2. Silver Stain Analysis of the TAP fractions

A silver staining of the different fractions of the TAP purification showed that there was depletion of many nonspecific proteins throughout the purification (Figure 11C). Also, there were some bands that may indicate potential interacting proteins of AID for the AID-TAP fusions and not for the TAPalone (Figure 11C). The final eluate of the TAP purification contained a mixture of proteins enriched for the proteins of the complexes formed by the bait protein. The proteins that were present owing to contamination were expected to be comparable to the background obtained in the TAPalone. The sensitivity of detection by the silver stain for smaller proteins is lower because there are fewer amino acids for the binding of the Ag^{+} ions. Due to this reason, the detection of very low amounts of smaller proteins in the final eluate was borderline or nearly absent.

From the western blot and silver stain analysis, it was concluded that the TAP purification was feasible in the DT40 system with protein amounts expressed corresponding to 5-10 copies of mRNA per *hprt*. The final eluates obtained from the purification were concentrated by TCA precipitation to carry out in-gel tryptic digestion.

3.1.3. Trypsin Digestion and nano-Liquid Chromatography of the final eluates

The final eluates of the TAP purification were trypsinised by an in-gel method. The resulting peptides were eluted out of the gel, lyophilised and finally dissolved in 0.1% Trifluroacetic acid (TFA). Each final eluate of a given sample was split into two fractions at this point and processed further as two separate LC/MALDI experiments. The dissolved peptides of each fraction of a sample were purified and separated by reverse phase nano-LC

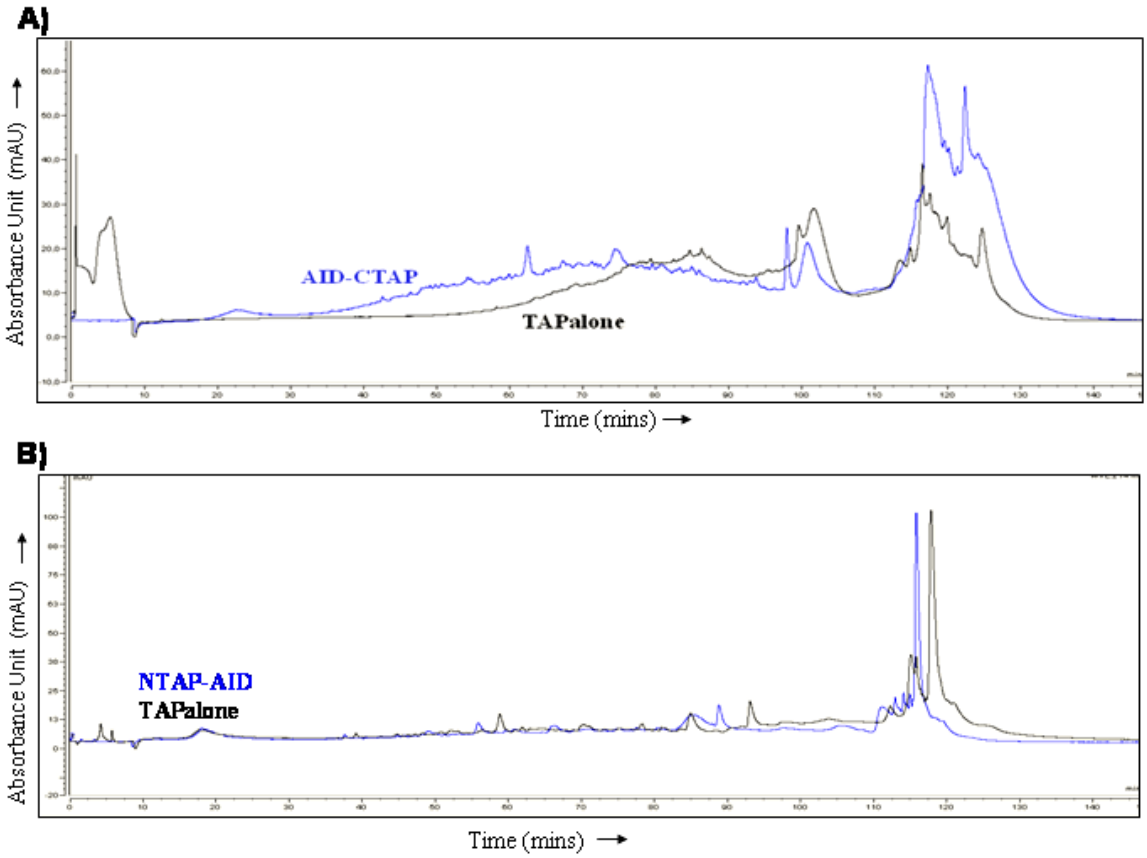

***Figure 12*: The chromatogram of the nano-LC separation of AID-TAP fusion peptides.** *The chromatogram of the peptides of A) AID-CTAP (blue) vs. TAPalone (black) and B) NTAP-AID (blue) vs. TAPalone (black) are shown. The intensity of the peptide peaks are expressed in absorbance units (mAU) and plotted against the retention time (in mins).*
Abbreviations: mAU – milli absorbance units; AID – activation induced cytidine deaminase

based on the hydrophobicity of the peptides. During this separation, the UV detector generated an output in form of peaks representing the quantity and number of different peptides in the sample. Figure 12 shows a liquid chromatography profile of the AID-CTAP and NTAP fusions compared to the TAPalone.

The separated peptides eluting out of the LC unit were loaded on a MALDI target along with the CHCA matrix by the probot microfraction collecter from Dionex. The samples were spotted such that a total of 275 spots were loaded for each sample. The target was then loaded onto the 4700 proteomics analyser from Applied Biosystems for MALDI TOF-TOF analysis, during which each spot was identified by the analyser by its retention time.

The CTAP fusion protein samples had specific peptide peaks that were not present in the TAPalone (Figure 12A) while NTAP fusions of all purifications showed nearly no significant peptide peaks compared to the TAP alone (Figure 12B).

3.1.4. MALDI TOF-TOF analysis of the peptides of the AID fusion eluates

During the MALDI analysis, the peptides were ionised by a LASER beam and were accelerated across the vaccum chamber with varying velocities according to the mass/charge ratio of the peptides. The peptides were identified by a detector that extrapolated the mass of the peptides based on the time of flight (TOF) compared to that of a known standard. The peptides thus identified were more for the AID-CTAP and NTAP fusion samples than for the TAPalone. For instance, in the same experiment of the LC profile shown in Figure 12A, there were 872 and 579 unique peptides identified for the AID-CTAP and TAPalone samples, respectively. The 4700 proteomic analyser is also capable of MS/MS optics that was used to identify these peptides with higher accuracy. During the MS/MS optics, the peptide ions previously identified during the MS optics were selected. These peptides were subjected to high energy collision induced dissociation (CID) by activation of the peptide ions after collisions with a gas. These high energy collisions result in fragmentation of the peptide into smaller fragments of lower masses. These additional fragmentation patterns of the peptides generated a raw MS/MS data of the individual peptides identified by the MS optics.

3.1.5. Generation of an NCBI Gallus database and MASCOT analysis for AID-TAP fusions

The data generated by the MALDI TOF-TOF optics were processed by the MASCOT software. The MASCOT search algorithm is based on the Mowse scoring algorithm that has been described earlier (Pappin et al. 1993) combined with a probability based scoring. This software is able to assign an ion score for each peptide based on the significance and reliability of the match between a peptide and a protein sequence in the database. The ion scores were added together for the identification of a protein which had the best peptide coverage. The total ion scores thus calculated were used to generate a list of proteins arranged in the order of significance that represented the proteins that may be present in the samples analysed.

Many of the chicken proteins are not sufficiently conserved with the other taxonomic groups. In order to assess which protein database served as the most optimal database to analyse the MALDI data, the MASCOT analysis was done with three different databases, namely Swissprot, NCBI (entire), and NCBI Gallus databases.

The NCBI Gallus database was downloaded especially for this study from the NCBI website by the following procedure. All proteins entries with a “Gallus” search tag were displayed in FASTA format in the NCBI website, resulting in 36,215 entries as on the date of creating the database. The sequences were then exported to the clipboard by using the <send

to> function in the webpage and pasted into a text file. The text file with all the sequences was saved and then set up in the MASCOT software search engine as per the instructions given on the Matrix Science company webpage for setting up a database in the MASCOT server (http://www.matrixscience.com/help/seq_db_setup.html). The database is frequently updated for new protein sequence entries and the latest sequences of existing entries.

The original lists for the AID fusions generated with the analyses using all three databases are provided in the Appendix 1. The use of the NCBI *Gallus* database for the MASCOT search analysis yielded the most optimal results, as there were significant scores for AID and the potential interaction partners previously identified in the analysis with the Raji human cell line (Tobollik 2007). The AID fusions generated more significant and unique proteins compared to the TAPalone. The results of the two fractions of a given sample were compiled into a single list of proteins. The TAPalone control also generated a list of proteins that may be considered the background contaminants which were substracted from the AID fusion lists. Table 2 shows a simplified overview of the proteins identified as potential interaction partners of AID, generated using the NCBI Gallus database. The original lists with more details are included in the Appendix 1.

The bait protein AID was identified with a significant score. Although the bait protein is enriched in the fusion samples during TAP, only 1 to 2 peptides were identified for AID with the NCBI Gallus database, while the same data when analysed with the swissprot database could identify 4 to 5 peptides. This may be due to the fact that the AID cDNA in the TAP constructs used was that of the human protein sequence which shares only 89% homology with the chicken AID protein.

The known and previously identified interaction partners of AID were also found in the MALDI analysis of the AID fusions. Tubulin, for instance, is a known interaction partner of AID and implicated as a potential cytoplasmic retention factor in the regulation of nuclear exclusion of AID (Wu et al. 2005). Although tubulin is often considered as a potential contaminating protein in MS analyses, it was found with a significant score for AID fusions with a better sequence coverage than in the TAPalone. For instance in the purification of CTAP-AID (pST10-10B), tubulin was identified with many peptides while in the TAPalone (pSK1-1A) it was found with only 2-3 peptides. In fact, in one purification (TAP3), tubulin was only identified in the fusion sample and not in the TAP alone. The Ubiquitin-protein Ligase EDD1 and Ubiquitin are implicated in the ubiquitin proteosome system and were previously identified in the proteomic analysis for AID interaction partners in Raji, a human B cell line (Tobollik 2007). These proteins were also identified with a significant score in the

AID fusion samples generated from the DT40 cell line. Besides these, there were also many other proteins identified which are categorized as "others" in the table 2. The relevance of these proteins to AID function was not evident and to investigate the functional link of AID with these proteins was beyond the scope of this project. Based on the fact that the bait protein AID and the previously identified proteins of the ubiquitin proteasome system were found in the MALDI analysis with a significant score, it could be concluded that the proteomic approach of TAP combined with MS analysis was successfully established in the DT40 cell line. The approach was then applied to study the Rad18 interaction network in DT40 cells.

Proteins identified with significant score	
TAP Tagged Bait Protein	Activation Induced Cytidine Deaminase
Ubiquitin Proteosome system previously identified in a similar study in the human cell line – Raji (Tobollik 2007)	Ubiquitin-protein Ligase EDD1
	Ubiquitin
Potential cytoplasmic retention factor – known interaction (Wu et al. 2005)	Tubulin
Heat shock proteins	HSP 90 alpha
Others, such as …	Proteasome activator complex subunit 3
	Dedicator of cytokinesis protein 7
	Rho guanine nucleotide exchange factor 3
	ADP/ATP translocase 2
	complement component 4 binding protein, alpha isoform 3
	DnaJ-class molecular chaperone with C-terminal Zinc finger domain
	PREDICTED: similar to pDJA1 chaperone
	Nuclear pore complex protein hnup153
	Downstream of kinase 3 protein
	galectin-3-binding protein-like (Tumor associated antigen 90K)
	PREDICTED: similar to ubiquitin-specific protease USP32
Unknown Proteins	Hypothetical protein – Unknown – gi|118107414
	Unknown (protein for MGC:160383) – gi|120538297
Potential Contaminants	Keratin
	Trypsin
	Calmodulin
	Actin

***Table 2*: A compilation of some of the potential interactions identified for AID-TAP fusions when using the NCBI Gallus database for the MASCOT search analysis.** *The bait, known interaction partners and previously identified potential interactors are mentioned in the appropriate categories. The relevance of the other potential new interaction partners to AID function was not evident and a few of them are listed as "others" in this table selected as examples with no particular criterion for selection. The original lists with all the proteins are given in the appendix 1.*

3.2. Study of the Rad18 interaction network in DT40 cells

Since the TAP method was successfully established in DT40 cells using AID-TAP fusions, it was then adapted for analysing the Rad18 interaction network in the DT40 cell line. The chicken Rad18 protein shares only 48% homology with the human Rad18 and hence the antibodies available for the human protein did not crossreact with the chicken Rad18 protein. Therefore, in order to be able detect the fusion protein on western blots beyond the TEV cleavage step, it was necessary to add a HA tag in the cloning of the Rad18-TAP fusion protein. The pZome vector was used for expressing the fusion in rad18$^{-/-}$ cells, in order to achieve close to physiological expression levels.

3.2.1. Exogenous expression of Rad18-HA-TAP fusions in rad18$^{-/-}$ DT40 cells

The clones obtained by stable transfection of Rad18-HA-TAP constructs were analysed for the mRNA and protein levels of the fusions by qRT-PCR (Figure 13A) and western blot analysis (Figure 13B).

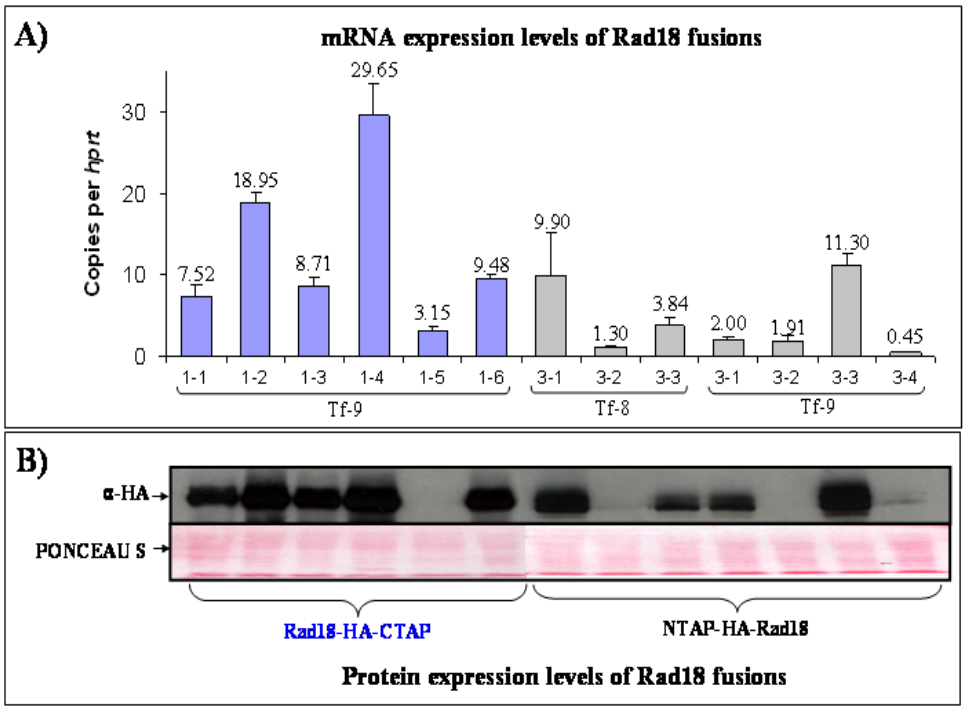

***Figure 13*: Expression levels of Rad18-HA-TAP fusions**
A) qRT-PCR data for Rad18-HA-TAP mRNA expression normalised to hprt expression. The values derived from Rad18-HA-CTAP clones expressed from pZome vector are given in blue and those of the NTAP-HA-Rad18 are shown in grey. Mean and standard deviation derived from two quantifications are indicated.
B) Western blot analysis of Rad18-HA-TAP fusions detected with anti-HA reagent. Ponceau S staining is shown as a control of equal loading.
Abbreviations: hprt – Hypoxanthine phosphoribosyltransferase; HA – Hemagglutinin epitope

As observed earlier for the AID-TAP fusions, most of the clones showed a correlation of their mRNA and protein amounts. Expression ranges between 3.15 and 29.65 mRNA copies per HPRT were obtained for the Rad18-HA-CTAP fusions and between 0.45 and 11.3 mRNA copies per HPRT for the NTAP-HA-Rad18 fusions. The CTAP fusion clone number Tf9/1-1 expressing 7.52 mRNA copies per HPRT and the NTAP fusion clone number Tf9/3-3 expressing 11.3 mRNA copies per HPRT were chosen for further analysis. Since the TAPalone clones obtained in the rad18$^{-/-}$ cells did not express the tag sufficiently for a successful TAP, these clones were not used as a negative control for the TAP method. The TAPalone clone generated in the wildtype DT40 cells, which was used earlier for the establishment of the technique, was used as the negative control for all the experiments except the cisplatin colony survival assay (which will be described in the section 3.2.4). The Rad18-HA-TAP fusions were characterised for functionality, complex formation and nuclear localisation before they were used in TAP.

3.2.2. Native PAGE of Rad18 fusion protein complexes

The Rad18-TAP fusions were assessed for their ability to form complexes with other proteins in the cell as a large tag might affect the interaction of Rad18 with other proteins. The extracts of Rad18 fusion and TAPalone clones were subjected to native PAGE.

Considering the known interaction partners of the complexes mediating TLS and error free bypass (Ulrich and Jentsch 2000), the potential size of such complexes were estimated for Rad18 fusions to be a minimum of 244kDa and 461kDa, respectively. The protein sizes of Rad6 and Rad18 were taken into account for calculating the potential complex for TLS while Rad5, Ubc13, Mms2, SHPRH and HTLF were also included to estimate the size of the complex that mediates error-free template switch bypass. The native PAGE revealed that Rad18 does form specific complexes of the size of about 720kDa or more while in the TAPalone this complex was absent (Figure 14A). The ponceau stain of *NativeMark*™ *Unstained* Protein Standard was used to make a rough estimated of the complex size.

3.2.3. Cellular localization of Rad18 fusion proteins

The Rad18 fusions were then characterised for their cellular localisation. For this, the clones expressing the fusions and the TAPalone were fractionated for their nuclear and cytoplasmic components and analysed by western blot. The quality of separation was assessed by analysing for GAPDH and p53 in the fractions. The GAPDH was not detectable in the nuclear fractions but only in the cytoplasmic fractions, implying that the nuclear fractions were pure. As a control that the nuclear fraction is not completely devoid of proteins, p53

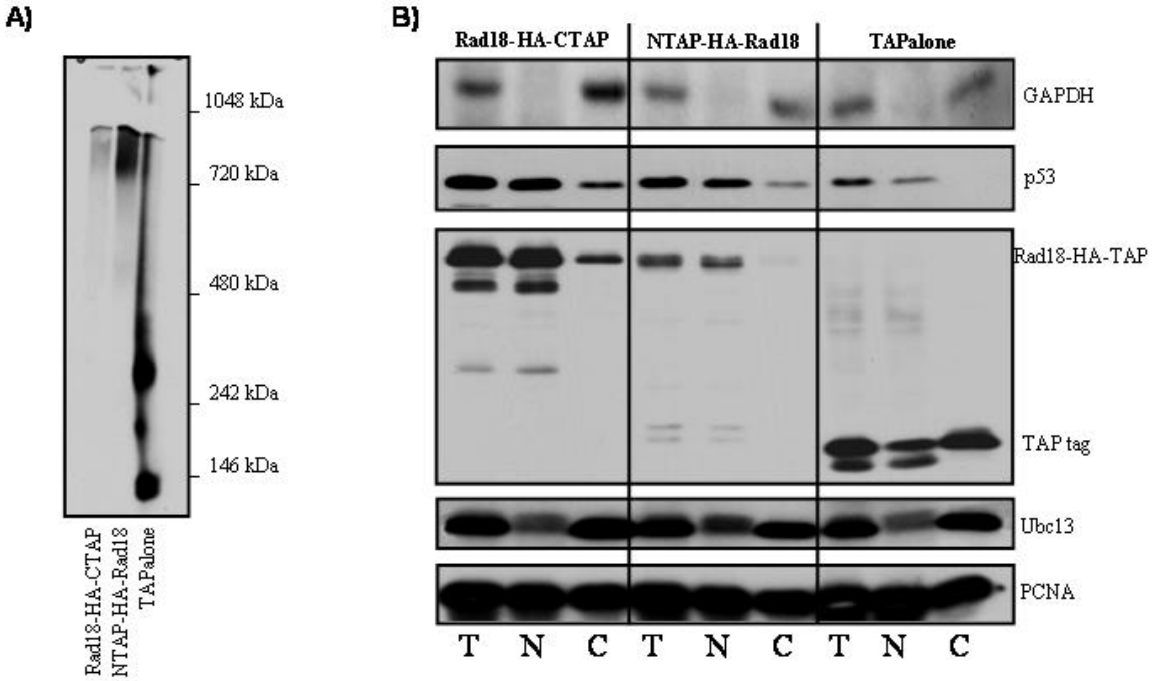

***Figure 14*: A) Native PAGE of Rad18 fusions and TAPalone.** *Native extracts of Rad18-HA-TAP fusions and TAPalone were subject to PAGE and probed with PAP reagent. The* NativeMark™ *Unstained Protein Standard was used in combination with PonceauS stain of the PVDF membrane to estimate the complex size.*
B) Nuclear/cytoplasmic localisation of Rad18-HA-TAP fusions and TAPalone control. *GAPDH and p53 were analysed to assess the quality of separation of nuclear and cytoplasmic fractions. The localisation of the Rad18-HA-TAP fusions and TAPalone was analysed using the PAP reagent and the localisation pattern of known interaction partners, Ubc13 and PCNA were also verified with the appropriate reagents.*
Abbreviations: PAGE – Polyacrylamide gel electrophoresis; PAP – peroxidase antiperoxidase; PVDF - Polyvinylidene difluoride; GAPDH – Glyceraldehyde 3-phosphate dehydrogenase; PCNA – Proliferating cell nuclear antigen; T – Total extract; N – Nuclear fraction; C – cytoplasmic fraction

protein was also detected predominantly in the nucleus. Thus it was concluded that the fractionation was successfully accomplished (Figure 14B).

Subsequently, the localisation of the Rad18 fusions and the TAP tag alone was determined using the PAP reagent. It was observed that majority of the Rad18 fusions was detectable in the nuclear fraction where the known function of the protein is implicated. The TAPalone remained predominantly in the cytoplasm although some amount was also detected in the nuclear fraction. This may be due to passive diffusion since the protein is only 20kDa in size. The cellular localisation of the known Rad18 interaction partners such as Ubc13 and PCNA was also ascertained. Ubc13 was predominantly in the cytoplasm and at detectable levels in the nucleus. PCNA was detected in both the nuclear and cytoplasmic fractions.

3.2.4. Functional Characterization of Rad18-HA-TAP fusions

The rad18$^{-/-}$ DT40 cells are known to be more sensitive to cisplatin than the wildtype cells (Yamashita et al. 2002). Hence the functionality of the fusions was analysed by assessing the survival of the clones upon DNA damage after treating the cells with different doses of cisplatin and plating them on methyl cellulose as described earlier (Simpson and Sale 2006). In brief, 2x10^5 cells of DT40 wild type, rad18$^{-/-}$, Rad18-HA-CTAP clone, NTAP-HA-Rad18, and rad18$^{-/-}$ TAPalone were each treated with increasing doses of cisplatin for 1hour at 37°C. The cells were then plated on methyl cellulose media in 6 well plates and incubated at 37°C for 10 to 14 days. The same numbers of untreated cells were also plated as control. Colonies formed by the surviving cells were counted for all the doses and normalised to the number of colonies formed by untreated cells (0μM). The values were plotted on a graph as shown in the Figure 15.

The results of this experiment were consistent with the known phenotype. The Rad18-HA, –CTAP and –NTAP fusion expression in the rad18$^{-/-}$ cells restored the resistance to cisplatin to a similar level as in the wild type cells, while the TAPalone clone remained almost as sensitive as the rad18$^{-/-}$ cells. The experiments were set up in triplicates for statistical significance and repeated for consistency. The results showed that the Rad18-HA-TAP fusions are as functional as the wild type protein in supporting survival of DNA damage.

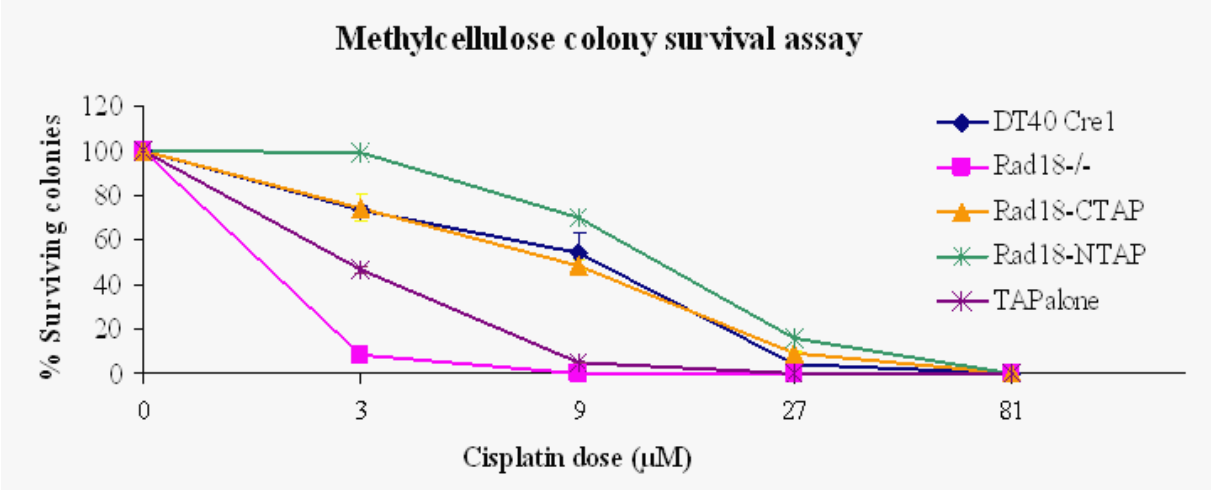

***Figure 15*: Survival curves of the methylcellulose colony survival assay with increasing doses of cisplatin (in μM).** *The rad18-/- and rad18-/-TAPalone cells showed sensitivity to increasing doses of cisplatin while the Rad18-HA-TAP fusions survived similar to the wildtype DT40 cells. The percentage survival at each dose was normalised to the untreated control. The experiment was set up in triplicates and the mean and standard deviation are also represented in the survival curves shown above.*

3.2.5. Isolation of Rad18-HA-TAP fusion complexes by the TAP method

The Rad18 fusions, thus characterized for expression, complex formation, cellular localisation and functionality, were then used to perform a TAP to isolate the complexes formed by the fusion protein. The TAP of Rad18 fusions was done as previously implemented for the AID fusions. The different fractions were collected and the purification was analysed by western blotting and silver stain analysis as previously shown for AID purifications. From the western blot analysis it was observed that the Ig binding was successful with a variability of 20% to 80% in different purifications and samples. The recovery of the TEV eluate and the calmodulin binding were nearly 95 - 100%. The final elution from the calmodulin beads worked with an efficiency of 5% to as much as 20% of the amount contained in the TEV eluate (Figure 16A).

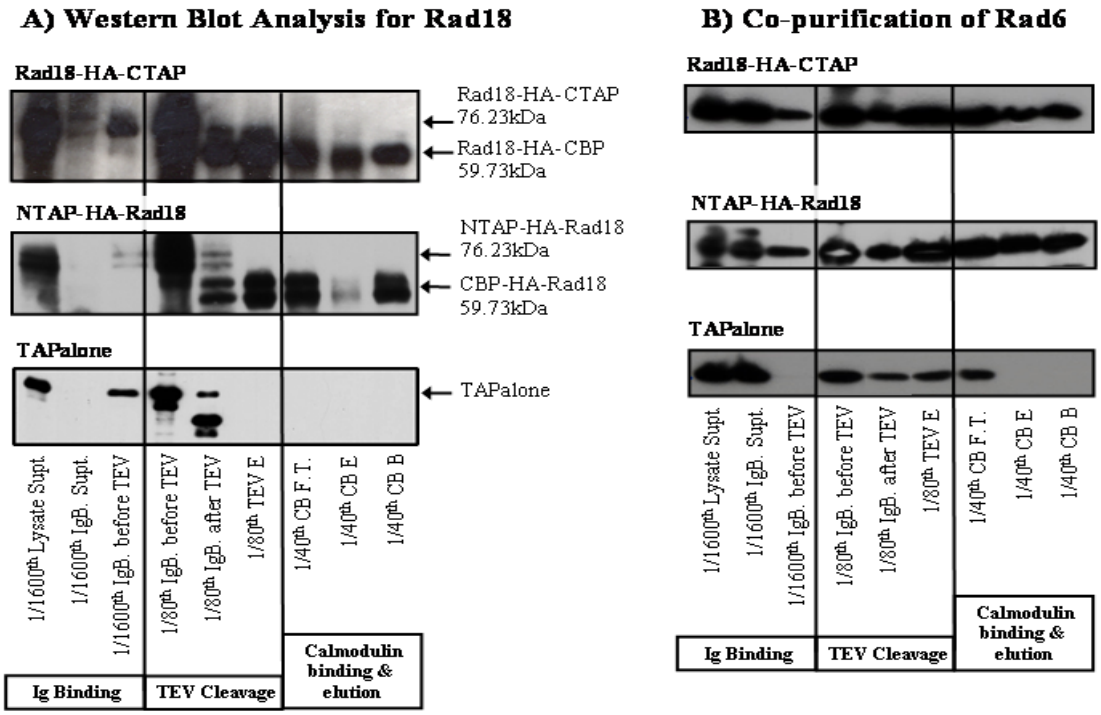

***Figure 16*: Western blot analysis of tandem affinity purification of Rad18-HA-TAP fusions**
A) The success of the TAP method of Rad18-HA-TAP fusions was analysed with anti-HA antibody. PAP reagent that detects the TAP tag was used for the TAP alone control. The fraction of the volume loaded to the total volume of each fraction is indicated. The Ig binding (lanes 1 to 3), the TEV protease cleavage step (lanes 4 to 6) and the calmodulin binding and elution (lanes 7 to 9) were shown to be successful.
B) Co-purification of Rad6. The CB-E of the Rad18 fusions show copurification of Rad6 while the TAPalone control lost the Rad6 in the CB F.T.
Abbreviations: IgB Supt. – Ig beads Supernatant; IgB vor TEV – Ig beads before TEV; IgB after TEV – Ig beads after TEV protease cleavage ; TEV E – TEV protease eluate; CB F.T. – Calmodulin binding flow through; CB E – calmodulin binding eluate; CB B – calmodulin binding beads

The TAP fractions of Rad18 fusions were also analysed for the copurification of a known interaction partner of Rad18. Rad6 is present in the Rad18 complexes involved in TLS as well as in the error-free bypass. Rad6 was co-purified with the Rad18 fusions but was lost in the CB flow through for the TAPalone control (Figure 16B), implying that the complexes were intact throughout the purification steps.

3.2.6. Silver Stain analysis of the Rad18 TAP fractions

A silver staining of the different TAP fractions showed that there was protein depletion throughout the purification. There were some specific bands for the NTAP fusion expressing clones and not for the TAPalone control while the CTAP showed detectable bands only when more protein was loaded. These results indicated that the purification was successful (Figure 17). In the NTAP fusion sample, specific bands displaying a potential complex were detected in two purifications.

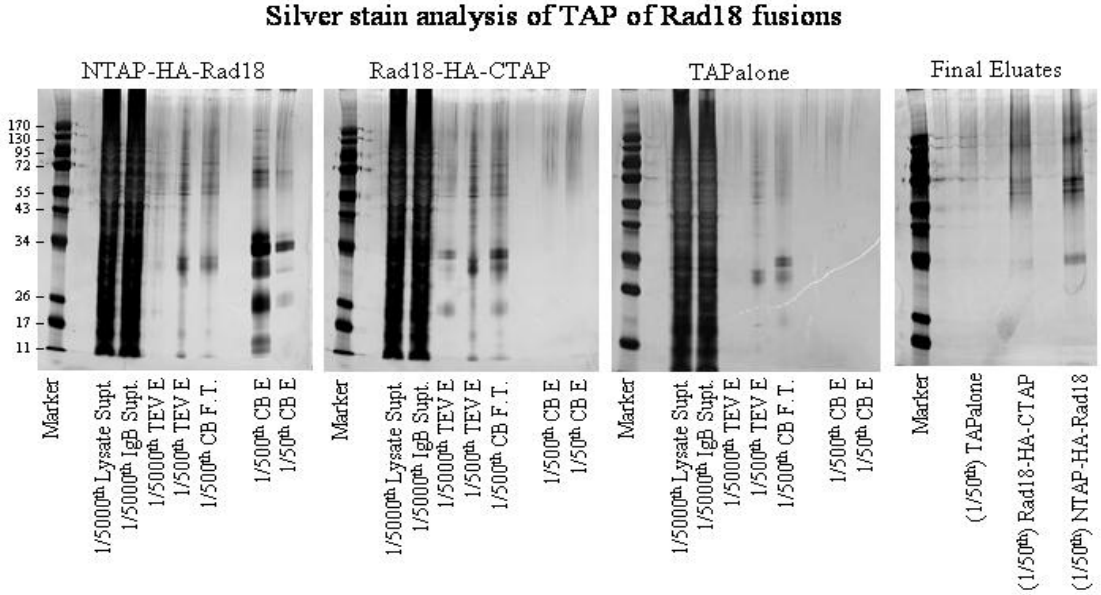

***Figure 17*: Silver stain analysis of TAP method of Rad18-HA-TAP fusions**
Protein depletion throughout the purification and specific bands for the final eluates of the fusions indicate successful TAP for Rad18 fusions. The first three panels show the different steps of the purification for CTAP, NTAP and TAP alone. The volume loaded to the total volume of each fraction is shown in the parentheses. The fourth panel shows the final eluates of the fusions and the TAPalone of the same purification experiment loaded in a separate gel for better staining. The detection of distinct bands in the CB E of the NTAP fusion (first panel) was not improved when it was loaded 10 fold more in the next lane and also not reproducible in the separate gel for loading 10-fold more of the final eluates alone (fourth panel). The reason for this discrepancy is unclear. Abbreviations: IgB Supt. – Ig beads Supernatant; IgB vor TEV – Ig beads before TEV; IgB after TEV – Ig beads after TEV protease cleavage ; TEV E – TEV protease eluate; CB F.T. – Calmodulin binding flow through; CB E – calmodulin binding eluate; CB B – calmodulin binding beads

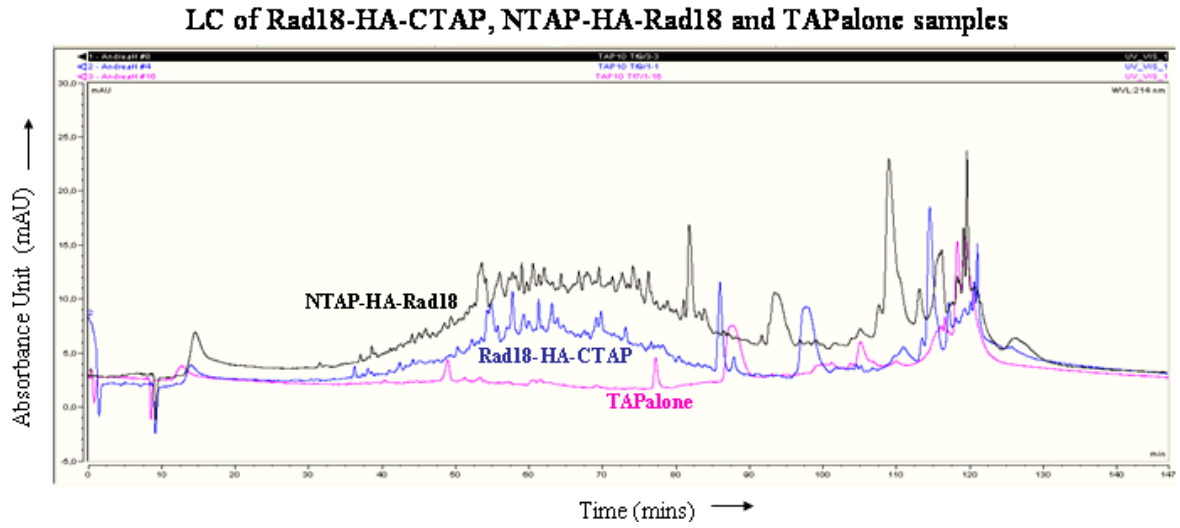

***Figure 18*: The chromatogram of the nano-LC separation of peptides of Rad18-HA-TAP fusions and TAPalone.** *Specific peaks were detected for the fusions compared to the TAPalone. Key: Blue line – Rad18-HA-CTAP; Black line – NTAP-HA-Rad18; Pink line – TAPalone.*

3.2.7. LC-MALDI analysis of Rad18 TAP samples

The final eluates of the TAP were processed as done before for the AID-TAP fusions. The peptides generated by trypsin digest were split into two fractions and each fraction was separately processed further. The peptides in the sample were subjected to reverse phase nano-LC. The nano-LC profile revealed specific peptide peaks for the Rad18 fusions against very low background peaks for the TAPalone (Figure 18). The separated peptides were spotted with the matrix on a MALDI target, which was analysed by the 4700 proteomic analyser. There were many peptides identified for the Rad18 fusions compared to the TAP alone control during MALDI analysis. For instance, in a particular experiment, there were 1408 unique peptides identified in the NTAP-HA-Rad18 fusion sample while in the TAPalone, 1156 peptides were identified. The MALDI data were then analysed by the MASCOT software to identify potential interaction partners of Rad18.

3.2.8. MASCOT analysis for Rad18 fusions

The MASCOT analysis revealed more significant proteins for the Rad18 fusion samples than for the TAPalone control. For instance, in a particular purification, a list of 44 significant proteins was generated for the fusion sample, while the TAPalone samples produced a list of only 18 significant proteins. The 44 unique proteins included the bait protein, Rad18 and known interaction partners, Rad6 and ubiquitin. Table 3 shows a sample list of significant proteins identified for Rad18 fusion in one of the purifications. Although Rad6 was shown to

Rank	Protein Name	Peptide Count	Total Ion Score C.I.%	Best Ion Score C.I.%
1	hypothetical protein [Gallus gallus] Rad18	23	100,0	100,0
2	heat shock cognate 70 [Gallus gallus]	6	100,0	100,0
6	unnamed protein product [Gallus gallus] Tubulin	7	100,0	100,0
7	PREDICTED: similar to glutamine rich protein [Gallus gallus]	5	100,0	100,0
8	nuclear protein matrin 3 [Gallus gallus]	5	100,0	100,0
9	Jun-binding protein	3	100,0	100,0
10	hypothetical protein [Gallus gallus] coatomer protein complex, subunit alpha [Gallus ga	5	100,0	99,7
11	hypothetical protein [Gallus gallus] Calcium/calmodulin-dependent protein kinase type	4	100,0	100,0
12	PREDICTED: similar to beta prime cop [Gallus gallus]	3	100,0	100,0
14	hypothetical protein [Gallus gallus] Stress-70 protein, mitochondrial precursor (75 kDa	2	100,0	100,0
15	PREDICTED: similar to ribosomal protein L18a [Gallus gallus]	3	100,0	99,5
16	hypothetical protein [Gallus gallus] Proteasome activator complex subunit 3 (Proteasome a	3	100,0	100,0
17	ribosomal protein S3A [Gallus gallus]	2	100,0	99,9
18	hypothetical protein [Gallus gallus] heterogeneous nuclear ribonucleoprotein H1 (H) [G	2	100,0	100,0
19	PREDICTED: similar to Heterogeneous nuclear ribonucleoprotein U (scaffold attachment f	2	100,0	100,0
20	60S ribosomal protein L15 (L10)	2	100,0	99,7
21	PREDICTED: similar to DNA strand-exchange protein SEP1 isoform 2 [Gallus gallus]	1	100,0	100,0
23	hypothetical protein [Gallus gallus] phosphofructokinase, platelet [Gallus gallus]	2	100,0	95,7
24	hypothetical protein [Gallus gallus] Enah/Vasp-like [Gallus gallus]	2	100,0	97,3
25	hypothetical protein [Gallus gallus] ribosomal protein L4 [Gallus gallus]	2	100,0	96,4
26	PREDICTED: similar to Rpl17 protein [Gallus gallus]	1	100,0	100,0
28	hypothetical protein [Gallus gallus] Elongation factor 1-alpha 1 (EF-1-alpha-1) (Elongati	2	100,0	94,8
29	hypothetical protein [Gallus gallus] Rho GTPase activating protein 25 [Gallus gallus]	1	99,9	99,9
30	unnamed protein product [Gallus gallus] 60S ribosomal protein L13 (Breast basic conse	1	99,9	99,9
32	PREDICTED: similar to calcineurin A alpha [Gallus gallus]	2	99,8	68,9
33	ribosomal protein S8 [Gallus gallus]	1	99,8	99,8
34	PREDICTED: similar to MGC89673 protein [Gallus gallus]	1	99,7	99,7
35	ribosomal protein L18 [Gallus gallus]	1	99,6	99,6
36	PREDICTED: similar to Leucine-rich repeats and calponin homology (CH) domain containi	1	99,2	99,2
37	60S acidic ribosomal protein P0 (L10E)	1	99,1	99,1
38	hypothetical protein [Gallus gallus] small nuclear ribonucleoprotein D3 polypeptide 18k	1	98,9	98,9
41	kinesin family member C1 [Gallus gallus]	1	97,7	97,7
42	ribosomal protein L14 [Gallus gallus]	1	96,9	96,9
44	PREDICTED: similar to 40S ribosomal protein S2 [Gallus gallus]	1	96,2	96,2
45	retinoblastoma binding protein 4 [Gallus gallus]	1	96,1	96,1
46	PREDICTED: hypothetical protein [Gallus gallus] C9orf10b	1	95,9	95,9
43	PREDICTED: similar to Rpl10a-prov protein [Gallus gallus]	1	95,8	96,8
47	PREDICTED: hypothetical protein [Gallus gallus] RPL15	1	95,4	95,4

***Table 3*: An example of the primary list of the potential interactions identified for NTAP-HA-Rad18 fusions**

copurify with Rad18 in the western blot analysis of the TAP method, it was identified in the MASCOT analysis only with a single peptide and only in the CTAP fusion sample of a single TAP purification. It was identified in other samples sometimes with a non-significant score. New potential interaction partners of Rad18 were also identified with significant scores.

The proteins that were considered for further analysis were those that met more than one of the following criteria of significance. Those that were identified: 1) in more than one sample or purification with a significant score and 2) with a reliable y (when the fragmentation occurs at the C-terminus of the peptide bond) and b (when the fragmentation occurs at the N-terminus) MS/MS fragmentation for a given peptide. A detailed description about the MS and MS/MS optics is given in the part 5.2.12 of the methods section. Table 4 shows a shortened list of potential interaction partners of Rad18 with its known functions, based on these criteria. The original lists of the Rad18 fusions and TAP alone are provided in the Appendix 2.

Several ribosomal proteins were identified as potential Rad18 interaction partners that are multifunctional proteins which have many different functions in the cell besides their role

PROTEIN	No. of significant peptides						Known function
	C (8)	N (8)	T (8)	C (10)	N (10)	T (10)	
Rad18	**16**	**23**	**0**	**20**	**13**	**0**	**Bait**
Rad6	**1**	**1***	**0**	**0**	**0**	**0**	**Known interaction**
Jun binding protein	2	3	0	1	1	0	Ribosomal function Putative tumor supressor
RPS3a/ v-FTE1	0	2	0	3	2	0	Ribosomal function v-Fos Transformation effector
RPL18a	2	3	0	0	0	0	Ribosomal functions Putative Jun regulator
RhoGAP25	0	1	0	1	0	0	Rho regulation
RBBP4 (vertebrates) CAF1 (in yeast)	0	1	0	0	0	0	PI3K/Akt pathway By epistasis analysis, linked to Rad6 pathway in yeast

*** - peptide not significant**

***Table 4*: An overview of the known and interesting potential interaction partners identified for the Rad18-HA-TAP fusions.** *The number of significant peptides and the known function(s) are indicated for each protein. These short listed proteins were considered for further analysis. Abbreviations: C – CTAP fusion sample; N – NTAP fusion sample; T – TAPalone sample; the numbers (8) and (10) indicate the experiment numbers of two different purifications.*

in ribosomes. The ribosomal protein (RP) L10 is known to be a structural and functional homolog of human QM and chicken Jun binding protein or Jun interaction factor (JIF)-1 (Monteclaro and Vogt 1993; Chavez-Rios et al. 2003). The Jun binding protein was often identified with many significant peptides in the MALDI analysis of Rad18 fusions. This protein is considered as a tumor suppressor gene expressed in non-tumorigenic revertants of Wilm's tumor cells (Dowdy et al. 1991; Monteclaro and Vogt 1993). Several studies have revealed that the JIF-1 protein binds to c-Jun, inhibiting the activating protein 1 (AP1) function (Monteclaro and Vogt 1993; Chavez-Rios et al. 2003), thereby regulating the JNK/AP1 pathway.

The RP S3a is yet another ribosomal protein known to play a role in cellular transformation and apoptosis (Naora and Naora 1999). The monoallelic disruption of the rat RPS3a which is identical to the v-Fos transformation effector protein 1 (fte1) gene in v-fos-transformed fibroblasts resulted in the loss of the transformed phenotype (Kho et al. 1996). As an EBNA5 binding protein, fte1/RPS3a is involved in inhibiting growth and differentiation and plays a role in v-fos mediated cellular transformation (Lecomte et al. 1997; Kashuba et al. 2005). Therefore this protein could also be linked to the regulation of JNK/AP1 pathway.

RPS3a also inhibits apoptosis in association with Bcl-2 by inhibiting PARP activity (Song et al. 2002).

RP L18a contains two hydrophobic zipper-like domains that could bind to the Leucine Zipper motif of c-Jun and hence RP L18a is considered as a putative cellular regulator of the Jun protein (Gramatikoff et al. 1995). However this function has not been further characterised.

The Rho GTPase activating protein 25 (RhoGAP25) could be implicated in the regulation of the JNK/AP1 pathway since Rho GTPases are essential for the activation of the JNK pathway upon DNA damage and Rho GAPs inactivate the GTPases by accelerating the intrinsic GTPase activity leading to the GDP-bound form. Rho GAP25 is also known to be downregulated in Burkitt lymphoma cells (Hummel et al. 2006).

The Retinoblastoma binding protein 4 (RBBP4) homolog Chromatin Assembly Factor1 (CAF-1) subunit has been linked to the Rad6 pathway by epistasis analysis in yeast (Game and Kaufman 1999). RBBP4 is also a part of histone deacetylase complex 1 (Nicolas et al. 2000), histone deacetylase complex 3 (Nicolas et al. 2001), and histone deacetylase transferase 1 (Wolffe et al. 2000). Therefore RBBP4 seems to play a role in chromatin assembly, remodelling and modification. Besides, it could also be linked to the regulation of the PI3K/AKT pathway since overexpression of RBBP4 conferred radiation sensitivity on several cancer cell lines via dephospohorylation of Akt (Torres-Roca et al. 2005).

All these protein interactions were found to be interesting for further analysis and experiments for confirmation by co-immunoprecipitation with Rad18 and characterisation of the functionality were then pursued.

3.2.9. Immunoprecipitation attempts for confirmation of some potential Rad18 interaction partners

The co-immunoprecipitation (Co-IP) experiments to confirm interesting potential interactions were attempted for RP L10/ JIF-1 with the exogenously expressed Rad18-HA-CTAP fusion clones, since there was no antibody available for the endogenous chicken Rad18 protein and the antibody that was available for the JIF-1 protein only detected the chicken protein. To avoid interference of the protein A moiety of the TAP tag during the IP, the cell extracts were subjected to TEV cleavage as done for the TAP purification and the TEV eluate was used as the input for the IP with JIF-1 antibody. An isotype matched antibody and lysate without antibody were used as controls. The precipitate was then analysed for co-precipitation of Rad18 using anti-HA antibody (Figure 19A). Rad18 was detected in the immune precipitate with the JIF1 antibody as well as the two controls and the background was not lost

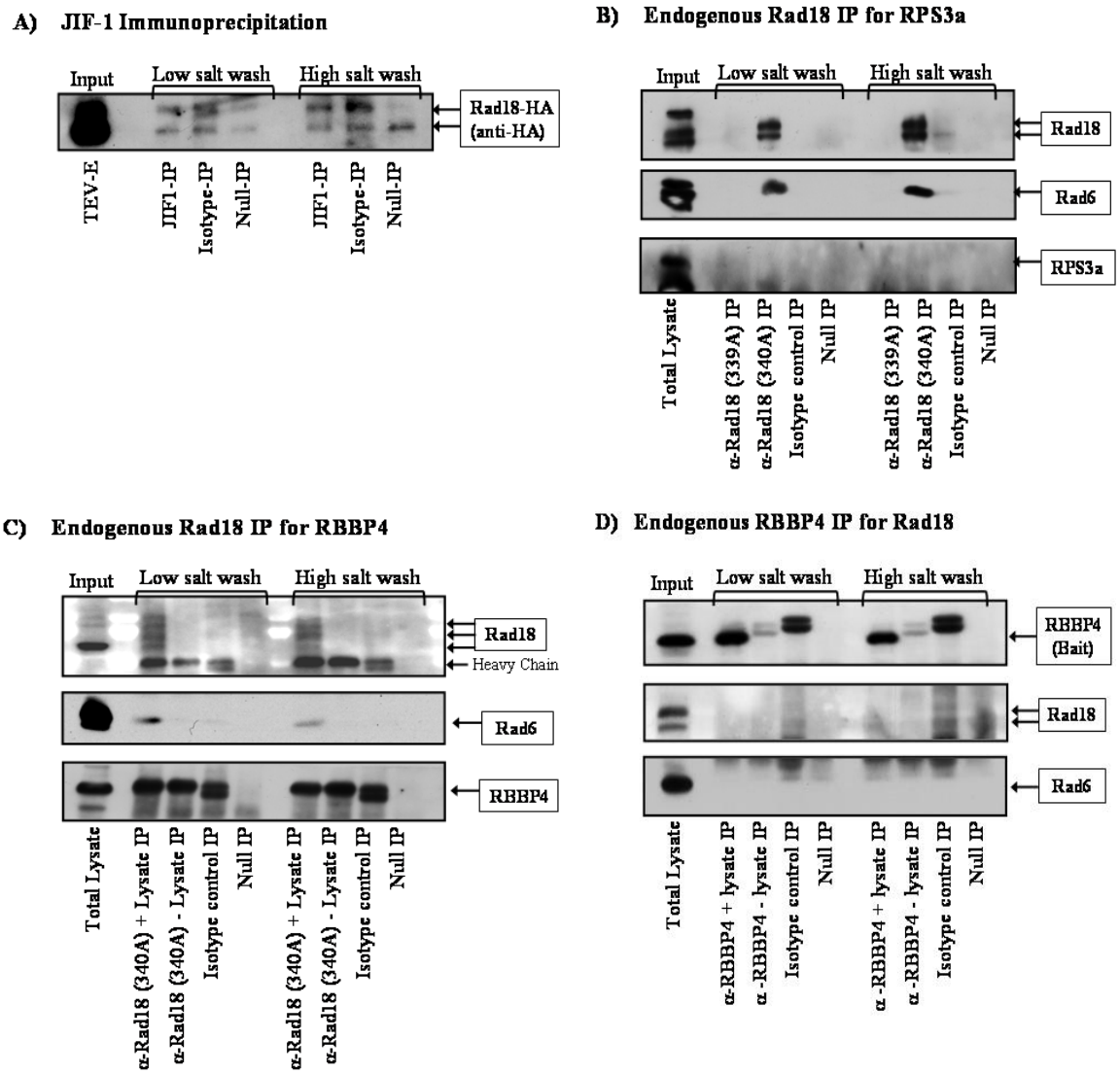

<u>Figure 19</u>: Co-immunoprecipitation experiments for interesting potential Rad18 interaction partners.

A) IP of Jun binding protein or JIF1 in DT40 cells expressing Rad18-HA_TAP fusions. The TAP extracts of Rad18 fusions were subjected to IgG binding and TEV cleavage to get rid of the protein A moiety of the TAP tag that may interfere with the IP. TEV E was used as the IP-input in this case. Immunoprecipitates of JIF-, isotype control and null antibody control were washed either with low-salt or high-salt buffer. Co-immunoprecipitation of Rad18 was analysed with anti-HA antibody.

B) & C) Immunoprecipitation of endogenous Rad18 in the human B cell line Raji, to analyse co-precipitation of (B) RPS3a and (C) RBBP4. The total cell lysate input was incubated with Rad18 antibodies along with appropriate controls as indicated. The Rad18 antibodies 339A and 340A are two antibodies obtained from Bethyl Laboratories, Inc that were raised against different epitopes of the human Rad18 protein. Rad6 was shown to co-precipitate with the Rad18 for the 340A anti-Rad18 antibody. The immunoprecipitates were washed with either low salt or high salt buffers.

D) Immunoprecipitation of endogenous RBBP4 in Raji cells.

Abbreviations: IP – Immunoprecipitaion; TEV – Tobacco etch virus; JIF-1 – Jun interaction factor 1; RBBP4 – Retinoblastoma binding protein 4; RPS3a – Ribosomal protein S3a; TEV E – TEV protease eluate; IP - immunoprecipitate

even with high salt washes. The success of the IP for RPL10/JIF1 could also not be ascertained owing to the background bands from the proteinG beads at the height of RPL10/JIF1. Due to these technical problems, the Rad18-RPL10 interaction could not be confirmed by CoIP.

In the meantime, a new Rad18 antibody with an IP potential became available for the endogenous human Rad18 protein. This reagent was used for CoIP experiments to confirm RPS3a and RBBP4, since antibodies for the human homologs of these proteins were also available. Figure 19B and 19C shows the IP immunoblots for the endogenous Rad18 protein in a human cell line, Raji. The success of the IP was confirmed by probing for Rad6, the known interaction partner of Rad18. The potential interaction of RPS3a with Rad18 was not evident in the IP though (Figure 19B). To confirm the interaction between RBBP4 and Rad18, CoIP was performed once with Rad18 as the bait protein and once with RBBP4 as the bait. The RBBP4 protein was not detectable in the IP with Rad18 antibody due to interference with the heavy chain signal as observed in the antibody without lysate control (Figure 19C). When the IP was performed with the RBBP4 antibody, Rad18 protein was not detectable in the precipitate (Figure 19D). Hence it was not possible to confirm the interaction between Rad18 and RBBP4.

3.2.10. Functional Link of Rad18 to the JNK pathway

The c-Jun N-terminal kinases/stress-activated protein kinases (JNK/SAPK) regulate the phosphorylation of the AP1-like transcription factors, Jun/Fos and Jun/ATF heterodimers that are activated upon genotoxic stress. The JNK/SAPK are members of the MAP Kinase family that regulate cell survival by promoting DNA repair and apoptosis. The dual phosphorylation of SAPK/JNK is known to be activated upon DNA damage induced stalling of replication forks (Fritz and Kaina 2006). Since Rad18 is a key player in the recognition, response and repair of stalled replication forks, it could be hypothesised that Rad18 may have a role in the activation of the JNK/AP1 pathway.

Some of the interesting potential interactions partners identified by the proteomic analysis of Rad18 indicated a potential role of Rad18 in the modulation of the JNK pathway, although the interactions could not be confirmed owing to technical bottlenecks of the DT40 system. Independently, since Rad18 knockout DT40 cell lines were available to test the functional link of Rad18 to the JNK pathway upon DNA damage induced stalling of replication, Rad18 deficient and proficient DT40 cells were used to investigate this functional link.

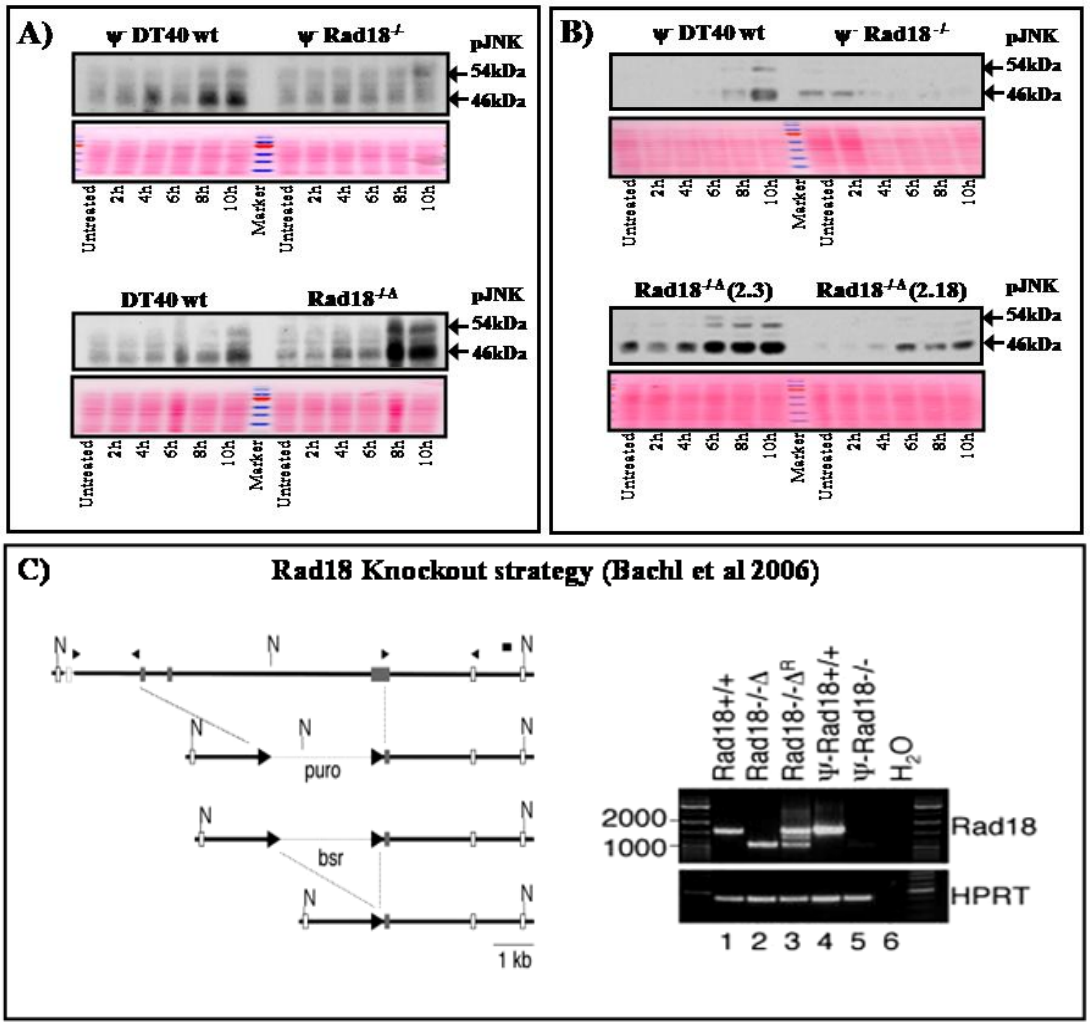

***Figure 20*: MMS induced activation of the JNK pathway upon stalled replication in Rad18 proficient and deficient DT40 cells**

A) The activation of the JNK pathway upon DNA damage in ψ- wild type vs. ψ- Rad18-/- and wild type Cre1 vs Rad18-/-Δ DT40 cells. The cells treated with 1mM MMS for different time points were analysed for the activation of JNK pathway by immunoblotting for pJNK.

B) Activation of the JNK pathway upon DNA damage induced stalled replication in ψ- wild type and ψ- Rad18-/- compared to that of ψ- Rad18-/-Δ single cell clones derived from the ψ- Rad18-/- cells. PonceauS stain is shown as a control for equal loading.

C) Source: Bachl et al. 2006. The difference between the ψ- Rad18-/- and Rad18-/-Δ cells in the Rad18 knockout strategy. The knockout strategy used to generate the Rad18 knockouts (left) and qRT-PCR to analyse the mRNA transcripts of the two Rad18 knockout DT40 cells compared to wildtype (right). The exons 1 to 7 of the Rad18 gene are represented as boxes. The exons 3, 4 and part of exon 5 were replaced by loxP flanked resistance marker cassettes. These exons correspond to 46-209 amino acid residues of the Rad18 protein that code for essential and conserved parts of the RING domain, thereby abolishing the Rad6/Rad18 interaction and hence the PCNA ubiquitination function of Rad18. The qRT-PCR for the complete Rad18 coding region indicates loss of the targeted exons in the knockouts but an in-frame spliced mRNA transcript of smaller size in the Rad18-/-Δ DT40 cells.

Abbreviations: pJNK – phosphorylated JNK1 (54kDa) and JNK2 (46kDa); MMS – methyl methane sulphonate

The ψ$^-$ Rad18$^{-/-}$ DT40 cells were generated from the ψ$^-$ DT40 cells that have their pseudo-V genes deleted (ψ$^-$) (Arakawa et al. 2004; Bachl et al. 2006). The two alleles of the Rad18 were inactivated using LoxP flanked blasticidin and puromycin resistance cassettes that replaced most of the RING domain (Bachl et al. 2006) (Figure 20C).

These cells were treated with 1mM Methyl Methanesulfonate (MMS), a DNA alkylating agent, harvested at different time points and analysed by western blot for phospho-JNK1 (46kDa) and phospho-JNK2 (54kDa) (abbreviated together as "pJNK"). The Rad18$^{-/-}$ cells showed clearly a lack of activation of the pathway when compared to the wild type cells (Figure20A), suggesting that Rad18 is involved in the activation of the JNK pathway upon DNA damage.

In order to further analyse this novel function of Rad18, a Rad18$^{-/-\Delta}$ clone was also tested along with the parental wild type Cre1 DT40 cells for this knockout. These Rad18$^{-/-\Delta}$ cells had been generated by tamoxifen induced removal of the resistance cassettes which resulted in the generation of an in-frame spliced mRNA transcript lacking the RING domain (Bachl et al. 2006) (Figure 20C). Surprisingly, these cells showed an increased activation of the JNK pathway (Figure 20A). From the known functional domains of Rad18 (Notenboom et al. 2007), it could be speculated that despite the lack of the RING domain in the Rad18$^{-/-\Delta}$ protein, the DNA binding domain was still retained. The in-frame spliced mRNA transcript in the Rad18$^{-/-\Delta}$ cells could potentially result in a truncated form of the protein that is able to bind to stalled replication forks but lacks the ability to perform its usual ubiquitination function. This could lead to a block or further delay in the repair of the fork resulting in an increased activation of the JNK pathway from these stalled forks.

In order to test this assumption, in a joint experiment with Samantha Pill, a diploma student in our group, ψ$^-$ Rad18$^{-/-\Delta}$ cell clones generated by tamoxifen induced removal of the resistance cassettes in the ψ$^-$ Rad18$^{-/-}$ cells were used. The ψ$^-$ wildtype, ψ$^-$ Rad18$^{-/-}$ parental and two ψ$^-$ Rad18$^{-/-\Delta}$ single cell clones were treated with 1mM MMS and assayed for the activation of JNK pathway as before. The ψ$^-$ Rad18$^{-/-\Delta}$ cell clones indeed showed an increased activation of the JNK pathway while the ψ$^-$ Rad18$^{-/-}$ parental cell line showed a complete lack of JNK activation compared to the ψ$^-$ wild type cells (Figure 20B).

It thus appeared that a Rad18 protein lacking the RING domain was able to activate the JNK pathway, implying that the RING domain of Rad18 and hence the ubiquitination of PCNA was not required for this activation. This was confirmed by analysing the activation of DNA damage induced JNK pathway in ψ$^-$ parental DT40 cells and a ψ$^-$ PCNA K164R mutant that cannot be ubiquitinated (Figure 21A). The activation of JNK was observed to be almost

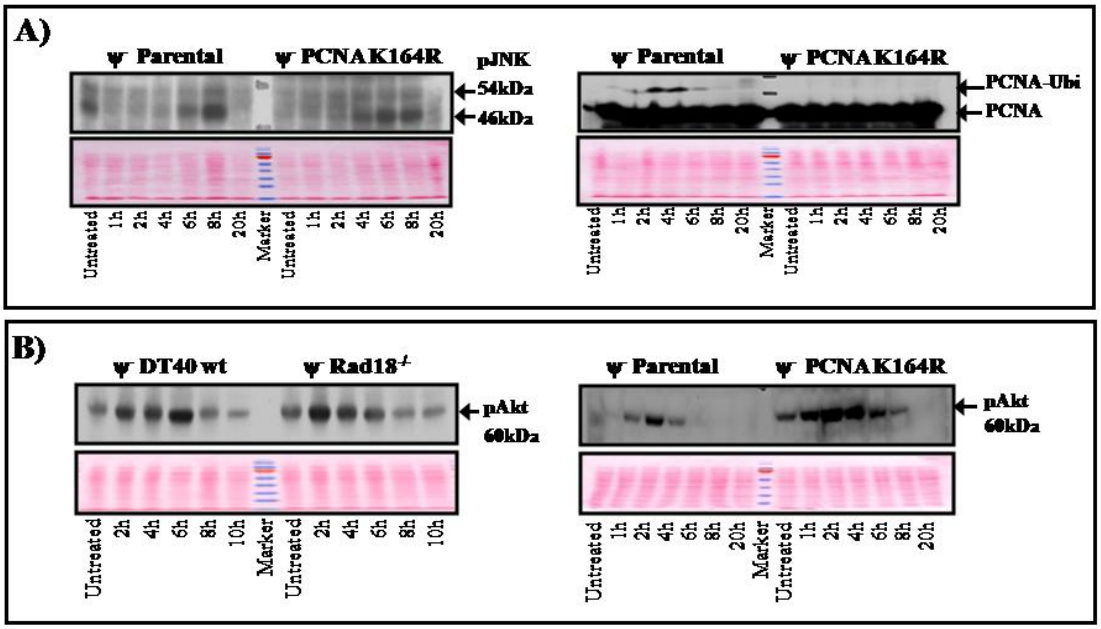

Figure 21:
A) The activation of the JNK pathway upon DNA damage in the ψ- parental and ψ- PCNA K164R mutant DT40 cells*. The monoubiquitination status of PCNA in the wild type and mutant cells is also shown as a control for the assay.*
B) DNA damage induced activation of PI3K/Akt pathway in ψ- wild type vs. ψ- Rad18$^{-/-}$ and the ψ- parental and ψ- PCNA K164R mutant DT40 cells*.*
PonceauS stain is shown as a control for equal loading.
Abbreviations: pAkt – phosphorylated Akt protein; PCNA – proliferating cell nuclear antigen; PCNA-Ubi – monoubiquitinated PCNA

equal in both the cells indicating that PCNA ubiquitination status does not affect this activation. The ubiquitination status of PCNA was also verified by western blot analysis (Figure 21A). These results show that DNA damage induced activation of the JNK pathway by Rad18 is a novel function of Rad18, independent of its PCNA ubiquitination function.

Since one of the potential Rad18 interaction partners identified, RBBP4 was linked to the regulation of the PI3K/Akt pathway via dephosphorylation of Akt, the potential role of Rad18 in this function was also tested. In order to verify this, the western blot analysis of MMS treated ψ- wild type vs. ψ- Rad18$^{-/-}$ and ψ- parental vs. PCNA K164R mutant was also probed for phosphorylated Akt (pAkt) (Figure 21B). It was observed that the presence or absence of Rad18 did not affect the activation of the Akt pathway and hence did not influence the role of RBBP4 in the dephosphorylation of Akt. This indicated that the phenotype observed for the activation of the JNK pathway was indeed biologically significant rather than being an incidental cell type specific difference. These results proved that Rad18 was required for DNA damage induced JNK activation that is not dependent on the RING domain and hence the ubiquitination function of the protein.

4. Discussion

The study of protein interaction networks is vital to acquire a comprehensive understanding of cellular processes. Most of these processes are executed by multiprotein complexes. The identification and characterisation of the components of these complexes would provide a better understanding of the organisation of the proteome into functional entities. Rad18, the protein studied in this project, is a key mediator of the Rad6 pathway. It plays a role in SHM (Bachl et al. 2006) and is also involved in mediating DNA damage responses via the ubiquitination of the 9-1-1 checkpoint clamp (Fu et al. 2008). The recognition of forked and single-stranded DNA structures by Rad18 triggers its recruitment to the stalled replication forks (Tsuji et al. 2008) via direct interaction with RPA (Davies et al. 2008). Consequently, it is becoming increasingly clear that Rad18 is a central player in many different pathways linked to DNA damage recognition, response and repair especially at the stalled replication fork. The study of the Rad18 interaction network was undertaken to understand more vividly the molecular interplay of different pathways modulated by Rad18.

This requires the isolation of native protein complexes to near homogeneity. Affinity chromatography is one of the most popular approaches to isolate protein complexes. In 1999, B. Seraphin and his research group developed a method for the purification of native protein complexes from yeast, the TAP method which is based on a combination of a high affinity purification step with a subsequent lower affinity purification step (Rigaut et al. 1999). The first step removes most of the nonspecific proteins in the extract, and allows a crude isolation of the fusion protein with its associated interaction partners. The removal of any remaining contaminating proteins from this first eluate requires a second purification step. It was found that even very small quantities of native complexes could be isolated with high yield using this method in the yeast system (Rigaut et al. 1999).

The introduction of the TAP method substantially improved the purification and systematic genome-wide characterisation of protein complexes in yeast (Rigaut et al. 1999; Puig et al. 2001; Gavin et al. 2002). This approach was adapted to higher eukaryotic cells often with modifications to implement a more effective method that was comparable to the yeast system. The iTAP strategy, for instance, comprises the conventional TAP approach combined with suppression of the corresponding endogenous protein by RNA interference in Drosophila melanogaster Schneider cells (Forler et al. 2003) or in mammalian cells (Bertwistle et al. 2004). In human cells, the TAP method has been applied for instance in HEK293, an embryonic kidney cancer cell line (Bouwmeester et al. 2004), and in the Raji, human B cell line (Tobollik 2007).

However, the TAP method has not been used in a vertebrate system that could offer the specific advantages of the yeast system. The DT40 chicken B cell line presents the possibility to knockout the endogenous protein owing to its high genetic stability and easy manipulation of the genome. The knockout of the endogenous gene followed by the expression of the TAP tagged fusion protein allows the assessment of the functionality of the fusion and avoids competition for interaction partners with the endogenous protein. Moreover the DT40 B cell line also constitutes a well established system for the study of gene conversion and SHM. Consequently, we decided to combine the advantages of the TAP method with DT40 to establish a system which parallels many advantages of the TAP combination with yeast.

The TAP method followed by mass spectrometric analysis is a valuable approach that provides an outline of the network of protein complexes thereby presenting a more fundamental perspective on the molecular communication of biological processes. This approach was established using AID-TAP constructs and applied to study the Rad18 interaction network in the DT40 chicken B-cell line. For this the GOI was tagged to the TAP tag. There are two alternatives to express the TAP tagged fusion protein, namely from the endogenous loci that could be modified to express the TAP tagged fusion protein or from exogenous expression vectors stably transfected into the cells. Ideally, endogenous expression of the TAP fusion is expected to achieve expression levels similar to the endogenous protein. However, modifying the endogenous loci may also result in the disruption of the promoter and regulatory elements in the 5'-region of the gene that controls its expression in case of the N-terminal modification. This may even lead to loss of expression of the gene. Alternatively, since exogenous expression vectors carrying AID-CTAP and NTAP-AID fusions were already available to test the approach, the latter alternative was opted for this study. The pCAG and pZome expression vectors that were tested differ by the type of promoter driving the expression of the fusions.

The AID-TAP fusions were expressed in the $AID^{-/-}$ DT40 cell line. The expression attainable by these vectors was measured at the mRNA and protein levels by qRT-PCR and western blotting, respectively. The protein amounts bear the final influence on the success of the purification, and owing to differences in the transcriptional and translational regulation, mRNA amounts need not necessarily correlate with the protein levels. However, the protein A moiety of the TAP tag can bind any antibody probed in the western blot analysis and generate very strong signals. Due to this reason, the signal of the fusion protein probed with the AID antibody for AID fusions or the HA antibody for the Rad18 fusion protein cannot be compared to the signal of the endogenous protein. Hence the comparison of the exogenous

fusion expression to the endogenous expression of the GOI was made only in the context of the mRNA amounts.

The qRT-PCR results indicated that the pCAG served as an overexpression system that could be used if needed, while the pZome vector provided expression at or close to physiological levels. Previous TAP purifications in vertebrate systems have often involved mild to moderate overexpression of the fusion protein (Bertwistle et al. 2004; Bouwmeester et al. 2004). The purifications performed with AID-TAP fusions in the human Raji cell line in an earlier study was successful with 6-fold overexpression of the AID-CTAP fusion and 30-fold overexpression of the NTAP-AID fusion compared to the endogenous AID in the context of mRNA levels (Tobollik 2007). The AID-TAP fusion protein expression in the DT40 cell line was compared to the protein amount that was used to perform a successful TAP in the Raji human cell line. From this comparison, it was deduced that a protein amount corresponding to 5-10 mRNA copies per *hprt* copy in the DT40 cell line was sufficient to make a successful TAP purification in the chicken B cells.

The Rad18-HA-CTAP and NTAP-HA-Rad18 fusions were expressed from the pZome expression vector in rad18$^{-/-}$ DT40 cells, since we could obtain clones expressing close to physiological to mild overexpression of the fusion protein using this vector. Comparing the relative band intensities of the fusions detected in the western blot to the relative mRNA copies determined by qRT-PCR, it was observed that there was a correlation between the mRNA and protein expression levels for both the AID-TAP clones as well as the Rad18-HA-TAP clones. Moreover the differences in the exogenous expression levels of the fusion protein in the various clones offered the possibility to choose the clone with an appropriate expression level required for optimal proteomic analysis. A clone with a mild overexpression at nearly 10 fold mRNA copies was used in this study. A higher overexpression of the fusion protein from the pCAG vector may also be employed in the future to achieve higher signal to noise ratio in the MALDI analysis. However, one has to be cautious in interpreting the interactions identified from an overexpression system, since this may attract non-specific interactions. This necessitates the confirmation of the interactions identified by an independent assay (Bertwistle et al. 2004).

The ability of the fusion protein to form complexes is crucial for studying the protein interaction networks. Therefore, the Rad18 fusion complexes were analysed by native PAGE and it was observed that the fusions do form complexes of more than 720kDa in size. The lack of an antibody for chicken Rad18 protein at this time limited the comparison of this complex to the endogenous context in the wild type and rad18$^{-/-}$ cells. When an antibody that cross reacts with the chicken Rad18 protein would be found, it could be used to characterise

the Rad18 complexes in a physiological context in future. A native PAGE is a rough estimation of the complexes and gel filtration or sucrose gradient ultracentrifugation methods might provide an even better alternative to estimate the exact complex size. The native PAGE technique may instead be used to monitor complex integrity during TAP purification or to assess complex changes upon induction of DNA damage in the cells.

Cellular localisation has a direct bearing on the functionality of the protein and its interaction partners. Therefore, it was interesting to study the localisation of the Rad18 fusions. The localisation of the endogenous Rad18 protein is known to be affected by the ubiquitination status of the protein (Miyase et al. 2005). The non-ubiquitinated Rad18 is predominantly detected in the nucleus while the monoubiquitinated form is specifically localized in the cytoplasm. In fact, it has been speculated that monoubiquitination serves to export the protein from the nucleus to the cytoplasm. The polyubiquitinated forms of Rad18 have been shown to trigger the degradation of the protein by the proteosome *in vitro* (Miyase et al. 2005). In this study, the Rad18-HA-TAP fusion proteins were found in both the nuclear and cytoplasmic fractions. It is interesting to note that a specific band of lower molecular weight was also detected but only in the nuclear fraction, which may correspond to the non-ubiquitinated species of the fusion in the nucleus.

The nuclear fraction of the TAPalone negative control also showed the presence of the TAP tag protein. This might indicate passive diffusion of the protein owing to its small size of 20kDa or may be due to slight contamination of the cytoplasmic fraction during the separation. The PAP reagent used to detect the TAP tag and the fusions is known to generate a strong signal and hence even mild contamination could be detected with a strong signal. The cellular localisation pattern of some of the known interaction partners of Rad18, namely Rad6 (Koken et al. 1996; Lyakhovich and Shekhar 2003), UBC13 (Ulrich and Jentsch 2000; Hoege et al. 2002) and PCNA (Szuts et al. 2005) was also found to be consistent with earlier findings.

Finally, an important aspect to be considered before performing a TAP was to ascertain that the fusion protein was able to reconstitute the function of the knocked-out endogenous protein. The TAP tag being large (≈ 20kDa) could influence the folding of the protein and/or the availability of the active site(s) of the protein to perform certain functions. The functionality of the fusion protein is assessed in terms of the known functions of the protein. The type of fusion, whether C-terminal or N-terminal could also influence the functionality of the protein, as seen for AID-TAP constructs earlier (Tobollik 2007). The AID-CTAP fusion was functional and the NTAP-AID fusion was non-functional for SHM, as assessed by the rate of SHM using a GFP reporter assay in human and DT40 cells (Tobollik 2007).

The Rad18 functionality was analysed by assaying the cell survival upon DNA damage (Tateishi et al. 2000; Yamashita et al. 2002). Analysis of the reconstitution of the PCNA ubiquitination function (Hoege et al. 2002) or of the influence on the rate of SHM (Bachl et al. 2006) were the other alternatives to assess the functionality of Rad18 fusions. However it is known that a certain degree of background PCNA ubiquitination does occur in Rad18 knockout cells (Szuts et al. 2006; Zhang et al. 2008). Also, SHM is a process achieved by complementary paths (Rada et al. 2004), some of which do not involve Rad18 and although the knockout of Rad18 showed a reduced frequency of SHM, it is not entirely abolished (Bachl et al. 2006). Therefore determining the sensitivity of the fusions to cisplatin compared to the wild type and rad18$^{-/-}$ cells was selected as the best alternative to assess the functionality of the Rad18 fusions.

The methylcellulose colony survival assay showed that both the Rad18-HA-CTAP and NTAP-HA-Rad18 fusions were able to reconstitute the sensitivity of the rad18$^{-/-}$ cells to cisplatin induced DNA damage. In fact the slight overexpression of the NTAP fusion appeared to render the cell survival even higher than that of the wild type, while the survival of the CTAP fusion resembled that of the wild type cells. This small difference might be due to the influence of the TAP tag on protein folding and the distance of the tag to the positions of the known functional domains of Rad18 (Notenboom et al. 2007). Despite this small difference, both the fusions were evaluated to be functional and the TAP tag did not seem to interfere with all interactions of the protein.

The TAP fused proteins thus characterised for expression, cellular localisation, complex formation and functionality were then subjected to TAP. The TAP technique was optimised earlier in the human Raji cell line by Stephanie Tobollik in the lab such that the protocol could be used for different cell types (Tobollik 2007). The technique was carried out in the DT40 cells as performed by S. Tobollik in the Raji cell line, except that the number of DT40 cells used for protein extraction was doubled since the DT40 cells are much smaller than the Raji cells. The short doubling time of DT40 cells was convenient for making this increase practically feasible.

The Western blot analysis showed that the AID-TAP fusions were successfully recovered in the purification process and RPA – a known interaction partner of AID (Chaudhuri et al. 2004) – was also co-purified. The binding of the Protein A moiety to the IgG beads was successful with a variation of 50% to 90% binding in independent experiments and different fusions within an experiment. There was a 60% to 90% variation in the efficiency of the TEV cleavage step but the elution of the cleaved protein was nearly 95 to 100%. The calmodulin binding and elution was the least efficient step, since much of the protein was lost

in the flow through or remained bound to the beads during elution and the final recovery was only 3 to 5% of the input. In the western blot analysis of the TAP fractions, degradation products of the fusions were sometimes observed. It is not known whether this might be due to the conditions of the purification itself, especially at the TEV protease cleavage step, or due to an overnight Ig binding step. Despite this mild degradation, it was possible to recover the full length protein in the final elution step of the TAP purification.

Similarly, Rad18 fusions were also successfully purified and Rad6, a known interaction partner of Rad18, was copurified. The recovery throughout the purification was much more efficient for the Rad18 fusions than for the AID fusions. The Ig binding varied within the range of 70 to 90% and the TEV cleavage step was always around 90% efficient. The final calmodulin binding and elution recovery was also substantially better for Rad18 fusions than for the AID fusions. The calmodulin binding was nearly 40 to 50% while about 30% or more of the TEV eluate was lost in the calmodulin flow through. The final eluate recovered was nearly 10 to 25% for the CTAP fusion and only 3-5% for the NTAP fusion.

It is possible that the long overnight Ig binding step might have an impact on complex integrity. But the co-purification of the known interaction partners, RPA with the AID fusion and Rad6 with the Rad18 fusion, showed that the complexes are at least partly intact. This could be verified by performing native PAGE of the different fractions of the purification. There are several possibilities to optimise the TAP technique in DT40 cells. The calmodulin elution might be improved for better recovery of the fusion protein by investigating the recovery with increasing salt or EGTA concentrations in the elution buffer. There are also possibilities to use other types of TAP tags which might be even more efficient in recovering the bait protein. For instance, a modified TAP tag in which the Protein A moiety was replaced by STREP tag to avoid the TEV cleavage step (Gloeckner et al. 2007) might be an alternative to test.

The recovered final eluate of the TAP purification was concentrated by TCA precipitation before further processing. Complex mixtures of proteins are usually processed by in-solution trypsin digest, which is more efficient in digestion of the proteins and recovery of peptides than the in-gel trypsin digestion. However, due to technical problems with chloroform-methonol precipitation, this method could not be implemented for the final TAP eluates. Instead, the final eluate containing a mixture of different proteins was run on SDS-PAGE gel for about 1cm and cut out to perform an in-gel tryptic digest. Although it is possible to analyse the final eluate by a longer SDS-PAGE, followed by visualisation of proteins using coomassie or deep purple® staining methods in order to cut out individual bands for in-gel trypsin digest, this approach was not implemented. This is because this

approach largely depends on the sensitivity of the staining methods used and the amount of protein recovered by the TAP method, both of which were variable between different experiments.

Despite the less efficient in-gel trypsin digest, the nano-LC detector showed specific peptide peaks for the fusion proteins compared to a lower background in the TAPalone control. The peaks for the Rad18 samples were even more distinct than for the AID samples. In many of these nano-LC profiles, however, high peaks appeared after the gradient separation which may indicate the presence of unresolved peptides or inefficiently digested proteins. The resolution of the peptide peaks for the samples during the gradient separation might be improved and the unresolved/undigested peaks may be avoided by adopting in-solution tryptic digest.

The separated peptides were subjected to MALDI TOF-TOF analysis in the 4700 proteomic analyser from Applied Biosystems. The LASER induced ionisation of the peptides is followed by the flight of the peptide in an electric field across a vaccum chamber. The mass of the peptide is calibrated according to the TOF properties of the peptides ionised. The peptides thus identified from each retention spot on the MALDI target were selected in a subsequent MS-MS optics analysis in order to identify the peptide sequence with higher accuracy using the MASCOT analysis software. There were more peptide precursors for MS/MS analysis for the fusions than for the TAPalone. The analysis of the AID samples by MASCOT yielded potential interaction partners previously identified in human cells. The bait protein was also identified with a significant score for the AID fusions. There were also other proteins identified for AID but without an obvious relevance to AID function. Although RPA was shown to co-purify with the fusion by western blot analysis, it was not identified in the MALDI analysis. The reason for this may be that the ionisation of the peptides upon LASER stimulation was not optimal to detect the protein by the LC-MALDI approach. This reason could be validated by performing a different MS approach such as the Orbitrap which is an electrostatic ion trap with an electrospray ionization source (ESI) technique. Since the bait – AID and previously identified interactions were found with significant scores by the LC-MALDI approach, it was concluded that the TAP method followed by LC-MALDI analysis was successfully adapted to the DT40 cell line to investigate the protein interaction networks of any protein of interest.

An improved trypsin digest and recovery of peptides or overexpression may be opted to obtain a higher signal to noise ratio. Besides these sample processing improvements, the sensitivity of the MALDI is also a factor in obtaining optimal protein lists. A MALDI analyser with higher sensitivity or an entirely different MS approach such as the Electro spray

ionisation method may also be used to obtain a better or different list of proteins, since different and/or more peptides may be ionised. A recent study comparing nanoLC –MALDI MS/MS and nanoLC-ESI-MS/MS techniques, showed that coupling nanoLC with both ESI and MALDI ionisation interfaces improved coverage, reduced suppression of ionization and improved quantitation, particularly in complex samples (Yang et al. 2007). The first eluate of the TAP may also be analysed to obtain a better identification of the interacting proteins that may be less abundant in the complex. However, it must be distinguished that there may be a chance of some specific interaction partners of the bait being identified in the negative control if the first purification eluate was used, since RPA or Rad6 was lost only in the second purification step in the TAPalone control.

It was also observed that the NCBI Gallus database generated better protein lists than Swissprot and entire NCBI databases. This was probably because the swissprot database is a curated database that is optimal for the AID TAP samples analysed in a human cell line (Tobollik 2007), but was not well updated for chicken protein sequences. On the other hand, the entire NCBI database was very huge containing more ambiguous sequences. In this case, the moderately conserved chicken proteins could likely not be identified by homology with other taxonomic groups. The NCBI database nevertheless did contain sequences of the chicken proteins that were constantly updated, so when the MASCOT analysis was performed with a manually downloaded database from NCBI for sequences restricted to those of Gallus gallus, the result of the analysis improved significantly. The only drawback of this approach was the fact that many chicken protein entries were initially made as hypothetical proteins and these would still interfere with the identification of the name of the protein. For instance, even the bait protein Rad18 was identified as “hypothetical protein” with very many peptides, and identified as Rad18 only upon blasting the sequence of the hypothetical protein. However, this is expected to be a temporary problem of the database and analysing the same experimental MALDI data again in the future could generate more and more refined protein lists.

In summary, the approach is feasible and valuable in the DT40 system. The advantages of the combination of the DT40 system with the TAP method and proteomic analysis may be considered comparable to the yeast system in which the TAP method was originally established. This combination can be used as a tool to understand complex biological networks in vertebrates. Such an extensive elucidation of TNFα/NF-κB signalling has been achieved using the TAP method in human HEK 293-cells (Bouwmeester et al. 2004) and easy genetic manipulation might allow similar extensive studies on cellular processes in the DT40 system. The current bottleneck of the approach in using DT40 cells is the limited availability of antibodies for chicken proteins. A curated chicken database comparable to the swissprot

database, devoid of ambiguities and hypothetical proteins might offer an additional advantage. But these bottlenecks are only temporary, and this approach may be applied for the analysis of other factors involved in somatic hypermutation and components of the Rad6 pathway, leading to an understanding of the cellular networks that may link these two processes in the B cell.

The MALDI analysis of Rad18 yielded the bait protein with the most significant score. The known interaction partners Rad6 and Ubc13 were also identified although only once with a single peptide. The Rad18 fusion samples also yielded interesting new potential interactions with many interesting functions, some of them also being multifunctional proteins. The relative number of unique proteins identified for the fusions and the TAPalone indicated that as many as 47 and 36 new potential interaction partners were identified for the Rad18-HA-CTAP fusion and NTAP-HA-Rad18 fusions respectively, after substracting the background proteins identified in the TAPalone. These substracted lists consisted of unique proteins many of which were multifunctional ribosomal proteins, RNA binding and splicing proteins and DNA binding proteins. There were also a few uncharacterised protein entries of unknown function.

The proteins that met more than one of the following criteria of significance were considered for further analysis: 1) those that were identified in more than one sample or purification with a significant score and 2) with a reliable MS/MS fragmentation for a given peptide. The reason for this was because there was very low chance that a false positive interaction could be identified more than once in different purifications and different types of fusions. Further, the MS/MS fragmentation gives the reliability of the peptide(s) with which the protein was identified. Therefore, the better the identification of the fragmentation pattern, the higher the accuracy of the sequence of the peptide identified. However, one must keep in mind that common contaminants such as keratin, trypsin, actin and tubulin also meet these criteria and hence the results of the MALDI analysis only generates a list of potential interaction partners that would have to be confirmed by functional analysis.

Some of the multifunctional proteins that were identified as potential Rad18 interaction partners were previously linked to the regulation of the JNK/AP1 pathway which is known to play a role in the cellular decision between apoptosis and survival during genotoxic and cytotoxic stress. These proteins, the Jun binding protein (alias JIF1 or RPL10), the ribosomal proteins S3a and L18a and RhoGAP25, were identified in independent TAP eluates and Rad18 C- and N- terminal TAP fusions. The ribosomal proteins are conventionally known for their function in translation (Roger A. Garrett 2000), but some of these proteins have been known to perform extraribosomal functions.

The ribosomal protein (RP) L10, a structural and functional homolog of human QM and chicken Jun binding protein or Jun interaction factor (JIF-1), is known to regulate the c-Jun protein although it does not resemble previously identified Jun regulators (Monteclaro and Vogt 1993; Chavez-Rios et al. 2003). The Jun binding protein is known to be a Wilm's tumor suppressor that may be involved in inhibiting Jun induced transformation (Dowdy et al. 1991; Monteclaro and Vogt 1993) and is also known as an inhibitor of the c-Jun protein in its activating protein 1 (AP1) function (Monteclaro and Vogt 1993; Chavez-Rios et al. 2003).

The RPS3a or FTE1 has been implicated in cellular transformation and apoptosis (Naora and Naora 1999), since the disruption of this gene in v-fos-transformed fibroblasts resulted in the loss of the transformed phenotype (Kho et al. 1996). It is an EBNA5 binding protein which is involved in inhibiting growth and differentiation or apoptosis regulating functions (Lecomte et al. 1997; Kashuba et al. 2005). It as also known that Bcl-2 in association with RPS3a is able to inhibit Poly (ADP-ribose) polymerase activity and in the absence of RPS3a, Bcl-2 failed to inhibit PARP activity. These results suggest that RPS3a may be involved as an inhibitor of apoptosis (Song et al. 2002). It has been found that RPS3a is involved in drug sensitivity only when cytotoxicity includes DNA damage (Hu et al. 2000).

The RPL18a is a putative Jun regulator (Gramatikoff et al. 1995) since it was shown to be able to bind to the leucine zipper motif of c-Jun. However there has been no further study published on this function.

Another interesting potential interaction partner identified was the RhoGAP25, that has been found to be downregulated in Burkitt lymphoma cells (Hummel et al. 2006), but there are no other functional characterisation of this protein. RhoGTPase family genes are cancer associated genes since genetic alterations in these genes lead to carcinogenesis through the dysregulation of Rho/Rac/Cdc42 – like GTPases. The Rho-GTPases are also essential for the activation of the JNK pathway upon DNA damage (Fritz and Kaina 2006). Rho GTPase activating proteins (Rho GAPs) inactivate the GTPases by catalysing the intrinsic GTPase activity to its GDP-bound form. Therefore in may be speculated that Rho GAP25 may also be involved in the regulation of the JNK pathway in this manner.

Besides these proteins, the RBBP4 was also identified as potential interactor of Rad18 with significant scores. The RBBP4 seems to be implicated in chromatin assembly, remodelling and modification. It is a homolog of the yeast Chromatin Assembly Factor1 (CAF-1) subunit C which has been linked to the Rad6 pathway by epistasis analysis (Game and Kaufman 1999). In Saccharomyces cerevisiae, CAC1, CAC2 and CAC3 are the three subunits of CAF-1, the deletion of any of which reduces the telomeric gene silencing and confers an increase in UV sensitivity. In this study, cac1 deletion in Rad18 and Rad6 mutants

did not increase the UV sensitivity of these cells, indicating an epistatic relation between the two genes. RBBP4 is also a part of the histone deacetylase complex 1 (Nicolas et al. 2000), complex 3 (Nicolas et al. 2001), and the histone deacetylase transferase 1 (Wolffe et al. 2000). Therefore the RBBP4 and Rad18 interaction could be involved in the influence of chromosome structure and modification. The overexpression of RBBP4 was concurrent with the dephosphorylation of Akt, suggesting that this function of RBBP4 may be mediated by antagonising the Ras pathway (Torres-Roca et al. 2005). The RBBP4 overexpression conferred radiation sensitivity on several cancer cell lines through the dephosphorylation of Akt protein. Therefore RBBP4 could also be linked to the regulation of PI3K/AKT pathway (Torres-Roca et al. 2005).

Thus the most significant potential interaction partners of Rad18 indicated a potential role of Rad18 in the modulation of the JNK/AP1 pathway, PI3K/Akt pathway and PARP inhibition. Since antibodies for chicken proteins are limiting but the strength of DT40 genetics was foreseeable, the functional analysis of the link between Rad18 and the JNK/AP1 pathway and the PI3K pathway were carried out in parallel to the co-immunoprecipitation experiments to confirm the interactions.

A number of immunoprecipitation (IP) approaches were carried out to confirm these interactions. Owing to lack of an antibody for chicken Rad18 protein, an IP of JIF-1 was attempted in the Rad18 fusion expressing clones after the extracts were subjected to TEV cleavage and elution. The Rad18 TEV-cleaved fusion was detectable in the precipitate, but also in the isotype and null antibody controls. Hence it was problematic to confirm the Rad18-JIF1 interaction in DT40 cell line by an IP method. The success of the IP was also not ascertained since the protein G and light chain interfered with the detection of JIF1.

Since an antibody with an IP potential for the human Rad18 protein has recently become available, a successful IP was established in the Raji human cell line with this reagent, which was verified by co-precipitation of Rad6. Antibodies for human RPS3a and RBBP4 were also available and where probed to verify their interaction with Rad18. It was observed that the RPS3a was not detectable in the precipitate and it was difficult to detect RBBP4 due to interference of signal from the heavy chain. The use of Trueblot® secondary antibodies also did not overcome the problems of heavy and light chains. The IP with RBBP4 antibody also did not co-precipitate Rad18, but the success of this IP could not be controlled to derive conclusions.

While a positive co-IP is a definite a proof of interaction, a negative co-IP does not necessarily imply that the interaction is not true. Further, the interaction may be specific for chicken and not for human. Lack of antibody for chicken proteins could hence be termed as a

"DT40 problem" and might be solved by tagging the proteins of interest to epitopes such as FLAG, MYC, etc. Such exogenous IP methods might be considered as a general solution to this problem. In order to perform such IPs for exogenous proteins, Rad18-HA fusions constructs in the pZome vector have already been generated (vide, methods). Other types of confirmation for the interactions may also be attempted, such as yeast two-hybrid assays, bimolecular fluorescence complementation, co-immune fluorescence, etc. For organisms that offer powerful genetic analysis methods such as the DT40 cell line, phenotypic analyses could also be used to confirm the functional significance of protein interactions.

Since many proteins identified by the MALDI analysis of Rad18-TAP eluates were implicated in the regulation of the JNK/AP1 pathway, a potential functional link of Rad18 to this pathway was analysed.

Exposure to genotoxic stress leads to cellular responses that affect cell survival via the stimulation of expression of various genes. This transcriptional activation is mediated by phosphorylation induced activation of pre-existing transcription factors such as c-Jun, c-Fos, ATF2, SRF-TCF, CREB and NFκB. The knockout of even one of these transcription factors impairs cell survival upon DNA damage. The SAPK and JNK regulates the phosphorylation of the AP1-like transcription factors and are both phosphorylated upon DNA damage induced stalling of replication forks (Fritz and Kaina 2006).

Since the activation of the JNK/AP1 pathway by DNA damage induced stalling of replication forks is already known (Fritz and Kaina 2006), it was imperative to perform independent functional assays to test whether this process also involved Rad18. For this, ψ^- wild type and ψ^- Rad18$^{-/-}$ DT40 cells were treated with 1mM MMS and immunoblotted for phospho-JNK (pJNK). The JNK proteins are phosphorylated by Mitogen activated protein kinase kinases (MAP2Ks) that activates the JNK proteins triggering the downstream signalling cascade of the JNK pathway. Hence pJNK was assessed as the measure of the activation of the JNK pathway. The results indicated that there was barely any detectable activation of the JNK pathway in the ψ^- Rad18$^{-/-}$ DT40 cells, while the wild type showed an activation of the pathway. However, when the Rad18 knockout in Cre1 DT40 cells, the Rad18$^{-/-\Delta}$ was tested, the activation of the pathway was substantially increased when compared to the wild type control. The differences between the two Rad18 knockouts is that the ψ^- Rad18$^{-/-}$ cells have the knockout resistance cassettes in the Rad18 loci and the resistance cassettes have been removed in the Rad18$^{-/-\Delta}$ giving rise to an in-frame spliced mRNA lacking the RING domain (Bachl et al. 2006) but retaining the SAP domain responsible for the binding of Rad18 to the DNA (Notenboom et al. 2007). This implies that the Rad18 function of the RING domain and hence the ubiquitination function is not required

for the JNK activation. This was indeed found to be true when the ψ^- PCNA K164R mutant and its parental ψ^- cells were tested in a similar fashion. The results showed that the activation of the JNK pathway was similar in these cells, both being proficient for Rad18 and the PCNA mutant being incapable of ubiquitination.

These results were further confirmed in a combined experiment with a diploma student by performing the assay in two independent single-cell ψ^- Rad18$^{-/-\Delta}$ clones generated de novo from the ψ^- Rad18$^{-/-}$ cells. It could be seen that the results were consistent with the newly generated ψ^- Rad18$^{-/-\Delta}$ cells as well. Thus there is substantial evidence of a novel Rad18 function in the activation of DNA damage induced JNK activation not involving the RING domain or PCNA ubiquitination.

Since RBBP4 plays a role in the dephosphorylation of Akt, the effect of Rad18 on the DNA damage associated activation of the PI3K/Akt pathway was also investigated in Rad18 proficient and deficient DT40 cell lines. It was found that DNA damage induced phosphorylation of Akt was not affected by the presence of absence of Rad18. However, this assay may serve as a biological verification that the effects measured by the JNK activation assay were indeed due to a biological impact of Rad18 on the JNK pathway and not due to clonal differences between the Rad18$^{-/-}$ and Rad18$^{-/-\Delta}$ cell types.

The activation of the JNK pathway upon DNA damage had been known for quite some time (Bode and Dong 2003; Dent et al. 2003) and the activation of the JNK pathway by DNA damage induced stalling of replication forks was thought to be mediated by DNA-dependent protein kinase catalytic subunit (DNA-PKcs) and Cockayne syndrome protein CSB (Fritz and Kaina 2006). In the present study, a novel role of Rad18 in MMS induced activation of the JNK pathway was identified, although it is still not known whether this function is mediated by Rad18 directly or via potential interaction partner(s).

One might think that the activation of JNK pathway during transcription coupled repair is mediated by CSB, during double strand break repair via DNA-PKcs and the activation of JNK pathway during repair of stalled replication could then be mediated via Rad18. However, this would not explain why the inactivation of *either* of these components would lead to a defect in JNK activation upon MMS treatment, which results in DNA lesions that mostly activate the BER and Rad6 pathways. This leads to a new question: Is DNA-PKcs and/or CSB epistatic with Rad18? It would therefore be interesting to answer this question by testing the effect of multiple knockouts of these three genes, individually and in combination, on the activation of the JNK pathway upon DNA damage. The DT40 Cre1 system offers the possibility to embark on such an approach.

Alternatively, the activation of JNK pathway upon DNA damage by Rad18 may be a specific feature of the DT40 cell type or may be specific for *Gallus gallus* species. In order to ascertain this, one may also investigate the role of Rad18 in the activation of JNK pathway upon DNA damage in other cell lines and/or other species.

Future perspectives

Reconstitution of Rad18 in the $Rad18^{-/-}$ cells is expected to prove the novel function of Rad18 in the activation of JNK pathway from the stalled replication forks and experiments are already ongoing to meet this requirement. Since the Rad18 protein is already well characterised for its various functional domains (Notenboom et al. 2007), another future perspective would be to map the domain of the Rad18 protein that is involved in this novel function by mutational analysis.

The activation of the JNK pathway might be mediated by increasing the kinase activity or reducing the phosphatase activity. Hence the ability of Rad18 to enhance upstream kinases and/or inhibit upstream phosphatases of the JNK pathway could be investigated to understand the mechanism of activation of the JNK pathway by Rad18. It would also be important to study the biological effect(s) of the JNK activation to know the impact of this novel function of Rad18 on cell survival and apoptosis, since the downstream targets of JNK/AP1 pathway affect both (Shaulian and Karin 2002). The role of Rad18 on other pathways such as the NFκB pathway, other MAPK signalling pathways, and cell cycle checkpoint signalling, Ig gene diversification, etc could also be investigated as the recent findings indicate the involvement of Rad18 in some of these signalling pathways or processes besides its classical role in the Rad6 pathway (Bachl et al. 2006; Bi et al. 2006; Szuts et al. 2006; Dávid Szüts 2008; Davies et al. 2008; Fu et al. 2008).

An improved TAP procedure in combination with a more sensitive MS analysis would also be pursued and the new potential interactions identified would be confirmed by optimising the IP protocol for endogenous human Rad18 protein and also by IP using the exogenous HA tagged Rad18 and Myc tagged potential interaction partners in DT40 cells. The Rad18 fusions may also be overexpressed and analysed by more sensitive mass spectrometric approaches to identify new potential interactions that may substantiate the novel link to the JNK pathway and also may provide interaction information linking Rad18 to other DNA damage repair and response pathways or cell cycle control. Mutagenic analysis may be followed to map the domains of Rad18 protein to other novel functions or interactions that may be thus identified.

5. Materials

5.1. Chemicals and reagents

All Chemicals and materials used were purchased from the following companies:

Applied Biosystems (Foster City, USA), BD Biosciences (Heidelberg), Biochrom (Berlin), BioRad (Munich), Bruker Daltonik (Bremen), Costar (Bodenheim), Dianova (Hamburg), Eppendorf (Hamburg), Fluka (Taufkirchen-Munich), GE Healthcare Europe (previously Amersham Biosciences, Freiburg), Greiner (Frickenhausen, Nuertlingen), Integra Biosciences (Fernwald), Invitrogen (Karlsruhe), Kodak (Rochester, USA), Labor Schubert & Weiß GmbH (Munich), Laborteam K+K (Munich), MBI-Fermentas (St. Leon-Rot), Merck (Darmstadt), Millipore (Bedford, USA), MP Biomedicals (Eschwege), NEB (Schwalbach), neolab (Heidelberg), Nunc (Wiesbaden), PAA (Pasching, Austria), Perbio Science (Bonn), Promega (Mannheim), Qiagen (Hilden), Roche Applied Science (Mannheim), Roth (Karlsruhe), Sigma-Aldrich (Taufkirchen-Munich), Stratagene (Amsterdam, Netherlands).

5.2. Equipments

Biological incubator shakers	New Brunswick Scientific
Electrophoretic apparatus	BioRad
Eppendorf table centrifuge	Eppendorf
Developer Machine X-OMAT	Kodak
Electroporation equipment Gene Pulser II	BioRad
Cell culture CO_2 Incubator	Heraeus Christ Instruments
PCR cycler	Biometra
Light Cycler	Roche
Photometer	Eppendorf
Laminar sterile hood	Haereus Christ Instruments
Centrifuges	Eppendorf; Sorvall; Beckman; Hettich
Spectrophotometer	Eppendorf

5.3. Kits

All kits were used according to manufacturer's instructions.

GFX Micro Plasmid Prep Kit (Amersham Biosciences, Freiburg)

Jet Star 2.0 Plasmid Purification Kit (Genomed, Löhne)

QIAgen Gel Extraction Kit (Qiagen, Hilden)

QIAgen PCR Purification Kit (Qiagen, Hilden)

RNeasy Kit (Qiagen, Hilden)

1st Strand cDNA Synthesis Kit (Roche Applied Science, Mannheim)

FastStart DNA Master SYBR Green I Kit (Roche Applied Science, Mannheim)

DC Protein Assay (BioRad, Munich)

ECL Kit (Amersham Biosciences, Freiburg)

5.4. Bacteria

The Escherichia coli strain, DH5α was used for cloning.

Genotype: F-, φdlacZ Δ M15, endA1, recA1, hsdR17 (rk-, mk-), supE44, thi-1, gyrA96, relA1, Δ(lacZYA-argF)U169, λ-

5.5. Enzymes

Table 5: List of Enzymes used

Enzymes and buffers	Supplier
T4-DNA-Ligase and 10x ligase buffer	Roche Applied Science
Restriction enzymes & (10x) reaction buffers	MBI-Fermentas, New England Biolabs and Roche Applied Science.
Taq-Polymerase and buffer	Roche Applied Science and Qiagen
TurboPfu-Polymerase	Stratagene
acTEV Protease	Invitrogen
Trypsin Gold	Promega

5.6. Antibodies

Table 6: List of primary antibodies

Primary reagents	Dilution	Host	Reactivity	Source
AID 5G9	1:5	Rat	Hu, Ch	E.Kremmer, Helmholtz Zentrum
HA 3F10	1:100	Rat	epitope	E.Kremmer, Helmholtz Zentrum
RPA RBF 4E4	1:5	Rat	Hu, Ch	E.Kremmer, Helmholtz Zentrum
GAPDH	1:5000	Mouse	Hu, Ch	Abcam
Tubulin	1:1000	Rabbit	Hu, Ch	Abcam
PCNA	1:10000	Mouse	Hu, Ch	Abcam
Ubiquitin	1:2000	Mouse	Hu, Ch	Santa Cruz
p53	1:500	mouse	Hu, Ch	Santa Cruz
Rad6	1:5000	Rabbit	Hu, Ch	Bethyl Laboratories
Ubc13	1:1000	Mouse	Hu, Ch	Abcam
JIF-1 (QM)	1:500	Rabbit	Ch	Santa Cruz
RPS3a	1:1000	Mouse	Hu, Ch	Abnova
RBBP4	1:1000	Mouse	Hu, Ch	Abcam
Rad18 Rad18	1:1000	Mouse Rabbit	Hu Hu	Abcam Bethyl laboratories; used for IPs
pJNK	1:1000	Rabbit	Hu, Ch	Abcam
pAkt	1:1000	Rabbit	Hu, Ch	Cell signalling
PAP	1:2000	Rabbit	–	Sigma; for detection of TAP tag

Hu – Human; Ch – Chicken

Table 7: List of secondary antibodies

Secondary reagents	Dilution	Host	Antigen	Source
anti-mouse-HRP	1:5000	goat	Mouse	Promega
anti-rat-HRP	1:5000	goat	Rat	Jackson Immuno Research
anti-rabbit-HRP	1:3000	goat	Rabbit	Cell Signalling

5.7. Oligonucleotides

Table 8: Primers for qRT-PCR

Primer Name	**Nucleotide sequence (5´→ 3´)**
SGS-Rad18-SFor1	GAT GTA GCT AAC CGT TGT CTT C
SGS-Rad18-SFor2	GGT CTG GCA GGA ACA GAT TGG
SGS-Rad18-SFor5	CTG CCA TAG GAT TGC CAG CAG G
SGS-Rad18-SRev1	CTG CTG AGA CAG CTG TCC AG
SGS-Rad18-SRev4	GGC AAA GAC GCA GGA GTC TTG G
SGS-Rad18-SRev5	CTC TTC ACT AGC TCA TCT AAC GTC
SGS-Rad18-SRev6	GTA TCC AAG ACC AAC TGG ACC AG
SGS-NTAP-SFor1	GCT AAA TGA TGC TCA GGC GCC G
C-TAP1	GTA TCG GCA GAG TCG TCG GTT G
SGS-AID-SFor1	GGG AAG TAC AGA GCA TTC CAC G
SGS-AID-SRev1	GAG GTG AAC CAT GTG ATG CGG
SGS-HPRT-SFor1	TAT TGT TGG AAC TGG AAG GAC AAT G
SGS-HPRT-SRev1	ACT CAC TGC TGT ATA TAT TCA TCA G

Table 9: Oligonucleotides used for cloning the Rad18-HA-TAP fusions

Primer Name	**Nucleotide Sequence (5´→ 3´)**	**Enzyme**
SGS-Rad18-For3	GGG ACTAGT GAATTC GGG TCG CC **ATG** GCC CTG G	SpeI, EcoRI
SGS-Rad18-Rev2	CCC GGATCC *TGCATAGTCCGGGACGTCATAGGGATA* C GCGGCCGC GCT CTT CTT CCT CTT GCT CCT G	BamHI, NotI
SGS-Rad18-For4	GGG CCAGCACAGTGG GG *TATCCCTATGACGTCCCGGACTATGCA* **ATG** GCC CTG GCG CTG CCC G	BstXI
SGS-Rad18-Rev3	CCC GTC GAC CCT ACA CCC AGT GGC TCT GC	SalI

SGS-Rad18-For3 and SGS-Rad18-Rev2 was used for CTAP cloning
SGS-Rad18-For4 and SGS-Rad18-Rev3 was used for NTAP cloning
Underlined – restriction sequence used for the cloning of the PCR fragment into the pZome expression vector; *Italicised* – HA tag sequence; **Bold** – Start codon

Table 10: Oligonucleotides used for cloning the Rad18-HA construct

Oligo Name	**Nucleotide Sequence (5´→ 3´)**	**Enzyme**
SG-Ct-Oligo1	GATCC **TAG** GGGCCC G	ApaI
SG-Ct-Oligo2	TCGAC GGGCCC **CTA** G	ApaI

Oligo1 and Oligo2 – complementary strand sequences that generate BamHI (5') and SalI (3') restriction overhangs upon annealing.
Underlined – Apa1 Restriction site for testing insertion after cloning; **Bold** – Stop codon

5.8. Plasmids

The plasmids pZome-1C carrying the C-terminal TAP tag and pZome-1N carrying the N-terminal TAP tag were obtained from the company Cellzome, Heidelberg, Germany. The NTAP-AID construct in pCAG (pST 8-2), the AID-CTAP construct in pZome (pST 7-2) and pCAG (pST10-10) vectors were available from Stephanie Tobollik, Helmholtz Zentrum Muenchen (Tobollik 2007).

5.9. Cell lines

Table 11: Source and particulars of the cell lines used

Cell line	**Source**	**Remarks**
Chicken B-cell line – DT40		
Cre1	H. Arakawa, Neuherberg	The "wild type" DT40 cells
Rad18$^{-/-\Delta}$	B. Jungnickel, Grosshadern	Rad18 knockouts in Cre1 wt cells in which the resistance cassettes were removed by tamoxifen induced Cre recombinase
Ψ^{-} OR Ψ^{-} AID$^{-/-®}$	H. Arakawa, Neuherberg	Pseudo-V gene knockout => Ig gene conversion defective; endogenous AID knockout and exogenous AID-GFP expression (puromycin resistant)
Ψ^{-} AID$^{-/-}$	B. Jungnickel, Grosshadern	The loxP flanked AID expression cassette was removed by Tamoxifen induced Cre recombinase by Christina Glon
Ψ^{-} Rad18$^{-/-}$	B. Jungnickel, Grosshadern	Rad18 knockout, Puromycin + Blasticidin resistance cassettes present
Ψ^{-} Parental	H. Arakawa, Neuherberg	A subclone of Ψ^{-} cells. Pseudo-V gene knockout with endogenous AID knockout and exogenous AID expression (puromycin resistant)
Ψ^{-} PCNA K164R	H. Arakawa, Neuherberg	PCNA mutant + exogenous AID expression (puromycin resistant)
Human B-cell line:		
Raji ATCC	J. Bachl, München	Burkitt Lymphoma cell line, EBV-positiv

5.10. Softwares

The following software programs were used:

Sci Ed Central (Clone Manager 6)	Sequence analysis
Microsoft office 2003	Data processing and compilation
Adobe Photoshop 6.0	Image processing
Chromeleon®	nano-HPLC
μCarrier (microcarrier)	Probot Microfraction Collector
GPS Data Explorer 2.0	MS/MS-analysis
MASCOT	Search engine
NCBI Gallus	Protein database

6. Methods

6.1. Standard methods

Standard methods were performed according to Sambrook and Russel (2001) or according to the manufacturer protocol.

6.2. Cloning of the Rad18-HA-TAP fusions

Rad18-HA-CTAP clone (SG-RC1):

The Rad18 cDNA was amplified with the SGS-Rad18-For3 and SGS-Rad18-Rev2 primers to add an HA tag to the C- terminus of the protein. Then the PCR fragment and the pZome-1C vector (obtained from Cellzome, Germany) were each restriction digested with SpeI and BamHI. The PCR fragment was ligated into the pZome vector that already carried the TAP tag, at 4°C overnight in the presence of T4 DNA ligase and its appropriate buffer. The ligated vector was sequenced to ensure sequence fidelity.

NTAP-HA-Rad18 clone (SG-RN1)

The Rad18 cDNA was amplified with the SGS-Rad18-For4 and SGS-Rad18-Rev3 primers, to add a HA tag to the N- terminus of the protein. Then the PCR fragment and the pZome-1N vector (obtained from Cellzome, Germany) were restriction digested with BstXI and SalI. The PCR fragment was ligated into the pZome vector that already carried the TAP tag, at 4°C overnight in the presence of T4 DNA ligase and its appropriate buffer. The ligated vector was sequenced to ensure sequence fidelity.

6.3. Cloning of Rad18-HA (R18-HA1)

The cloning was carried out by removing the TAP tag from the SG-RC1 vector by restriction digestion with BamHI and SalI. The oligos SG-Ct-Oligo1 and SG-Ct-Oligo2 were annealed by mixing 250μM of the oligo at equimolar concentration and subjecting it to 95°C for 5 mins followed by gradual cooling to room temperature (RT). The BamHI and SalI digested vector was then ligated with the annealed oligo at 4°C overnight in the presence of T4 DNA ligase and its appropriate buffer, to generate the Rad18-HA (C-terminal) fusion expressed from the pZome vector.

6.4. RNA isolation and cDNA synthesis

The total mRNA from approximately $3x10^6$ cells was isolated using the RNeasy Kit (Qiagen, Hilden) according to the manufacturer's specifications. A maximum of 1µg total RNA was reverse transcribed using the 1st strand cDNA Synthesis Kit (Roche Applied Science, Mannheim, Germany) in order to generate the cDNA. The p-oligo(dT) 15 primer and reverse transcriptase enzyme were used for this reaction. The cycle conditions were: annealing of primers for 10 minutes at 25°C, reverse transcription at 42°C for 1 hour, denaturation of the enzyme at 99°C for 5mins. The cDNAs obtained were stored at -20°C and used whenever required for qRT-PCR reactions. The qRT-PCR in the Light Cycler was carried out according to the instructions from Roche.

6.5. SDS PAGE & western blot analysis

Approximately $3x10^6$ cells were washed with PBS and pelleted. The pellets were lysed using 2x Laemmli buffer (Laemmli 1970). The protein contents of these cell lysates were estimated using the DC protein assay from Bio-Rad (Munich), according to the manufacturer's instructions. 60µg of protein per lane were subjected to electrophoresis in 12% SDS-polyacrylamide gels and transferred on to a Polyvinylidene difluoride (PVDF) membrane. After transfer, the membrane was blocked with 5% skim milk in PBS and incubated with the appropriate primary antibody overnight at 4°C. The membrane was then washed with PBS and incubated with the appropriate secondary antibody for 3h at RT. The membrane was again washed in PBS before treating with the Chemiluminescence reaction using the ECL or Advance™ ECL Western Blotting Detection Kits (both, GE Healthcare, Freiburg) to visualise the signal of the proteins probed. Note that the PAP reagent alone did not require probing with secondary antibody.

6.6. Native PAGE & blotting

$2x10^7$ cells were resuspended in 100µl lysis buffer (50 mM Tris-HCl [pH 8.0], 1% IGEPAL, 150mM NaCl and protease inhibitors - added fresh) and vortexed thoroughly for about 5 seconds. The mixture was incubated on ice (at 4°C) for 20-30 mins with sporadic vortexing. After incubation, the DNA was disrupted by ultrasonication. The samples were vortexed thoroughly for about 5 seconds and centrifuged for 10mins with 16400rpm (max. rpm) at 4°C. The lysate supernatant was mixed 1:1 with 2x sample buffer (125 mM Tris-HCl [pH 6.8], 30% glycerol and 0.02% bromophenol blue). 50ul of this sample was loaded in an SDS-free polyacrylamide gel (6.5%) and electrophoretic separation was performed in the

absence of SDS at 4°C. The Blotting was carried out in the absence of methanol with the same 1x buffer as the running buffer (14.4grams Glycin and 3.02grams Tris dissolved in 1 litre Millipore water) for 1.5hours and 450mA at 4°C. The membrane was blocked in 5% milk and probed by chemiluminiscence for the fusions with the PAP reagent as described before in section 5.2.5.

6.7. TAP extraction of GOI-TAP fusions

All steps were carried out on ice with all buffers and tubes pre-chilled and everything keratin free. $2x10^9$ cells (for DT40 Rad18-NTAP) and $1x10^9$ cells (for DT40 Rad18-CTAP) were pelleted and resuspended in 5ml extract buffer (30mM Tris-HCl, 150mM NaCl, 10µM ZnCl2, 1.5mM MgCl2, 10% Glycerol, 1mM β-ME, 0.5M PMSF and complete –E) and cell clumps were dislodged by homogenizing in the DOUNCE homogenizer by moving the pestle up and down very slowly and gently for 5 times. To the cell suspension, 5ml lysis buffer (30mM Tris-HCl, 150mM NaCl, 10µM ZnCl2, 1.5mM MgCl2, 10% Glycerol, 1mM β-ME, 0.5M PMSF complete –E and 0.5% IGEPAL) was added and homogenized as before for 10 times. The extract was centrifuged for 1hr, at 4°C, with a minimum of 13,000rpm. The supernatant was used subsequently for TAP or for CoIPs or stored at -20°C until use.

6.8. Tandem Affinity Purification

Ig Binding

450µl Ig beads for each extract were washed in 5ml IPP150 buffer (10mM Tris-HCl, 150mM NaCl, 10µM ZnCl2, 1% IGEPAL) three times by centrifugation at 600rpm 4°C, 1 min. 10ml of the lysate supernatant of the TAP extract were added to the washed Ig beads and incubated with rotation overnight at 4°C.

TEV Cleavage and Elution

The beads that were incubated overnight with the TAP lysate supernatant were centrifuged for 2 minutes at 600rpm, 4°C and the supernatant was removed. The beads were washed 3 times with 10ml IPP 150 buffer and the final wash was made with 10ml of the TEV cleavage buffer (10mM Tris-HCl, 150mM NaCl, 10µM ZnCl2, 1% IGEPAL, 0.5mM EDTA, 1mM β-ME) and the supernatant was removed as much as possible at this step. The 400µl beads were gently resuspended in the remaining volume of the TEV Cleavage Buffer and transfered into labeled luerlock columns (small), with filter, lid and stopper. Again 400µl of TEV cleavage buffer was added to the transferred beads followed by 10µl TEV protease enzyme (100 units). This was then incubated with moderate rotation for 3 hours at 15°C. The

TEV eluate is collected by placing the column in eppendorf tubes after removing the stopper followed by centrifugation at 1000 rpm for 1 min, 4°C.

Calmodulin Binding

The BioRad columns were equilibrated with 2ml CB buffer (10mM Tris-HCl, 150mM NaCl, 10µM ZnCl2, 1% IGEPAL, 1mM Mg Acetate, 1mM Imidazole, 2mM CaCl2, 10mM β-ME) on ice. 400µl of Calmodulin resins (slurry) were washed 3 times with 500µl CB buffer. 3ml CB buffer, 800µl TEV eluate + 200µl TEV cleavage buffer (making TEV eluate to 1ml) + 3µl CaCl2 were taken in the BioRad columns. To this, 400µl of the washed Calmodulin resin was added and closed to incubate on a roller at 4° C room for 3 hours.

Calmodulin Elution

After incubation, the CB flow through was collected and the CB resins were washed three times with 10ml CB buffer by allowing the buffer to flow through the column placed over a collecting falcon tube. The stoppers of the columns were then closed and 500µl of Calmodulin Elution buffer (10mM Tris-HCl (pH 8), 150mM NaCl, 1% IGEPAL, 1mM Mg Acetate, 1mM Imidazole, 2mM EGTA, 10mM β-ME) was added to the resins and incubated for 15 minutes on ice. After 15 minutes, the CB eluate was collected in pre-lubricated eppendorf tubes and this elution step was repeated to maximise the recovery. All fractions were stored at -20°C until further use.

6.9. TCA protein precipitation

An equal volume of 20% (w/v) TCA was added to the protein samples, mixed by vortexing and incubated on ice for 20mins. The proteins were pelleted in a cooling centrifuge at maximum speed for 10mins. The supernatant was removed and the protein pellet was washed with 200µl ice-cold acetone for three times. The pellets were dried at RT and dissolved in the sample buffer used for SDS PAGE by incubating at 70°C in a shaker for 20 mins at 550rpm. The samples are stored -20°C

6.10. Silver stain analysis

The silver staining of using SDS-polyacrylamide gel electrophoresis separated proteins was carried out after Blum (Blum et al. 1987).

6.11. In-Gel Trypsin Digest

The protein sample was loaded in the NuPAGE gel system (Invitrogen) and subjected to electrophoresis for about 1cm length. The gel portion containing the sample was cut out and divided into two fractions. Each fraction was then cut into smaller pieces and transferred to labelled keratin-free 500µl eppendorf tubes. The gel pieces were immersed in 50µl ABC Buffer (50mM NH_4HCO_3 in 30% acetonitrile) and incubated for 5min at 37°C. Then the buffer was removed and discarded. This wash was carried out 3-4 times. The alkylation of the proteins was done by incubating the gel pieces in 50µl DTT solution (3.5mg in 500µl deionised water) for 15min at 55°C. Then, the sample was allowed to cool and then incubated with 50µl Iodoacetamide solution (18.6mg in 1ml deionised water) in the dark for 15min at RT. Then the gel pieces were washed for at least 3 times with ABC buffer (mandatory).

The gel pieces were then incubated with 100µl of 100% acetonitril for 15min at RT. The acetonitrile was then removed and this step was repeated until all the gel pieces turned completely white and shrunken in size. After this, the remaining acetonitrile was completely vaporized at RT or at 37°C with the lids of the eppendorf tubes open. To the dried gel "crumbs" 1µl of the trypsin digest solution (5µl Trypsin 0.03µg/µl mixed fresh with 180µl of the 10mM NH_4HCO_3 digest buffer) was added directly on the gel and in about 5mins, the gels swelled back taking in all the digest solution. The digest solution was added until they are completely immersed in the solution within the range of 4µl to maximum of 10µl. This reaction mix was incubated overnight at 37°C. After the overnight digestion, the excess digest solution (if any) was collected in a new labelled siliconized eppendorf tubes. Then, 10µl of the elution buffer (80% Acetonitrile/ 1%TFA) was added to the gel pieces and sonicated for 5min in an ultrasonication bath. The samples were then centrifuged shortly and the eluate was collected. The elution step was repeated until the gel pieces became white and shrunken again. The eluate was lyophilised in the SpeedVac lyophiliser. Just before using for the HPLC, the peptide pellet was redissolved in 19µl 0.1% TFA for each of the two fractions of the samples and 9µl of each was pooled for the HPLC.

6.12. Reverse phase Nano-Liquid Chromatography

The peptides digested by the in-gel trypsin digest method were separated on a reverse-phase chromatography. The stationary phase of the column consists of porous silica particles, coated with 18-alkyl chain. The peptides are absorbed on the hydrophobic surface of the column and are eluted with an increasing gradient wash with acetonitrile (ACN). The

separation was performed by the Ultimate HPLC unit from Dionex. The flow rate of the HPLC buffers (buffer A: 5%ACN /0.1%TFA in water, buffer B: 80%ACN / 0.08% TFA in water) was 200nl/min. The linear gradient from 50 to 100% buffer B was used for the separation of the peptides for about 82min, followed by a 6-minute-long washing step with 100% buffer B. By using a pre-column with the same carrier material, the salt that may be present in the sample was removed before further mass spectrometric analysis. After the separation, the absorption of peptides was detected in a UV detector at a wavelength of 214 nm. The peptides that were separated were collected along with the matrix by an automated PROBOT microfraction collector according to the instructions given by the manufacturer. The PROBOT mixed the peptide eluating from the LC with a matrix solution (5mg/ml a-cyano-4-hydroxy cinnamic acid [CHCA] in 0.1% TFA, 70% ACN) in the ratio of 1:4 and distributed the mixture into 275 fractions, with a retention time of 30 seconds per fraction on a MALDI target. The samples were then ready for the MALDI analysis.

6.13. MALDI TOF-TOF

The device used was the 4700 proteomic analyser that is equipped to perform MALDI-TOF/TOF (matrix assisted laser desorption/ionization time of flight/time of flight) analysis (Applied Biosystems, Foster City, USA). During the analysis, peptides with masses 800 to 5500 Daltons (Da) were analyzed. The masses of individual peptides were extrapolated based on the time taken for them to travel through a defined path in high vacuum (Time of Flight - TOF). The speed of flight of the peptide ions is directly proportional to $1/\sqrt{m}$ (where m = mass of the ion). This implies that the heavier ions require a longer time of flight and the mass of the charged ions can be accurately estimated based on the TOF. The tandem mass spectrometry or MS/MS was applied for the identification of peptides from a peptide mixture during which a particular peptide identified by the first MS analysis was identified in the second MS analysis and subjected to collision in a gas chamber. This leads to the fragmentation of the peptides into individual fragments.

For a given peptide the fragmentation pattern is predictable and this is achieved by the division of the amide linkages between the various amino acids of the peptide. The ions are created as a b-ion, when the fragmentation occurs at the N-terminus of the peptide bond and as a y-ion, if the fragmentation occurs at the C-terminus. Besides these, other types of fragmentations also occurs, namely a, c, x and z ions according to their positions from the amide bond. The information about the fragmentation pattern for a given peptide was used by

the MASCOT software to identify the peptide mass and sequence. The parameters used for the analysis of the samples were as follows: The LASER was used with a frequency of 200Hz and a wavelength of 355 nm. For an MS analysis, the number of LASER shots per spectrum was 2500 and for the subsequent MS/MS optics, the number of shots per spectrum was increased to 4500 and the LASER intensity was increased by 200 units compared to the MS optics. The 4700 analyser software generates the list of masses and automatically selects the peptide precursors for MS/MS measurement. The mass was calibrated based on the peptide standard (Bruker Daltonik, Bremen). The resulting MS/MS spectra were loaded in the GPS Explorer 2.0 (Applied Biosystems, Foster City, USA) and a search against an appropriate protein database (SwissProt/NCBI-entire/NCBI Gallus) was made with the help of an integrated MASCOT search algorithm.

With the MASCOT search engine, a probability-based molecular weight search is possible (the probability model is not published in detail). The parameters for the MASCOT search were set as follows: the enzyme used was selected as trypsin; Carbamide methylation was fixed and the methionine oxidation was specified as variable. The database was selected as NCBI Gallus, the minimum peptide rank was set at 3, the maximum peptide score was set to 10 and the ppm was set to 100. The GPS Explorer software analysis assigned two scores of significance, the best ion score and the total ion score. The best ion score is the highest score of among all the peptides identified for a given protein and the total ion score is the score obtained by the sum of all the scores for all the peptides identified for a protein. The proteins were sorted according to the total ion score C.I. % (confidence interval %), a value calculated by the MASCOT analysis software based on the best ion scores of the peptides identified for the protein. The software assigned this score for every protein identified by taking into consideration the best ion score, the total ion score and the nature of the database and so on. A huge un-curated database such as NCBI was considered with more stringency than the curated ones like Swissprot. A protein with a total ion score C.I. % of ≥95% was considered significant. The proteins that were considered for further analysis were not only significant (≥95%) but those that met the following additional criteria: 1) those that were identified in more than one sample or purification with a significant score and 2) identified with a reliable y and b MS/MS fragmentation for a given peptide.

6.14. Co-immunoprecipitation in the Rad18-HA-TAP DT40 cells

The immunoprecipitation in the Rad18-HA-TAP clones was carried out by first removing the protein A part of the TAP tag that might interfere with the IP. For this, TAP extract of the cells was set up for overnight Ig binding as per the TAP protocol. After overnight incubation, the beads were centrifuged with 5000rpm at 4°C for 1min and the supernatant was removed as "IgB Supt". The beads (about 50µl) were then washed 3 times with 500µl of the TAP extract Buffer (by adding 500µl buffer, followed by centrifugation and discarding the supernatant wash). Then the bound protein was eluted by TEV protease cleavage step (as described previously) and the TEV eluate was incubated with the bait antibody and protein G beads with the appropriate controls. After overnight incubation, the beads were pelleted and the supernatant was collected as the IP supernatant. The pellets were then washed with low-salt or high salt buffer for 5 times with 500µl lysis buffer, followed by centrifugation and discarding the supernatant (wash). The pellet was then processed with 2x sample buffer and analysed by immunoblotting.

6.15. Endogenous co-immunoprecipitation in Raji cells

The cell number of $6x10^6$ cells was used for each IP which as extracted as per the TAP extraction protocol described earlier. The bait antibody, with and without lysate, isotype matched antibody with lysate and a sample with only lysate and no antibody (null) were set up in duplicate so that one set would be washed with low salt (150mM of NaCl) and the other with high salt (300mM NaCl). 500µl of the TAP lysate was added to the protein G beads that were preincubated for 1h with 5µg of the antibody. These were incubated with rotation for 3-4 hours at 4°C. After incubation, the beads were centrifuged with 5000rpm at 4°C for 2 min. The supernatant was removed and the pellet was washed 5 times with low salt or high salt buffer whichever was appropriate. The washed pellet (about 50ul) is the immune precipitate with the beads and it was processed for western blot analysis.

6.16. Cell culture

All cell culture methods were carried out under sterile conditions in the laminar hood (Heareus Christ instruments, Dusseldorf) with sterile glass or plastic pipettes. The cells were incubated (Heareus Christ instruments, Dusseldorf) at 5% CO2, 95% humidity and 41°C for chicken DT40 cells and 37°C for the Raji human cells in culture.

Table 12: Chicken Media for the DT40 cell culture:

Volume added	Components of DT40 cell culture media	Final concentration
500ml	RPMI 1640 Medium (Invitrogen, Karlsruhe)	-
50ml	FCS (Biochrom KG, Berlin und PAA, Pasching, Austria)	10 %
5ml	Penicillin (Invitrogen, Karlsruhe)	100 U/ml
5ml	Streptomycin (Invitrogen, Karlsruhe)	100 µg/ml
5ml	Glutamine (200 mM) (Gibco BRL, Schottland)	2 mM
5ml	Sodium Pyruvate (100 mM) (Gibco BRL, Schottland)	1 mM
50µl	β-mercaptoethanol (1M)	10 mM
5ml	Chicken serum (Sigma)	1%

The media for Raji human cells was prepared with the above ingredients except the β-mercaptoethanol and chicken serum.

6.17. Transfection of DT40 cells

About 25-50µg (about 50µl) of plasmid DNA was linearized outside of the genes of interest by digestion with an appropriate restriction enzyme in 500µl total volume for 3-5 hours at the appropriate temperature for the enzyme. Then 1ml of 100% ethanol was added to precipitate the DNA overnight in -20°C. The cells were seeded in a healthy growth density. The overnight precipitated DNA was centrifuged for 20min 14000rpm at 4°C and washed with 1ml 70% ethanol. The supernatant was discarded and the pellet was dried under the hood. The dried pellet was resuspended in 500µl sterile PBS solution. $1x10^7$ cells where washed and resuspended in 300µl of PBS and dissolved DNA was added to the cells, mixed and transferred into a pre-chilled electroporation cuvette. The cell-DNA mix was incubated on ice for 10min and the electroporated using a BioRad electroporator set at 25µF and 550 volts and kept on ice for another 10min. The cell/DNA solution was added to 10ml of chicken medium and 100µl was distributed into each of the wells of a 96-well microtiter plate. The cells were selected with 100µl of selective medium (containing twice the final concentration of the drug) added to each well after an overnight incubation for the cells to recover. Drug resistant colonies were retrieved after about ten days in the incubator.

6.18. Colony Survival assay for DT40 using chemical agents

The colony survival assay was carried out exactly as described earlier (Simpson and Sale 2006).

6.19. Nuclear/Cytoplasmic Fractionation

$5x10^6$ cells were washed in PBS and resuspended in 90µl Mendez A-Buffer (10mM Hepes pH 7.9, 10mM KCl, 1.5 mM MgCl2, 10% Glycerol, 0.34M Sucrose, 0.5mM DTT, Proteinase Inhibitors). 30µl of this fraction was aliquoted as "Total Extract". Then 40µl Mendez A-Buffer was mixed with 0,4µl 10% Triton-X 100 (1:100) and 40 µl Mendez A/ Triton X (final: 0,04% Triton-X 100; 1:250) was added to the remaining 60µl cell sample. The mix was incubated on ice for 10 mins and centrifuged for 4 min; 1300 rpm; 4°C (step A). The pellet and the supernatant were separated and each was processed further separately. The supernatant was centrifuged for 1h at full speed (ca.13000 rpm) and 4°C and the supernatant was taken into a clean eppendorf tube as the cytoplasmic fraction. The pellet from Step A is washed with 150µl Mendez A with centrifugation for 4 min; 1300 rpm; 4°C. The supernatant was discarded and the pellet is dissolved in 100µl Mendez A buffer as the nuclear fraction.

6.20. DNA damage induced activation of the JNK/AP1 pathway

The cells in a healthy growing density ($2.5x10^5$/ml) were seeded using $4.5x10^7$ cells in 150ml media without MMS and left overnight. The following day, the cells were counted to verify that they have been proliferating before treating with MMS. The cells were adjusted to an equal total number ($9x10^7$) just before starting the assay in case they were at different numbers provided they had doubled and look healthy. The total volume of the culture was made up to 180ml with fresh media and 20ml of this culture was pelleted for the untreated protein pellet. An appropriate amount of MMS that equals 1mM final concentration in the remaining 150ml culture was added and mixed thoroughly by pipetting. The cells were harvested at 2, 4, 6, 8, and 10h incubation time points. The cell pellets were extracted for total protein and analysed by western blot analysis with a phospho-JNK (pJNK) antibody.

References

Abraham, R. T. (2001). "Cell cycle checkpoint signaling through the ATM and ATR kinases." Genes Dev **15**(17): 2177-96.

Ahne, F., B. Jha, et al. (1997). "The RAD5 gene product is involved in the avoidance of non-homologous end-joining of DNA double strand breaks in the yeast Saccharomyces cerevisiae." Nucleic Acids Res **25**(4): 743-9.

Allen, C. D., T. Okada, et al. (2007). "Imaging of germinal center selection events during affinity maturation." Science **315**(5811): 528-31.

Arakawa, H., S. Furusawa, et al. (1996). "Immunoglobulin gene hyperconversion ongoing in chicken splenic germinal centers." Embo J **15**(10): 2540-6.

Arakawa, H., J. Hauschild, et al. (2002). "Requirement of the activation-induced deaminase (AID) gene for immunoglobulin gene conversion." Science **295**(5558): 1301-6.

Arakawa, H., K. Kuma, et al. (1998). "Oligoclonal development of B cells bearing discrete Ig chains in chicken single germinal centers." J Immunol **160**(9): 4232-41.

Arakawa, H., D. Lodygin, et al. (2001). "Mutant loxP vectors for selectable marker recycle and conditional knock-outs." BMC Biotechnol **1**: 7.

Arakawa, H., G. L. Moldovan, et al. (2006). "A role for PCNA ubiquitination in immunoglobulin hypermutation." PLoS Biol **4**(11): e366.

Arakawa, H., H. Saribasak, et al. (2004). "Activation-induced cytidine deaminase initiates immunoglobulin gene conversion and hypermutation by a common intermediate." PLoS Biol **2**(7): E179.

Aravind, L. and E. V. Koonin (2000). "SAP - a putative DNA-binding motif involved in chromosomal organization." Trends Biochem Sci **25**(3): 112-4.

Bachl, J., C. Carlson, et al. (2001). "Increased transcription levels induce higher mutation rates in a hypermutating cell line." J Immunol **166**(8): 5051-7.

Bachl, J., I. Ertongur, et al. (2006). "Involvement of Rad18 in somatic hypermutation." Proc Natl Acad Sci U S A **103**(32): 12081-6.

Back, J. W., V. Notenboom, et al. (2002). "Identification of cross-linked peptides for protein interaction studies using mass spectrometry and 18O labeling." Anal Chem **74**(17): 4417-22.

Bailly, V., J. Lamb, et al. (1994). "Specific complex formation between yeast RAD6 and RAD18 proteins: a potential mechanism for targeting RAD6 ubiquitin-conjugating activity to DNA damage sites." Genes Dev **8**(7): 811-20.

References

Bailly, V., S. Lauder, et al. (1997). "Yeast DNA repair proteins Rad6 and Rad18 form a heterodimer that has ubiquitin conjugating, DNA binding, and ATP hydrolytic activities." J Biol Chem **272**(37): 23360-5.

Bartek, J. and J. Lukas (2007). "DNA damage checkpoints: from initiation to recovery or adaptation." Curr Opin Cell Biol **19**(2): 238-45.

Bertwistle, D., M. Sugimoto, et al. (2004). "Physical and functional interactions of the Arf tumor suppressor protein with nucleophosmin/B23." Mol Cell Biol **24**(3): 985-96.

Bi, X., L. R. Barkley, et al. (2006). "Rad18 regulates DNA polymerase kappa and is required for recovery from S-phase checkpoint-mediated arrest." Mol Cell Biol **26**(9): 3527-40.

Blastyak, A., L. Pinter, et al. (2007). "Yeast Rad5 protein required for postreplication repair has a DNA helicase activity specific for replication fork regression." Mol Cell **28**(1): 167-75.

Blum, H., H. Beier, et al. (1987). "Improved silver staining of plant proteins, RNA and DNA in polyacrylamide gels." Electrophoresis **8**(2): 93-99.

Bode, A. M. and Z. Dong (2003). "Mitogen-activated protein kinase activation in UV-induced signal transduction." Sci STKE **2003**(167): RE2.

Bouwmeester, T., A. Bauch, et al. (2004). "A physical and functional map of the human TNF-alpha/NF-kappa B signal transduction pathway." Nat Cell Biol **6**(2): 97-105.

Bransteitter, R., P. Pham, et al. (2003). "Activation-induced cytidine deaminase deaminates deoxycytidine on single-stranded DNA but requires the action of RNase." Proc Natl Acad Sci U S A **100**(7): 4102-7.

Branzei, D., M. Seki, et al. (2004). "Rad18/Rad5/Mms2-mediated polyubiquitination of PCNA is implicated in replication completion during replication stress." Genes Cells **9**(11): 1031-42.

Broomfield, S., B. L. Chow, et al. (1998). "MMS2, encoding a ubiquitin-conjugating-enzyme-like protein, is a member of the yeast error-free postreplication repair pathway." Proc Natl Acad Sci U S A **95**(10): 5678-83.

Broomfield, S., T. Hryciw, et al. (2001). "DNA postreplication repair and mutagenesis in Saccharomyces cerevisiae." Mutat Res **486**(3): 167-84.

Buerstedde, J.-M. and S. Takeda (1991). "Increased ratio of targeted to random integration after transfection of chicken B cell lines." **67**(1): 179-188.

Carlson, L. M., W. T. McCormack, et al. (1990). "Templated insertions in the rearranged chicken IgL V gene segment arise by intrachromosomal gene conversion." Genes Dev **4**(4): 536-47.

References

Chaudhuri, J., C. Khuong, et al. (2004). "Replication protein A interacts with AID to promote deamination of somatic hypermutation targets." Nature **430**(7003): 992-8.

Chavez-Rios, R., L. E. Arias-Romero, et al. (2003). "L10 ribosomal protein from Entamoeba histolytica share structural and functional homologies with QM/Jif-1: proteins with extraribosomal functions." Mol Biochem Parasitol **127**(2): 151-60.

Christensen, D. E., P. S. Brzovic, et al. (2007). "E2-BRCA1 RING interactions dictate synthesis of mono- or specific polyubiquitin chain linkages." Nat Struct Mol Biol **14**(10): 941-8.

Cleaver, J. E. (1968). "Defective repair replication of DNA in xeroderma pigmentosum." Nature **218**(5142): 652-6.

Cox, B. S. and J. M. Parry (1968). "The isolation, genetics and survival characteristics of ultraviolet light-sensitive mutants in yeast." Mutat Res **6**(1): 37-55.

Dávid Szüts, L. J. S., Sarah Kabani, Mitsuyoshi Yamazoe and Julian E. Sale (2008). "A role for RAD18 in homologous recombination in DT40." Mol. Cell. Biol.

Davies, A. A., D. Huttner, et al. (2008). "Activation of ubiquitin-dependent DNA damage bypass is mediated by replication protein a." Mol Cell **29**(5): 625-36.

de Laat, W. L., N. G. Jaspers, et al. (1999). "Molecular mechanism of nucleotide excision repair." Genes Dev **13**(7): 768-85.

Dent, P., A. Yacoub, et al. (2003). "MAPK pathways in radiation responses." Oncogene **22**(37): 5885-96.

Di Noia, J. and M. S. Neuberger (2002). "Altering the pathway of immunoglobulin hypermutation by inhibiting uracil-DNA glycosylase." Nature **419**(6902): 43-8.

Di Noia, J. M. and M. S. Neuberger (2004). "Immunoglobulin gene conversion in chicken DT40 cells largely proceeds through an abasic site intermediate generated by excision of the uracil produced by AID-mediated deoxycytidine deamination." Eur J Immunol **34**(2): 504-8.

Dohmen, R. J., K. Madura, et al. (1991). "The N-end rule is mediated by the UBC2(RAD6) ubiquitin-conjugating enzyme." Proc Natl Acad Sci U S A **88**(16): 7351-5.

Dowdy, S. F., K. M. Lai, et al. (1991). "The isolation and characterization of a novel cDNA demonstrating an altered mRNA level in nontumorigenic Wilms' microcell hybrid cells." Nucleic Acids Res **19**(20): 5763-9.

Finkel, T. and N. J. Holbrook (2000). "Oxidants, oxidative stress and the biology of ageing." Nature **408**(6809): 239-47.

References

Forler, D., T. Kocher, et al. (2003). "An efficient protein complex purification method for functional proteomics in higher eukaryotes." Nat Biotechnol **21**(1): 89-92.

Fortini, P., B. Pascucci, et al. (1998). "Different DNA polymerases are involved in the short- and long-patch base excision repair in mammalian cells." Biochemistry **37**(11): 3575-80.

Friedberg, E. C., A. R. Lehmann, et al. (2005). "Trading places: how do DNA polymerases switch during translesion DNA synthesis?" Mol Cell **18**(5): 499-505.

Friedberg, E. C. e. a. (1995). DNA repair and mutagenesis, ASM Press, Washington DC.

Fritz, G. and B. Kaina (2006). "Late activation of stress kinases (SAPK/JNK) by genotoxins requires the DNA repair proteins DNA-PKcs and CSB." Mol Biol Cell **17**(2): 851-61.

Fu, Y., Y. Zhu, et al. (2008). "Rad6-Rad18 mediates a eukaryotic SOS response by ubiquitinating the 9-1-1 checkpoint clamp." Cell **133**(4): 601-11.

Game, J. C. and P. D. Kaufman (1999). "Role of Saccharomyces cerevisiae chromatin assembly factor-I in repair of ultraviolet radiation damage in vivo." Genetics **151**(2): 485-97.

Gavin, A. C., M. Bosche, et al. (2002). "Functional organization of the yeast proteome by systematic analysis of protein complexes." Nature **415**(6868): 141-7.

Gloeckner, C. J., K. Boldt, et al. (2007). "A novel tandem affinity purification strategy for the efficient isolation and characterisation of native protein complexes." Proteomics **7**(23): 4228-34.

Gramatikoff, K., W. Schaffner, et al. (1995). "The leucine zipper of c-Jun binds to ribosomal protein L18a: a role in Jun protein regulation?" Biol Chem Hoppe Seyler **376**(5): 321-5.

Hanna, M. G., Jr. (1964). "An Autoradiographic Study of the Germinal Center in Spleen White Pulp During Early Intervals of the Immune Response." Lab Invest **13**: 95-104.

Hess, M. T., U. Schwitter, et al. (1997). "Bipartite substrate discrimination by human nucleotide excision repair." Proc Natl Acad Sci U S A **94**(13): 6664-9.

Hoege, C., B. Pfander, et al. (2002). "RAD6-dependent DNA repair is linked to modification of PCNA by ubiquitin and SUMO." Nature **419**(6903): 135-41.

Hoeijmakers, J. H. (2001). "Genome maintenance mechanisms for preventing cancer." Nature **411**(6835): 366-74.

Hofmann, R. M. and C. M. Pickart (1999). "Noncanonical MMS2-encoded ubiquitin-conjugating enzyme functions in assembly of novel polyubiquitin chains for DNA repair." Cell **96**(5): 645-53.

Honjo, T., M. Muramatsu, et al. (2004). "AID: how does it aid antibody diversity?" Immunity **20**(6): 659-68.

Hu, Z. B., M. D. Minden, et al. (2000). "Regulation of drug sensitivity by ribosomal protein S3a." Blood **95**(3): 1047-55.

Huang, H., A. Kahana, et al. (1997). "The ubiquitin-conjugating enzyme Rad6 (Ubc2) is required for silencing in Saccharomyces cerevisiae." Mol Cell Biol **17**(11): 6693-9.

Hudson, D. F., C. Morrison, et al. (2002). "Reverse genetics of essential genes in tissue-culture cells: 'dead cells talking'." Trends Cell Biol **12**(6): 281-7.

Hummel, M., S. Bentink, et al. (2006). "A Biologic Definition of Burkitt's Lymphoma from Transcriptional and Genomic Profiling." N Engl J Med **354**(23): 2419-2430.

Jacob, J., G. Kelsoe, et al. (1991). "Intraclonal generation of antibody mutants in germinal centres." Nature **354**(6352): 389-92.

Janeway, C. A., P. Travers, M. Walport, and M. Shlomchik. (2004). Immunobiology, Garland Science, New York and London.

Janis Kuby, R. A. G., Thomas J. Kindt, Barbara A. Osborne (2003). Immunology, W.H. Freeman & Co, New York.

Jentsch, S., J. P. McGrath, et al. (1987). "The yeast DNA repair gene RAD6 encodes a ubiquitin-conjugating enzyme." Nature **329**(6135): 131-4.

Johnson, R. E., S. Prakash, et al. (1999). "Efficient bypass of a thymine-thymine dimer by yeast DNA polymerase, Poleta." Science **283**(5404): 1001-4.

Jones, J. S., S. Weber, et al. (1988). "The Saccharomyces cerevisiae RAD18 gene encodes a protein that contains potential zinc finger domains for nucleic acid binding and a putative nucleotide binding sequence." Nucleic Acids Res **16**(14B): 7119-31.

Kannouche, P. L., J. Wing, et al. (2004). "Interaction of human DNA polymerase eta with monoubiquitinated PCNA: a possible mechanism for the polymerase switch in response to DNA damage." Mol Cell **14**(4): 491-500.

Kashuba, E., M. Yurchenko, et al. (2005). "Epstein-Barr virus-encoded EBNA-5 binds to Epstein-Barr virus-induced Fte1/S3a protein." Exp Cell Res **303**(1): 47-55.

Kho, C. J., Y. Wang, et al. (1996). "Effect of decreased fte-1 gene expression on protein synthesis, cell growth, and transformation." Cell Growth Differ **7**(9): 1157-66.

Koken, M. H., J. W. Hoogerbrugge, et al. (1996). "Expression of the ubiquitin-conjugating DNA repair enzymes HHR6A and B suggests a role in spermatogenesis and chromatin modification." Dev Biol **173**(1): 119-32.

Laemmli, U. K. (1970). "Cleavage of structural proteins during the assembly of the head of bacteriophage T4." Nature **227**(5259): 680-5.

Langerak, P., A. O. Nygren, et al. (2007). "A/T mutagenesis in hypermutated immunoglobulin genes strongly depends on PCNAK164 modification." J Exp Med **204**(8): 1989-98.

Lawrence, C. (1994). "The RAD6 DNA repair pathway in Saccharomyces cerevisiae: what does it do, and how does it do it?" Bioessays **16**(4): 253-8.

Lecomte, F., J. Szpirer, et al. (1997). "The S3a ribosomal protein gene is identical to the Fte-1 (v-fos transformation effector) gene and the TNF-alpha-induced TU-11 gene, and its transcript level is altered in transformed and tumor cells." Gene **186**(2): 271-7.

Li, Z., C. J. Woo, et al. (2004). "The generation of antibody diversity through somatic hypermutation and class switch recombination." Genes Dev **18**(1): 1-11.

Lindahl, T. (1974). "An N-glycosidase from Escherichia coli that releases free uracil from DNA containing deaminated cytosine residues." Proc Natl Acad Sci U S A **71**(9): 3649-53.

Liu, M., J. L. Duke, et al. (2008). "Two levels of protection for the B cell genome during somatic hypermutation." Nature **451**(7180): 841-5.

Lowe, S. W., E. Cepero, et al. (2004). "Intrinsic tumour suppression." Nature **432**(7015): 307-15.

Lyakhovich, A. and M. P. Shekhar (2003). "Supramolecular complex formation between Rad6 and proteins of the p53 pathway during DNA damage-induced response." Mol Cell Biol **23**(7): 2463-75.

M. J. Hobart, T. H. R. P. N. G. E. S. S. C. N. S. S. P. (1981). "Immunoglobulin heavy chain genes in humans are located on chromosome 14." Annals of Human Genetics **45**(4): 331-335.

Margison, G. P. and M. F. Santibanez-Koref (2002). "O6-alkylguanine-DNA alkyltransferase: role in carcinogenesis and chemotherapy." Bioessays **24**(3): 255-66.

Marti, T. M., C. Kunz, et al. (2002). "DNA mismatch repair and mutation avoidance pathways." J Cell Physiol **191**(1): 28-41.

Matsumoto, Y., K. Kim, et al. (1994). "Proliferating cell nuclear antigen-dependent abasic site repair in Xenopus laevis oocytes: an alternative pathway of base excision DNA repair." Mol Cell Biol **14**(9): 6187-97.

Matsumoto, Y., K. Kim, et al. (1999). "Reconstitution of proliferating cell nuclear antigen-dependent repair of apurinic/apyrimidinic sites with purified human proteins." J Biol Chem **274**(47): 33703-8.

McBride, O. W., P. A. Hieter, et al. (1982). "Chromosomal location of human kappa and lambda immunoglobulin light chain constant region genes." J Exp Med **155**(5): 1480-90.

McCormack, W. T. and C. B. Thompson (1990). "Chicken IgL variable region gene conversions display pseudogene donor preference and 5' to 3' polarity." Genes Dev **4**(4): 548-58.

Memisoglu, A. and L. Samson (2000). "Base excision repair in yeast and mammals." Mutat Res **451**(1-2): 39-51.

Mitchell, D. L. and R. S. Nairn (1989). "The biology of the (6-4) photoproduct." Photochem Photobiol **49**(6): 805-19.

Miyase, S., S. Tateishi, et al. (2005). "Differential regulation of Rad18 through Rad6-dependent mono- and polyubiquitination." J Biol Chem **280**(1): 515-24.

Moertl, S., G. I. Karras, et al. (2008). "Regulation of double-stranded DNA gap repair by the RAD6 pathway." DNA Repair (Amst) **7**(11): 1893-906.

Monteclaro, F. S. and P. K. Vogt (1993). "A Jun-binding protein related to a putative tumor suppressor." Proc Natl Acad Sci U S A **90**(14): 6726-30.

Motegi, A., H. J. Liaw, et al. (2008). "Polyubiquitination of proliferating cell nuclear antigen by HLTF and SHPRH prevents genomic instability from stalled replication forks." Proc Natl Acad Sci U S A **105**(34): 12411-6.

Motegi, A., R. Sood, et al. (2006). "Human SHPRH suppresses genomic instability through proliferating cell nuclear antigen polyubiquitination." J Cell Biol **175**(5): 703-8.

Mullenders, L. H., A. C. van Kesteren van Leeuwen, et al. (1988). "Nuclear matrix associated DNA is preferentially repaired in normal human fibroblasts, exposed to a low dose of ultraviolet light but not in Cockayne's syndrome fibroblasts." Nucleic Acids Res **16**(22): 10607-22.

Muramatsu, M., K. Kinoshita, et al. (2000). "Class switch recombination and hypermutation require activation-induced cytidine deaminase (AID), a potential RNA editing enzyme." Cell **102**(5): 553-63.

Muramatsu, M., V. S. Sankaranand, et al. (1999). "Specific expression of activation-induced cytidine deaminase (AID), a novel member of the RNA-editing deaminase family in germinal center B cells." J Biol Chem **274**(26): 18470-6.

Nakajima, S., L. Lan, et al. (2006). "Replication-dependent and -independent responses of RAD18 to DNA damage in human cells." J Biol Chem **281**(45): 34687-95.

Naora, H. and H. Naora (1999). "Involvement of ribosomal proteins in regulating cell growth and apoptosis: Translational modulation or recruitment for extraribosomal activity?" Immunol Cell Biol **77**(3): 197-205.

Nelson, J. R., C. W. Lawrence, et al. (1996). "Thymine-thymine dimer bypass by yeast DNA polymerase zeta." Science **272**(5268): 1646-9.

Nicolas, E., S. Ait-Si-Ali, et al. (2001). "The histone deacetylase HDAC3 targets RbAp48 to the retinoblastoma protein." Nucleic Acids Res **29**(15): 3131-6.

Nicolas, E., V. Morales, et al. (2000). "RbAp48 belongs to the histone deacetylase complex that associates with the retinoblastoma protein." J Biol Chem **275**(13): 9797-804.

Niwa, H., K. Yamamura, et al. (1991). "Efficient selection for high-expression transfectants with a novel eukaryotic vector." Gene **108**(2): 193-9.

Notenboom, V., R. G. Hibbert, et al. (2007). "Functional characterization of Rad18 domains for Rad6, ubiquitin, DNA binding and PCNA modification." Nucleic Acids Res **35**(17): 5819-30.

Ohmori, H., E. Ohashi, et al. (2004). "Mammalian Pol kappa: regulation of its expression and lesion substrates." Adv Protein Chem **69**: 265-78.

Pappin, D. J., P. Hojrup, et al. (1993). "Rapid identification of proteins by peptide-mass fingerprinting." Curr Biol **3**(6): 327-32.

Pascucci, B., M. Stucki, et al. (1999). "Long patch base excision repair with purified human proteins. DNA ligase I as patch size mediator for DNA polymerases delta and epsilon." J Biol Chem **274**(47): 33696-702.

Pasqualucci, L., P. Neumeister, et al. (2001). "Hypermutation of multiple proto-oncogenes in B-cell diffuse large-cell lymphomas." Nature **412**(6844): 341-6.

Peltomaki, P. (2001). "DNA mismatch repair and cancer." Mutat Res **488**(1): 77-85.

Pham, P., R. Bransteitter, et al. (2003). "Processive AID-catalysed cytosine deamination on single-stranded DNA simulates somatic hypermutation." Nature **424**(6944): 103-7.

Phizicky, E. M. and S. Fields (1995). "Protein-protein interactions: methods for detection and analysis." Microbiol Rev **59**(1): 94-123.

Picologlou, S., N. Brown, et al. (1990). "Mutations in RAD6, a yeast gene encoding a ubiquitin-conjugating enzyme, stimulate retrotransposition." Mol Cell Biol **10**(3): 1017-22.

Prelich, G., C. K. Tan, et al. (1987). "Functional identity of proliferating cell nuclear antigen and a DNA polymerase-delta auxiliary protein." Nature **326**(6112): 517-20.

Puig, O., F. Caspary, et al. (2001). "The tandem affinity purification (TAP) method: a general procedure of protein complex purification." Methods **24**(3): 218-29.

Rada, C., J. M. Di Noia, et al. (2004). "Mismatch recognition and uracil excision provide complementary paths to both Ig switching and the A/T-focused phase of somatic mutation." Mol Cell **16**(2): 163-71.

Rajewsky, K. (1996). "Clonal selection and learning in the antibody system." Nature **381**(6585): 751-8.

Revy, P., T. Muto, et al. (2000). "Activation-induced cytidine deaminase (AID) deficiency causes the autosomal recessive form of the Hyper-IgM syndrome (HIGM2)." Cell **102**(5): 565-75.

Reynaud, C. A., V. Anquez, et al. (1987). "A hyperconversion mechanism generates the chicken light chain preimmune repertoire." Cell **48**(3): 379-88.

Reynaud, C. A., A. Dahan, et al. (1989). "Somatic hyperconversion diversifies the single Vh gene of the chicken with a high incidence in the D region." Cell **59**(1): 171-83.

Rigaut, G., A. Shevchenko, et al. (1999). "A generic protein purification method for protein complex characterization and proteome exploration." Nat Biotechnol **17**(10): 1030-2.

Roger A. Garrett, A. T. M. (2000). The Ribosome: Structure, Function, Antibiotics, and Cellular Interactions, ASM Press.

Saberi, A., M. Nakahara, et al. (2008). "The 9-1-1 DNA clamp is required for immunoglobulin gene conversion." Mol Cell Biol **28**(19): 6113-22.

Sale, J. E. (2004). "Immunoglobulin diversification in DT40: a model for vertebrate DNA damage tolerance." DNA Repair (Amst) **3**(7): 693-702.

Saribasak, H., N. N. Saribasak, et al. (2006). "Uracil DNA glycosylase disruption blocks Ig gene conversion and induces transition mutations." J Immunol **176**(1): 365-71.

Schwickert, T. A., R. L. Lindquist, et al. (2007). "In vivo imaging of germinal centres reveals a dynamic open structure." Nature **446**(7131): 83-87.

Sedgwick, B. (1997). "Nitrosated peptides and polyamines as endogenous mutagens in O6-alkylguanine-DNA alkyltransferase deficient cells." Carcinogenesis **18**(8): 1561-7.

Shaulian, E. and M. Karin (2002). "AP-1 as a regulator of cell life and death." Nat Cell Biol **4**(5): E131-6.

Shiloh, Y. (2003). "ATM and related protein kinases: safeguarding genome integrity." Nat Rev Cancer **3**(3): 155-68.

Shinkura, R., S. Ito, et al. (2004). "Separate domains of AID are required for somatic hypermutation and class-switch recombination." Nat Immunol **5**(7): 707-12.

Shiomi, N., M. Mori, et al. (2007). "Human RAD18 is involved in S phase-specific single-strand break repair without PCNA monoubiquitination." Nucleic Acids Res **35**(2): e9.

Simpson, L. and J. Sale (2006). Colony survival assay. Reviews and Protocols in DT40 Research**:** 387-391.

Simpson, L. J. and J. E. Sale (2005). "UBE2V2 (MMS2) is not required for effective immunoglobulin gene conversion or DNA damage tolerance in DT40." DNA Repair (Amst) **4**(4): 503-10.

Song, D., S. Sakamoto, et al. (2002). "Inhibition of poly(ADP-ribose) polymerase activity by Bcl-2 in association with the ribosomal protein S3a." Biochemistry **41**(3): 929-34.

Srivenugopal, K. S., X. H. Yuan, et al. (1996). "Ubiquitination-dependent proteolysis of O6-methylguanine-DNA methyltransferase in human and murine tumor cells following inactivation with O6-benzylguanine or 1,3-bis(2-chloroethyl)-1-nitrosourea." Biochemistry **35**(4): 1328-34.

Stucki, M., B. Pascucci, et al. (1998). "Mammalian base excision repair by DNA polymerases delta and epsilon." Oncogene **17**(7): 835-43.

Sung, P., S. Prakash, et al. (1990). "Mutation of cysteine-88 in the Saccharomyces cerevisiae RAD6 protein abolishes its ubiquitin-conjugating activity and its various biological functions." Proc Natl Acad Sci U S A **87**(7): 2695-9.

Szuts, D., C. Christov, et al. (2005). "Distinct populations of human PCNA are required for initiation of chromosomal DNA replication and concurrent DNA repair." Exp Cell Res **311**(2): 240-50.

Szuts, D., L. J. Simpson, et al. (2006). "Role for RAD18 in homologous recombination in DT40 cells." Mol Cell Biol **26**(21): 8032-41.

Takata, M., M. S. Sasaki, et al. (1998). "Homologous recombination and non-homologous end-joining pathways of DNA double-strand break repair have overlapping roles in the maintenance of chromosomal integrity in vertebrate cells." Embo J **17**(18): 5497-508.

Tateishi, S., Y. Sakuraba, et al. (2000). "Dysfunction of human Rad18 results in defective postreplication repair and hypersensitivity to multiple mutagens." Proc Natl Acad Sci U S A **97**(14): 7927-32.

Tobollik, S. (2007). Untersuchung der Regulation und Interaktionen der Aktivierungsinduzierten Cytidindeaminase (AID) in humanen B-Lymphozyten. Faculty of Biology. Munich, Ludwig-Maximilians-University. **PhD**.

Torres-Roca, J. F., S. Eschrich, et al. (2005). "Prediction of radiation sensitivity using a gene expression classifier." Cancer Res **65**(16): 7169-76.

Tsuji, Y., K. Watanabe, et al. (2008). "Recognition of forked and single-stranded DNA structures by human RAD18 complexed with RAD6B protein triggers its recruitment to stalled replication forks." Genes Cells **13**(4): 343-54.

Ulrich, H. D. and S. Jentsch (2000). "Two RING finger proteins mediate cooperation between ubiquitin-conjugating enzymes in DNA repair." Embo J **19**(13): 3388-97.

Unk, I., I. Hajdu, et al. (2008). "Human HLTF functions as a ubiquitin ligase for proliferating cell nuclear antigen polyubiquitination." Proc Natl Acad Sci U S A **105**(10): 3768-73.

Unk, I., I. Hajdu, et al. (2006). "Human SHPRH is a ubiquitin ligase for Mms2-Ubc13-dependent polyubiquitylation of proliferating cell nuclear antigen." Proc Natl Acad Sci U S A **103**(48): 18107-12.

van der Laan, R., E. J. Uringa, et al. (2004). "Ubiquitin ligase Rad18Sc localizes to the XY body and to other chromosomal regions that are unpaired and transcriptionally silenced during male meiotic prophase." J Cell Sci **117**(Pt 21): 5023-33.

Watanabe, K., S. Tateishi, et al. (2004). "Rad18 guides poleta to replication stalling sites through physical interaction and PCNA monoubiquitination." Embo J **23**(19): 3886-96.

Winding, P. and M. W. Berchtold (2001). "The chicken B cell line DT40: a novel tool for gene disruption experiments." J Immunol Methods **249**(1-2): 1-16.

Wolffe, A. P., F. D. Urnov, et al. (2000). "Co-repressor complexes and remodelling chromatin for repression." Biochem Soc Trans **28**(4): 379-86.

Wu, X., P. Geraldes, et al. (2005). "The double-edged sword of activation-induced cytidine deaminase." J Immunol **174**(2): 934-41.

Xin, H., W. Lin, et al. (2000). "The human RAD18 gene product interacts with HHR6A and HHR6B." Nucleic Acids Res **28**(14): 2847-54.

Yamashita, Y. M., T. Okada, et al. (2002). "RAD18 and RAD54 cooperatively contribute to maintenance of genomic stability in vertebrate cells." Embo J **21**(20): 5558-66.

Yang, X. H., B. Shiotani, et al. (2008). "Chk1 and Claspin potentiate PCNA ubiquitination." Genes Dev **22**(9): 1147-52.

References

Yang, Y., S. Zhang, et al. (2007). "A comparison of nLC-ESI-MS/MS and nLC-MALDI-MS/MS for GeLC-based protein identification and iTRAQ-based shotgun quantitative proteomics." J Biomol Tech **18**(4): 226-37.

Yasuda, M., E. Kajiwara, et al. (2003). "Immunobiology of chicken germinal center: I. Changes in surface Ig class expression in the chicken splenic germinal center after antigenic stimulation." Dev Comp Immunol **27**(2): 159-66.

Zan, H., A. Komori, et al. (2001). "The translesion DNA polymerase zeta plays a major role in Ig and bcl-6 somatic hypermutation." Immunity **14**(5): 643-53.

Zeng, X., D. B. Winter, et al. (2001). "DNA polymerase eta is an A-T mutator in somatic hypermutation of immunoglobulin variable genes." Nat Immunol **2**(6): 537-41.

Zhang, S., J. Chea, et al. (2008). "PCNA is ubiquitinated by RNF8." Cell Cycle **7**(21).

Zou, L. and S. J. Elledge (2003). "Sensing DNA damage through ATRIP recognition of RPA-ssDNA complexes." Science **300**(5625): 1542-8.

Zou, L., D. Liu, et al. (2003). "Replication protein A-mediated recruitment and activation of Rad17 complexes." Proc Natl Acad Sci U S A **100**(24): 13827-32.

Appendix

CONTENTS:

Appendix 1 – MASCOT analysis of TAP of AID fusions
Analysis with swissprot, NCBI-entire and NCBI Gallus databases

Exp. No	Sample Name
TAP3	Tf2/3B: NTAP-AID
TAP3	Tf7/1-16: TAPalone
TAP10	pST10-10B: AID-CTAP
TAP10	pSK1-1A: TAPalone

Appendix 2- MASCOT analysis of TAP of Rad18 fusions
Analysis with NCBI Gallus database

Exp. No	Sample Name
TAP8(12)	Tf9/1-1: Rad18-HA-CTAP
TAP8(12)	Tf9/3-3: NTAP-HA-Rad18
TAP8(12)	Tf7/1-16: TAPalone
TAP10	Tf9/1-1: Rad18-HA-CTAP
TAP10	Tf9/3-3: NTAP-HA-Rad18
TAP10	Tf7/1-16: TAPalone

KEY:

Tf# – Transfection experiment number
TAP# – TAP experiment number
bold font – Bait protein; known and interesting interaction partners

Appendix 1 - MASCOT analysis of TAP of AID Fusions

1.1.1. NTAP-AID fusion TAP3: Tf2/3B

Results with swissprot database: 21 significant proteins

Rank	Protein Name	Species	Peptide Count	Total Ion Score C.I. %	Best Ion Score C.I. %	Total Ion Score	Best Ion Score	Accession Number	Protein MW	Protein PI
1	(P07437) Tubulin beta-2 chain	Homo sapiens	11	100,00	100,00	596,06	111,69	TBB2_HUMA	50095,14	4,78
5	(P13602) Tubulin beta-2 chain (Beta-2 tubulin)	Xenopus laevi	9	100,00	100,00	455,31	111,69	TBB2_XENL	50148,04	4,81
7	(P19378) Heat shock cognate 71 kDa protein (Heat shock 70 kDa protein 8)	Cricetulus gris	6	100,00	100,00	325,55	83,41	HSP7C_CRIG	70989,2	5,24
6	**(P30436) Tubulin alpha chain**	Oncorhynchus	6	100,00	100,00	327,48	84,65	TBA_ONCKE	49967,29	4,92
3	(P68360) Tubulin alpha-1 chain (Alpha-tubulin 1)	Meriones ungu	9	100,00	100,00	507,86	84,65	TBA1_MERU	50803,86	4,94
2	(P68371) Tubulin beta-2C chain (Tubulin beta-2 chain)	Homo sapiens	10	100,00	100,00	538,95	111,69	TBB2C_HUM	50255,17	4,79
4	(Q5R1W4) Tubulin alpha-ubiquitous chain (Alpha-tubulin ubiquitous) (Tubulin K-alpha-	Pan troglodyte	9	100,00	100,00	491,35	84,65	TBAK_PANT	50787,9	4,98
13	**(Q75W64) Activation-induced cytidine deaminase (EC 3.5.4.5) (Cytidine aminohydr**	Canis familiari	2	100,00	100,00	112,19	72,57	AICDA_CAN	24270,28	9,46
16	**(Q80TP3) Ubiquitin-protein ligase EDD1 (EC 6.3.2.-) (Hyperplastic discs protein ho**	Mus musculus	3	100,00	96,11	83,85	34,69	EDD1_MOUS	311351,9	5,59
14	(Q9I8F9) Heat shock 70 kDa protein 1 (HSP70-1)	Oryzias latipes	2	100,00	99,89	94,21	50,05	HSP71_ORYI	70649,13	5,47
8	(Q9NY65) Tubulin alpha-8 chain (Alpha-tubulin 8)	Homo sapiens	6	100,00	100,00	301,84	84,65	TBA8_HUMA	50745,81	4,94
17	**(Q865C5) Ubiquitin**	Camelus drom	2	100,00	99,68	82,92	45,54	UBIQ_CAMD	8559,62	6,56
18	(Q8VCR8) Myosin light chain kinase 2, skeletal/cardiac muscle (EC 2.7.11.18) (MLCK2	Mus musculus	1	100,00	100,00	76,57	76,57	MYLK2_MOI	27840,16	6,01
19	(Q8R1A4) Dedicator of cytokinesis protein 7 (Fragment)	Mus musculus	1	100,00	100,00	72,57	72,57	DOCK7_MOU	84140,5	6,14
20	(Q28065) C4b-binding protein alpha chain precursor (C4bp)	Bos taurus	1	100,00	100,00	64,93	64,93	C4BP_BOVIN	70951,26	5,99
21	(O75165) DnaJ homolog subfamily C member 13 (Required for receptor-mediated endoc	Homo sapiens	1	99,95	99,95	53,80	53,80	DNJCD_HUM	256538,2	6,28
22	(Q99N50) Synaptotagmin-like protein 2 (Exophilin-4)	Mus musculus	2	99,69	52,83	45,64	23,85	SYTL2_MOU	107196,2	6,14
25	(P08955) CAD protein [Includes: Glutamine-dependent carbamoyl-phosphate synthase (E	Mesocricetus a	1	96,74	96,74	35,45	35,45	PYR1_MESA	245539,5	6,02
26	(Q9WUA3) 6-phosphofructokinase type C (EC 2.7.1.11) (Phosphofructokinase 1) (Phosp	Mus musculus	1	95,83	95,83	34,39	34,39	K6PP_MOUS	86426,7	6,73
27	(Q9QZK9) Deoxyribonuclease-2-beta precursor (EC 3.1.22.1) (Deoxyribonuclease II beta	Rattus norvegi	1	95,71	95,71	34,26	34,26	DNS2B_RAT	40959,58	9,33
28	(Q9NQ66) 1-phosphatidylinositol-4,5-bisphosphate phosphodiesterase beta 1 (EC 3.1.4.1	Homo sapiens	1	94,83	94,83	33,45	33,45	PLCB1_HUM	139334,5	5,9

1.1.1. NTAP-AID fusion TAP3: Tf2/3B

Results with NCBI-entire database: 29 significant proteins

Rank	Protein Name	Species	Peptide Count	Total Ion Score C.I. %	Best Ion Score C.I. %	Total Ion Score	Best Ion Score	Accession Number	Protein MW	Protein PI
1	beta-tubulin	Homo sapiens	8	100,00	100,00	515,22	111,69	gi|338695	50240,14	4,75
2	**tubulin alpha**	Rattus norvegi	9	100,00	100,00	507,86	84,65	gi|223556	50893,91	4,94
3	PREDICTED: similar to tubulin, alpha 1 [Bos taurus]	Bos taurus	9	100,00	100,00	507,86	84,65	gi|76610661	51941,36	4,96
4	unnamed protein product [Tetraodon nigroviridis]	Tetraodon nigr	9	100,00	100,00	507,86	84,65	gi|47218560	48551,65	5,14
5	tubulin, alpha, ubiquitous [Pan troglodytes]	Pan troglodyte	9	100,00	100,00	491,35	84,65	gi|77539752	50787,9	4,98
6	Tubulin, beta, 2 [Danio rerio]	Danio rerio	8	100,00	100,00	485,23	111,69	gi|34194061	50211,15	4,79
7	unnamed protein product [Tetraodon nigroviridis]	Tetraodon nigr	7	100,00	100,00	457,35	111,69	gi|47215416	43110,99	5,27
8	unnamed protein product [Tetraodon nigroviridis]	Tetraodon nigr	7	100,00	100,00	422,77	84,65	gi|47229080	54084,68	5,49
9	unnamed protein product [Tetraodon nigroviridis]	Tetraodon nigr	6	100,00	100,00	331,92	76,69	gi|47229078	46678,98	4,83
10	alpha-tubulin [Oncorhynchus keta]	Oncorhynchus	6	100,00	100,00	327,48	84,65	gi|64138	49967,29	4,92
11	Heat shock cognate 71 kDa protein (Heat shock 70 kDa protein 8)	Bos taurus	5	100,00	100,00	300,77	83,41	gi|123644	71423,5	5,49
12	MGC69074 protein [Xenopus laevis] TUBULIN	Xenopus laevis	5	100,00	100,00	265,00	86,53	gi|33417142	50812,44	5
13	alpha-tubulin 2 [Ciona intestinalis]	Ciona intestina	4	100,00	99,93	184,02	61,95	gi|21667229	44580,01	5,85
14	stress protein HSP70-1 [Xiphophorus maculatus]	Xiphophorus n	3	100,00	100,00	176,51	83,41	gi|17061835	70520,17	5,38
15	heat shock cognate 70 kDa protein [Pimephales promelas]	Pimephales pr	2	100,00	100,00	135,95	83,41	gi|43439894	71500,25	5,16
16	tubulin, alpha 4 [Homo sapiens]	Homo sapiens	2	100,00	100,00	134,41	84,65	gi|13376539	27756,88	8,65
19	Unknown (protein for MGC:80166) [Xenopus laevis]	Xenopus laevis	3	100,00	98,23	129,27	47,86	gi|49117900	51776,43	5,24
20	**AID [Homo sapiens]**	Mus musculus	2	100,00	99,99	112,19	72,57	gi|22297248	24323,27	9,5
21	PREDICTED: similar to Dedicator of cytokinesis protein 6 [Gallus gallus]	Gallus gallus	2	100,00	99,99	106,67	72,57	gi|50751700	262707,8	6,09
23	PREDICTED: similar to leucine-rich PPR motif-containing protein [Gallus gallus]	Gallus gallus	2	100,00	99,94	97,19	62,46	gi|50740428	177325,3	8,82
24	PREDICTED: similar to ubiquitous alpha-tubulin [Mus musculus]	Mus musculus	2	100,00	99,93	95,79	62,11	gi|63543117	29184,53	5,98
25	HSP70-1 protein [Oryzias latipes]	Oryzias latipes	2	100,00	98,93	94,21	50,05	gi|9652348	70649,13	5,47
26	Chain A, Crystal Structure Of A Multiple Hydrophobic Core Mutant Of Ubiquitin	Homo sapiens	2	100,00	96,98	82,92	45,54	gi|51247357	10027,28	6,71
27	Chain A, Rotamer Strain As A Determinant Of Protein Structural Specificity	Homo sapiens	2	100,00	96,98	82,92	45,54	gi|5821952	8559,62	6,56
29	Unknown (protein for IMAGE:4110141) [Homo sapiens] MYOSIN L KINASE	Homo sapiens	1	100,00	100,00	76,57	76,57	gi|14043538	27865,17	7,15
30	PREDICTED: complement component 4 binding protein, alpha isoform 3 [Bos taurus]	Bos taurus	1	99,97	99,97	64,93	64,93	gi|76680061	24697,41	5,71
31	mKIAA0678 protein [Mus musculus] (Predicted: similar to DnaJ (Hsp40) homolog, subfa	Mus musculus	1	99,55	99,55	53,80	53,80	gi|26006199	108883,6	5,65
33	t complex protein-10	Mus musculus	1	97,52	97,52	46,39	46,39	gi|201734	45562,6	5,6
36	MT5-MMP protein [Mus musculus]	Mus musculus	1	96,00	96,00	44,32	44,32	gi|4191265	70361,77	9,5

1.1.1. NTAP-AID fusion TAP3: Tf2/3B

Results with NCBI Gallus database: 42 significant proteins

Rank	Protein Name	Peptide Count	Total Ion Score C.I. %	Best Ion Score C.I. %	Total Ion Score	Best Ion Score	Accession Number	Protein MW	Protein PI
1	unnamed protein product [Gallus gallus] beta-tubulin	13	100,00	111,69	629,00	100,00	gi|63167	50095,14	4,78
2	Tubulin beta-3 chain (Beta-tubulin class-IV)	13	100,00	111,69	576,72	100,00	gi|135464	50285,15	4,78
3	**tubulin alpha**	10	100,00	84,65	519,21	100,00	gi|223280	46258,82	5
4	heat shock cognate 70 [Gallus gallus]	7	100,00	83,66	300,87	100,00	gi|2996407	71011,37	5,47
5	PREDICTED: similar to dedicator of cytokinesis 7 [Gallus gallus]	7	100,00	72,57	188,52	100,00	gi|118094735	240282	6,36
6	Tubulin alpha-2 chain (Testis-specific)	4	100,00	61,95	163,26	100,00	gi|135408	50450,43	4,86
7	heat shock protein Hsp70 [Gallus gallus]	4	100,00	83,66	137,27	100,00	gi|37590083	70097,88	5,66
8	PREDICTED: leucine-rich PPR-motif containing [Gallus gallus]	2	100,00	64,82	100,95	100,00	gi|118087977	157067,9	6,6
9	ubiquitin and ribosomal protein L40 [Gallus gallus]	3	100,00	47,81	93,63	99,88	gi|47604954	15015,08	9,87
10	PREDICTED: similar to abnormal spindle-like [Gallus gallus]	11	100,00	17,92	68,68	0,00	gi|118094036	396344,2	9,99
11	PREDICTED: similar to DnaJ domain-containing protein RME-8 [Gallus gallus]	3	100,00	53,80	65,12	99,97	gi|118085986	256634,5	6,35
12	gonad expressed transcript [Gallus gallus]	5	99,97	20,58	54,16	36,16	gi|60544838	178841,4	8,68
13	**PREDICTED: similar to activation-induced cytidine deaminase [Gallus gallus]**	3	99,91	19,22	49,03	12,69	gi|50729359	24271,34	9,52
14	**ubiquitin (34 AA) (1 is 2nd base in codon) [Gallus gallus]**	1	99,84	47,81	46,63	99,88	gi|833622	3725,891	8,5
15	PREDICTED: similar to extracellular reelin [Gallus gallus]	3	99,75	16,39	44,71	0,00	gi|118082072	406394	5,68
16	PREDICTED: similar to kendrin [Gallus gallus]	2	99,66	27,63	43,29	87,41	gi|118093369	411683,4	5,24
17	DEAD box helicase hypothetical protein [Gallus gallus]	3	99,37	20,06	40,65	28,04	gi|53129029	67769,69	9,48
18	PREDICTED: similar to polydom protein [Gallus gallus]	6	99,34	14,57	40,45	0,00	gi|118104463	394023,6	9,99
19	PREDICTED: similar to ubiquitin-specific protease USP32 [Gallus gallus]	3	99,22	16,69	39,69	0,00	gi|118100328	190511,5	6,11
20	cell division cycle 2-like 5 (cholinesterase-related cell division controller) PREDICTED: hypothetical pr	4	99,22	18,28	39,68	0,00	gi|118086240	183307,3	10,72
21	PREDICTED: similar to putative chromatin structure regulator [Gallus gallus]	2	99,08	30,18	38,97	93,00	gi|118100214	190283	4,79
22	phosphofructokinase, platelet [Gallus gallus]	1	99,01	38,67	38,67	99,01	gi|71895711	61728,38	6,25
23	PREDICTED: similar to beta V spectrin [Gallus gallus]	3	98,97	16,67	38,51	0,00	gi|118091638	405042,6	5,96
24	zinc finger and BTB domain containing 17 PREDICTED: hypothetical protein [Gallus gallus]	3	98,91	19,65	38,25	20,92	gi|118101131	69313,17	12,36
25	ankyrin 1, erythrocytic PREDICTED: hypothetical protein [Gallus gallus]	4	98,76	19,21	37,70	12,49	gi|118101396	97656,75	11,29
26	PREDICTED: similar to progestin induced protein, partial [Gallus gallus]	1	98,69	37,45	37,45	98,69	gi|118109032	14427,17	5,77
27	nebulin [Gallus gallus]	3	98,62	14,80	37,24	0,00	gi|13429929	278101,2	9,18
28	PREDICTED: similar to ADAM metallopeptidase with thrombospondin type 1 motif, 17 preproprotein [	4	98,56	15,48	37,05	0,00	gi|118095948	125508	8,69
29	solute carrier family 25 hypothetical protein [Gallus gallus]	2	98,55	20,13	37,02	29,19	gi|53127891	37910,42	9,33
30	odz, odd Oz/ten-m homolog 4 (Drosophila) PREDICTED: hypothetical protein [Gallus gallus]	3	98,45	19,51	36,73	18,33	gi|118085248	332324,9	9,32
31	PREDICTED: similar to ATAD3A protein [Gallus gallus]	2	98,31	20,09	36,35	28,54	gi|118101028	67239,95	9,45
32	zinc finger protein 92 homolog hypothetical protein [Gallus gallus]	1	97,98	35,58	35,58	97,98	gi|60099021	37034,72	9,33
33	ISY1 splicing factor homolog (S. cerevisiae) PREDICTED: hypothetical protein [Gallus gallus]	2	96,99	19,83	33,84	24,13	gi|50754283	32438,57	5,19
34	PREDICTED: similar to KIAA1285 protein [Gallus gallus]	2	96,95	24,94	33,78	76,61	gi|118085428	122469,1	7,53
35	tight junction protein [Gallus gallus]	2	96,74	29,99	33,50	92,69	gi|3820580	131044,8	6,24
36	ethanolamine kinase 1 PREDICTED: hypothetical protein [Gallus gallus]	3	95,59	12,37	32,19	0,00	gi|118083058	65325,3	9,95
37	family with sequence similarity 110, member B PREDICTED: hypothetical protein [Gallus gallus]	1	95,30	31,91	31,91	95,30	gi|118086978	40934,97	9,38
38	PREDICTED: similar to phosphoinositide-3-kinase, class 2, beta polypeptide [Gallus gallus]	3	95,06	14,64	31,69	0,00	gi|118102381	231672,6	5,92
39	PREDICTED: similar to epsilon-adaptin [Gallus gallus]	2	94,96	18,28	31,61	0,00	gi|118095748	129600,4	5,63
40	PREDICTED: hypothetical protein [Gallus gallus]	2	94,82	17,16	31,48	0,00	gi|118094241	18748,73	11,63
41	PREDICTED: similar to Glutamate receptor, ionotropic, delta 2 [Gallus gallus]	2	94,73	16,37	31,41	0,00	gi|118089961	114744,6	5,98
42	PREDICTED: similar to CLIP-associating protein 2 [Gallus gallus]	3	94,70	17,59	31,39	0,00	gi|118086036	165787,1	8,59

1.1.2. TAPalone TAP3: Tf7/1-16

Results with swissprot database: 7 significant proteins

Rank	Protein Name	Species	Peptide Count	Total Ion Score C.I. %	Best Ion Score C.I. %	Total Ion Score	Best Ion Score	Accession Number	Protein MW	Protein PI
3	(Q8VCR8) Myosin light chain kinase 2, skeletal/cardiac muscle (EC 2.7.11.18) (MLCK2	Mus musculus	1	100,00	100,00	94,30	94,30	MYLK2_MOI	27840,16	6,01
6	(P08108) Heat shock cognate 70 kDa protein (HSP70)	Oncorhynchus	1	99,96	99,96	51,00	51,00	HSP70_ONCI	71581,22	5,24
7	(Q5ZKA5) Bifunctional methylenetetrahydrofolate dehydrogenase/cyclohydrolase, mitoc	Gallus gallus	1	99,88	99,88	46,46	46,46	MTDC_CHIC	36559,66	9,51
9	(Q13557) Calcium/calmodulin-dependent protein kinase type II delta chain (EC 2.7.11.17	Homo sapiens	1	99,35	99,35	39,17	39,17	KCC2D_HUM	56888,77	7,01
5	(Q9CSN1) Nuclear protein SkiP (Ski-interacting protein) (SNW1 protein)	Mus musculus	1	99,18	99,18	38,99	38,99	SNW1_MOUS	61494,52	9,49
6	(Q9QZK9) Deoxyribonuclease II beta precursor (EC 3.1.22.1) (DNase II beta) (DNase2-l	Rattus norvegi	1	96,76	96,76	33,02	33,02	DNS2B_RAT	40959,58	9,33
10	(Q5VZ89) Protein C9orf55	Homo sapiens	1	94,56	94,56	29,94	29,94	CI055_HUMA	182536,3	6,46

Results with NCBI-entire database: 6 significant proteins

Rank	Protein Name	Species	Peptide Count	Total Ion Score C.I. %	Best Ion Score C.I. %	Total Ion Score	Best Ion Score	Accession Number	Protein MW	Protein PI
3	Unknown (protein for IMAGE:4110141) [Homo sapiens]	Homo sapiens	1	100,00	100,00	94,30	94,30	gi|14043538	27865,17	7,15
1	Myosin light chain kinase 2, skeletal/cardiac muscle (MLCK2)	Rattus norvegi	1	100,00	100,00	91,00	91,00	gi|125494	66459,07	5,05
4	restricted expression proliferation associated protein-100 [Gallus gallus]	Gallus gallus	1	99,92	99,92	57,95	57,95	gi|45383291	85469,78	9,54
5	Heat-Shock Cognate 70kd Protein (44kd Atpase N-Terminal Fragment) (E.C.3.6.1.3) Mu	Bos taurus	1	99,60	99,60	51,00	51,00	gi|640325	42542,9	6,63
6	Mthfd2-prov protein [Xenopus laevis]	Xenopus laevi	1	98,85	98,85	46,46	46,46	gi|50418343	36560,25	8,81
7	PREDICTED: similar to Nuclear protein SkiP (Ski-interacting protein) (SNW1 protein) (	Gallus gallus	1	97,55	97,55	43,17	43,17	gi|50748542	61891,68	9,54
10	multifunctional calcium/calmodulin-dependent protein kinase II delta2 isoform [Homo sa	Homo sapiens	1	93,85	93,85	39,17	39,17	gi|4426595	56888,77	7,01

Results with NCBi Gallus database: 5 significant proteins

Rank	Protein Name	Peptide Count	Total Ion Score C.I. %	Best Ion Score C.I. %	Total Ion Score	Best Ion Score	Accession Number	Protein MW	Protein PI
1	hypothetical protein [Gallus gallus] TPX2, microtubule-associated protein homolog [Gallus gallus]	3	100,00	99,99	94,53	57,95	gi|53136376	86081,12	9,56
2	heat shock protein 70 [Gallus gallus]	1	99,97	99,97	51,00	51,00	gi|55742654	69935,75	5,53
3	hypothetical protein [Gallus gallus] methylene tetrahydrofolate dehydrogenase 2 [Gallus gallus]	1	99,92	99,92	46,46	46,46	gi|53131685	36559,66	9,51
4	PREDICTED: hypothetical protein [Gallus gallus]	1	99,84	99,84	43,17	43,17	gi|50748542	61891,68	9,54
5	hypothetical protein [Gallus gallus] calcium/calmodulin-dependent protein kinase (CaM kinase) II delta [	1	99,59	99,59	39,17	39,17	gi|53130868	54738,69	6,66

1.2.1. AID-CTAP fusion TAP10: pST10-10B

Results with swissprot database: 43 significant proteins

Rank	Protein Name	Species	Peptide Count	Total Ion Score C.I. %	Best Ion Score C.I. %	Total Ion Score	Best Ion Score	Accession Number	Protein MW	Protein PI
1	(Q5NVM9) Heat shock cognate 71 kDa protein (Heat shock 70 kDa protein 8)	Pongo pygmae	17	100,00	100,00	1348,39	144,20	HSP7C_PONI	71062,32	5,37
3	(Q9W6Y1) Heat shock cognate 71 kDa protein (Hsc70.1)	Oryzias latipes	11	100,00	100,00	882,05	144,20	HSP7C_ORYI	76577,16	5,8
4	(P68360) Tubulin alpha-1 chain (Alpha-tubulin 1)	Meriones ungu	10	100,00	100,00	818,80	158,97	TBA1_MERU	50803,86	4,94
5	(Q5R1W4) Tubulin alpha-ubiquitous chain (Alpha-tubulin ubiquitous) (Tubulin K-alpha-	Pan troglodyte	10	100,00	100,00	800,65	158,97	TBAK_PANT	50787,9	4,98
6	(P07437) Tubulin beta-2 chain	Homo sapiens	13	100,00	100,00	781,69	122,77	TBB2_HUMA	50095,14	4,78
8	(P68371) Tubulin beta-2C chain (Tubulin beta-2 chain)	Homo sapiens	12	100,00	100,00	661,61	122,77	TBB2C_HUM	50255,17	4,79
9	(P02554) Tubulin beta chain	Sus scrofa	12	100,00	100,00	658,78	122,77	TBB_PIG	50285,12	4,78
10	(Q90473) Heat shock cognate 71 kDa protein (Heat shock 70 kDa protein 8)	Danio rerio	7	100,00	100,00	586,07	144,20	HSP7C_BRAI	71158,08	5,18
12	(P13602) Tubulin beta-2 chain (Beta-2 tubulin)	Xenopus laevis	8	100,00	100,00	521,62	122,77	TBB2_XENL	50148,04	4,81
13	**(P30436) Tubulin alpha chain**	Oncorhynchus	7	100,00	100,00	511,64	115,86	TBA_ONCKE	49967,29	4,92
14	(Q91060) Tubulin alpha chain	Notophthalmu	7	100,00	100,00	496,53	158,97	TBA_NOTVI	50745,64	4,94
16	(Q9NY65) Tubulin alpha-8 chain (Alpha-tubulin 8)	Homo sapiens	6	100,00	100,00	359,70	110,65	TBA8_HUMA	50745,81	4,94
17	(Q28065) C4b-binding protein alpha chain precursor (C4bp)	Bos taurus	7	100,00	100,00	357,27	82,98	C4BP_BOVIN	70951,26	5,99
18	(P02827) Heat shock 70 kDa protein (HSP70)	Xenopus laevis	4	100,00	100,00	284,96	93,39	HSP70_XENI	71270,38	5,32
19	**(Q9GZX7) Activation-induced cytidine deaminase (EC 3.5.4.5) (Cytidine aminohydr**	Homo sapiens	5	100,00	100,00	282,88	92,27	AICDA_HUM	24337,28	9,5
20	(Q9I8F9) Heat shock 70 kDa protein 1 (HSP70-1)	Oryzias latipes	4	100,00	100,00	266,01	93,39	HSP71_ORYI	70649,13	5,47
22	(P02662) Alpha-S1-casein precursor	Bos taurus	4	100,00	100,00	231,95	87,47	CAS1_BOVIN	24570,45	4,98
23	(Q8R1A4) Dedicator of cytokinesis protein 7 (Fragment)	Mus musculus	4	100,00	100,00	212,40	71,50	DOCK7_MOU	84140,5	6,14
24	(P61289) Proteasome activator complex subunit 3 (Proteasome activator 28-gamma subu	Homo sapiens	3	100,00	100,00	210,24	112,81	PSME3_HUM	29601,6	5,69
25	(P11501) Heat shock protein HSP 90-alpha	Gallus gallus	5	100,00	100,00	202,39	84,32	HS90A_CHIC	84405,69	5,01
26	(Q9N1U2) Heat shock 70 kDa protein 6 (Hsp-70-related intracellular vitamin D-binding p	Saguinus oedip	3	100,00	100,00	199,85	92,61	HSP76_SAGO	71568,65	6,06
28	(P08107) Heat shock 70 kDa protein 1 (HSP70.1) (HSP70-1/HSP70-2)	Homo sapiens	3	100,00	100,00	189,50	92,61	HSP71_HUM	70294,14	5,48
31	(Q8K310) Matrin-3	Mus musculus	4	100,00	100,00	173,06	79,10	MATR3_MOU	95085,03	5,87
32	(P02668) Kappa-casein precursor [Contains: Casoxin C; Casoxin 6; Casoxin A; Casoxin I	Bos taurus	2	100,00	100,00	168,20	106,64	CASK_BOVI	21369,93	6,3
34	(P08070) Tubulin alpha-2 chain (Testis-specific)	Gallus gallus	3	100,00	100,00	158,76	71,17	TBA2_CHICH	50450,43	4,86
35	(P05141) ADP/ATP translocase 2 (Adenine nucleotide translocator 2) (ANT 2) (ADP,AT	Homo sapiens	3	100,00	100,00	157,58	80,46	ADT2_HUMA	32971,21	9,76
38	(P02663) Alpha-S2-casein precursor [Contains: Casocidin-1 (Casocidin-I)]	Bos taurus	2	100,00	99,99	106,20	60,80	CAS2_BOVIN	26173,33	8,54
39	(P00340) L-lactate dehydrogenase A chain (EC 1.1.1.27) (LDH-A)	Gallus gallus	1	100,00	100,00	101,66	101,66	LDHA_CHIC	36645,27	7,74
40	(P47859) 6-phosphofructokinase type C (EC 2.7.1.11) (Phosphofructokinase 1) (Phospho	Oryctolagus cu	3	100,00	94,52	84,58	32,71	K6PP_RABIT	87207,31	7,81
42	(Q91437) CAD protein [Includes: Glutamine-dependent carbamoyl-phosphate synthase (I	Squalus acanth	2	100,00	99,24	76,61	41,27	PYR1_SQUA	251116,9	6,44
43	(Q14671) Pumilio homolog 1 (Pumilio-1) (HsPUM)	Homo sapiens	2	100,00	99,66	65,48	44,83	PUM1_HUMA	127078,9	6,35
44	(P84172) Elongation factor Tu, mitochondrial precursor (EF-Tu) (Fragment)	Gallus gallus	1	99,99	99,99	62,79	62,79	EFTU_CHICH	38511,34	8,98
45	(P02754) Beta-lactoglobulin precursor (Beta-LG) (Allergen Bos d 5)	Bos taurus	2	99,91	73,46	50,35	25,86	LACB_BOVI	20269,42	4,93
46	(Q8BL97) Splicing factor, arginine/serine-rich 7	Mus musculus	2	99,89	71,44	49,51	25,54	SFRS7_MOU	31026,92	11,89
47	(Q9NZB2) Protein C9orf10	Homo sapiens	1	99,86	99,86	48,57	48,57	CI010_HUMA	117710,5	9,18
48	(Q9JMC3) DnaJ homolog subfamily A member 4 (MmDjA4)	Mus musculus	1	99,84	99,84	48,04	48,04	DNJA4_MOU	45500,18	7,51
49	(Q9H9L3) Interferon-stimulated 20 kDa exonuclease-like 2 (EC 3.1.-.-)	Homo sapiens	1	99,81	99,81	47,26	47,26	I20L2_HUMA	39414,68	9,94
50	(P49791) Nuclear pore complex protein Nup153 (Nucleoporin Nup153) (153 kDa nucleop	Rattus norvegi	1	99,52	99,52	43,29	43,29	NU153_RAT	154098,4	9,08
51	(P68103) Elongation factor 1-alpha 1 (EF-1-alpha-1) (Elongation factor 1 A-1) (eEF1A-1	Bos taurus	1	99,47	99,47	42,89	42,89	EF1A1_BOVI	50451,24	9,1
52	(P58875) SEC14-like protein 2 (Alpha-tocopherol-associated protein) (TAP) (bTAP)	Bos taurus	1	98,94	98,94	39,85	39,85	S14L2_BOVI	46626,87	8,23
53	(Q8BZN6) Dedicator of cytokinesis protein 10 (Fragment)	Mus musculus	1	98,72	98,72	39,03	39,03	DOC10_MOU	209578,8	8,3
55	(Q4KLP8) Shugoshin-like 1 (Xsgo)	Xenopus laevis	1	95,00	96,18	33,10	34,28	SGOL1_XEN	75219,51	9,55
57	(Q00839) Heterogeneous nuclear ribonucleoprotein U (hnRNP U) (Scaffold attachment fa	Homo sapiens	1	94,80	94,80	32,94	32,94	HNRPU_HUM	91033,22	5,76

1.2.1. AID-CTAP fusion TAP10: pST10-10B

Results with NCBI-entire database: 74 significant proteins

Rank	Protein Name	Species	Peptide Count	Total Ion Score C.I. %	Best Ion Score C.I. %	Total Ion Score	Best Ion Score	Accession Number	Protein MW	Protein PI
1	heat shock protein [Numida meleagris]	Numida melea	17	100,00	100,00	1357,43	144,20	gi|45544523	71055,31	5,37
3	heat shock protein 70 cognate [Silurus meridionalis]	Silurus meridi	11	100,00	100,00	931,16	144,20	gi|126116091	71072,35	5,37
5	Heat shock cognate 71 kDa protein (Hsc70.1)	Oryzias latipes	11	100,00	100,00	882,05	144,20	gi|21263753	76577,16	5,8
6	heat shock protein 8 [Danio rerio]	Danio rerio	10	100,00	100,00	825,42	144,20	gi|56790264	71412,28	5,32
7	unnamed protein product [Xenopus laevis]	Xenopus laevi	10	100,00	100,00	818,80	158,97	gi|65167	50513,77	4,96
8	PREDICTED: similar to Tubulin alpha-2 chain (Alpha-tubulin 2) [Canis familiaris]	Canis familiari	10	100,00	100,00	818,80	158,97	gi|74005772	51778,23	4,98
9	**tubulin, alpha, ubiquitous [Pan troglodytes]**	Pan troglodyte	10	100,00	100,00	800,65	158,97	gi|77539752	50787,9	4,98
11	unnamed protein product [Tetraodon nigroviridis]	Tetraodon nigr	9	100,00	100,00	779,79	158,97	gi|47218560	48551,65	5,14
12	unnamed protein product [Tetraodon nigroviridis]	Tetraodon nigr	11	100,00	100,00	725,51	122,77	gi|47221548	50111,14	4,78
14	alpha tubulin [Gillichthys mirabilis]	Gillichthys mi	7	100,00	100,00	629,07	158,97	gi|16517095	32174,92	5,35
15	hypothetical protein LOC393586 [Danio rerio]	Danio rerio	8	100,00	100,00	619,15	135,71	gi|41055387	71130,18	5,23
16	PREDICTED: similar to Tubulin, alpha 2 isoform 1 [Bos taurus]	Bos taurus	7	100,00	100,00	614,32	158,97	gi|119888608	50554,6	4,93
17	beta-tubulin [Halocynthia roretzi]	Halocynthia ro	10	100,00	100,00	611,87	122,77	gi|2443346	50460,18	4,73
18	unnamed protein product [Mus musculus]	Mus musculus	10	100,00	100,00	605,43	122,77	gi|74144588	50227,14	4,79
19	Chain B, Tubulin Alpha-Beta Dimer, Electron Diffraction	Sus scrofa	10	100,00	100,00	602,60	122,77	gi|3745822	48319,4	5,17
20	beta-2 tubulin [Gadus morhua]	Gadus morhua	9	100,00	100,00	600,10	122,77	gi|5923889	50028,06	4,71
21	HSC71 [Rivulus marmoratus]	Kryptolebias n	9	100,00	100,00	595,71	93,39	gi|7960186	71832,51	5,28
22	matrin 3 [Gallus gallus]	Gallus gallus	10	100,00	100,00	591,32	79,11	gi|45383822	101164,1	5,79
23	unnamed protein product [Tetraodon nigroviridis]	Tetraodon nigr	7	100,00	100,00	584,38	158,97	gi|47229080	54084,68	5,49
24	hypothetical protein LOC767746 [Danio rerio]	Danio rerio	9	100,00	100,00	559,74	122,77	gi|115529301	50013,08	4,85
25	PREDICTED: similar to Heat shock cognate 71 kDa protein (Heat shock 70 kDa protein 8	Canis familiari	7	100,00	100,00	550,28	132,53	gi|74008507	44232,59	5,33
27	Tubulin alpha chain	Oncorhynchus	7	100,00	100,00	511,64	115,86	gi|267071	49967,29	4,92
28	unnamed protein product [Tetraodon nigroviridis]	Tetraodon nigr	6	100,00	100,00	508,82	158,97	gi|47229078	46678,98	4,83
29	Tubulin alpha chain	Notophthalmu	6	100,00	100,00	468,92	158,97	gi|3024695	50745,64	4,94
31	alpha tubulin [Chionodraco rastrospinosus]	Chionodraco r	6	100,00	100,00	379,93	115,86	gi|10242286	50832,86	4,98
32	Mec-12 protein [Xenopus laevis]	Xenopus laevi	5	100,00	100,00	370,55	115,86	gi|50414753	50539,59	4,95
33	PREDICTED: hypothetical protein [Gallus gallus]	Gallus gallus	5	100,00	100,00	368,11	158,97	gi|118102310	50709,76	5,01
34	complement component 4 binding protein, alpha [Bos taurus]	Bos taurus	6	100,00	100,00	333,54	82,98	gi|27806291	70951,26	5,99
35	PREDICTED: hypothetical protein [Monodelphis domestica]	Monodelphis d	4	100,00	100,00	298,13	158,97	gi|126306763	50642,71	4,93
36	Unknown (protein for MGC:83630) [Xenopus laevis]	Xenopus laevi	4	100,00	100,00	284,96	93,39	gi|50415517	71404,42	5,32
37	inducible heat shock protein 70 [Rhabdosargus sarba]	Rhabdosargus	4	100,00	100,00	272,48	93,39	gi|40888897	70434,83	5,31
38	tubulin, alpha 2 [Danio rerio]	Danio rerio	5	100,00	99,99	257,72	71,17	gi|37362304	50686,71	5,02
39	**activation-induced cytidine deaminase [Homo sapiens]**	Homo sapiens	4	100,00	100,00	256,26	92,27	gi|10190700	24337,28	9,5
40	PREDICTED: similar to Tubulin beta-6 chain (Beta-tubulin class-VI) [Danio rerio]	Danio rerio	5	100,00	100,00	256,76	85,03	gi|125819301	52943,68	4,9
41	**AID [Homo sapiens]**	Cricetulus gris	4	100,00	100,00	256,26	92,27	gi|22297300	22268,16	9,37
42	PREDICTED: similar to dedicator of cytokinesis 7 [Gallus gallus]	Gallus gallus	5	100,00	99,99	252,29	71,50	gi|118094735	240282	6,36
43	heat shock 70 kDa protein 8 [Ictalurus punctatus]	Ictalurus punct	4	100,00	99,99	251,06	72,59	gi|90103366	10446,48	4,88
44	Hsp70 protein [Odontaspis ferox]	Odontaspis fer	3	100,00	100,00	249,89	135,71	gi|21427254	50809,53	6,57
46	alpha-tubulin 2 [Ciona intestinalis]	Ciona intestina	3	100,00	100,00	227,81	86,66	gi|21667229	44580,01	5,85
48	Unknown (protein for MGC:160383) [Xenopus laevis]	Xenopus laevi	4	100,00	99,99	218,71	69,98	gi|120538297	51688,48	5,24
49	Tuba8 protein [Xenopus laevis]	Xenopus laevi	4	100,00	99,99	213,46	69,98	gi|49117900	51776,43	5,24

50	Ki nuclear autoantigen - bovine (fragment)	Bos taurus	3	100,00	100,00	210,24	112,81	gi|321229	27927,64	5,77
51	PREDICTED: similar to Heat shock cognate 71 kDa protein (Heat shock 70 kDa protein 8	Canis familiari	3	100,00	100,00	207,96	104,55	gi|73999370	21758,62	4,78
52	casein alphaS1	Bos taurus	3	100,00	100,00	204,93	87,47	gi|225632	24477,38	4,85
53	Heat shock 70 kDa protein 6 (Hsp-70-related intracellular vitamin D-binding protein)	Saguinus oedip	3	100,00	100,00	199,85	92,61	gi|50400671	71568,65	6,06
54	PREDICTED: similar to C4b-binding protein alpha chain [Bos taurus]	Bos taurus	4	100,00	99,88	195,73	60,37	gi|76677514	22393,34	6,34
55	Chain A, Heat-Shock 70kd Protein 42kd Atpase N-Terminal Domain	Homo sapiens	3	100,00	100,00	189,50	92,61	gi|6729803	41972,74	6,69
56	PREDICTED: similar to glutamine rich protein [Gallus gallus]	Gallus gallus	3	100,00	99,99	189,46	72,24	gi|118094814	147864,4	5,64
57	kappa casein	Bos taurus	2	100,00	100,00	168,20	106,64	gi|226020	21253,92	7,74
58	PREDICTED: similar to ADP/ATP translocase 2 (Adenine nucleotide translocator 2) (AN	Canis familiari	3	100,00	100,00	158,76	80,46	gi|74008184	27930,6	9,64
59	tubulin, alpha 8 [Gallus gallus]	Gallus gallus	3	100,00	99,99	158,76	71,17	gi|45382095	50450,43	4,86
61	tubulin, alpha 4, isoform CRA_b [Homo sapiens]	Homo sapiens	2	100,00	100,00	149,66	110,65	gi|119591127	27784,89	8,66
62	unnamed protein product [Mus musculus]	Mus musculus	2	100,00	99,97	130,79	66,12	gi|74177777	54545,51	5,83
63	90-kDa heat shock protein [Sus scrofa]	Sus scrofa	2	100,00	100,00	121,35	84,32	gi|47522774	85120,86	4,93
64	LOC496021 protein [Xenopus laevis]	Xenopus laevis	2	100,00	99,99	106,50	71,17	gi|56269174	50088,43	5,02
65	casein alpha-S2 [Bos taurus]	Bos taurus	2	100,00	99,89	106,20	60,80	gi|27806963	26173,33	8,54
66	lactate dehydrogenase A [Gallus gallus]	Gallus gallus	1	100,00	100,00	101,66	101,66	gi|45384208	36776,31	7,75
70	PREDICTED: similar to Rho guanine nucleotide exchange factor 3 (Exchange factor four	Canis familiari	2	100,00	98,42	83,82	49,10	gi|73985381	101776,9	9,08
72	Unknown (protein for IMAGE:7592068) [Xenopus tropicalis]	Xenopus tropic	2	100,00	90,44	76,61	41,27	gi|138519856	248785,6	6,08
73	PREDICTED: similar to nuclear pore complex protein hnup153 [Gallus gallus]	Gallus gallus	2	100,00	94,00	76,12	43,29	gi|118086393	154357,8	9,19
74	MGC131121 protein [Xenopus laevis]	Xenopus laevis	1	99,99	99,99	72,62	72,62	gi|76780144	43014,85	5,09
75	heat shock protein 90 [Bufo gargarizans]	Bufo gargariza	1	99,99	99,99	70,43	70,43	gi|89515102	81482,34	5,09
76	PREDICTED: similar to Elongation factor Tu, mitochondrial precursor (EF-Tu), partial [(	Gallus gallus	1	99,93	99,93	62,79	62,79	gi|118127631	6271,02	6,45
77	hCG1747788 [Homo sapiens]	Homo sapiens	1	99,73	99,73	56,80	56,80	gi|119608911	14782,88	4,74
79	PREDICTED: similar to T07C4.10 [Rattus norvegicus]	Rattus norvegi	1	99,38	99,38	53,14	53,14	gi|109470433	121266,7	5,47
80	hypothetical protein LOC23196 [Homo sapiens]	Homo sapiens	1	98,22	98,22	48,57	48,57	gi|39652628	123008	9,07
81	DnaJ (Hsp40) homolog, subfamily A, member 4 [Rattus norvegicus]	Rattus norvegi	1	97,99	97,99	48,04	48,04	gi|70794764	62521,53	8,71
82	Dnaja1-prov protein [Xenopus laevis]	Xenopus laevis	1	97,99	97,99	48,04	48,04	gi|27503357	45726,97	6,87
83	MGC64353 protein [Xenopus laevis]	Xenopus laevis	1	97,99	97,99	48,04	48,04	gi|32450126	45341,77	6,25
84	PREDICTED: hypothetical protein isoform 8 [Pan troglodytes]	Pan troglodyte	1	97,59	97,59	47,26	47,26	gi|55588378	39286,58	9,93
85	PREDICTED: leucine-rich PPR-motif containing [Gallus gallus]	Gallus gallus	1	96,99	97,71	46,29	47,47	gi|118087977	157067,9	6,6
86	PREDICTED: centrosomal protein 170kDa isoform 1 [Gallus gallus]	Gallus gallus	1	96,51	96,51	45,64	45,64	gi|118088102	173321,9	6,86
87	pumilio [Xenopus laevis]	Xenopus laevis	1	95,79	95,79	44,83	44,83	gi|12082247	64323,01	8,93
88	similar to elongation factor 1 alpha [Bos taurus]	Bos taurus	1	93,42	93,42	42,89	42,89	gi|28189733	17940,3	8,44

1.2.1. AID-CTAP fusion TAP10: pST10-10B
Results with NCBI Gallus database: 40 significant proteins

Rank	Protein Name	Peptide Count	Total Ion Score C.I. %	Best Ion Score C.I. %	Total Ion Score	Best Ion Score	Accession Number	Protein MW	Protein PI
1	heat shock cognate 70 [Gallus gallus]	16	100,00	100,00	1175,66	144,20	gi|2996407	71011,37	5,47
2	unnamed protein product [Gallus gallus] **TUBULIN**	13	100,00	100,00	781,69	122,77	gi|63167	50095,14	4,78
3	**tubulin alpha**	8	100,00	100,00	731,21	158,97	gi|223280	46258,81	5
4	nuclear protein matrin 3 [Gallus gallus]	12	100,00	100,00	632,20	79,11	gi|17221616	101164,1	5,79
5	c-beta-3 beta-tubulin	11	100,00	100,00	627,05	122,77	gi|212830	50285,15	4,78
6	Tubulin beta-4 chain (Beta-tubulin class-III)	10	100,00	100,00	577,87	122,77	gi|135468	50844,44	4,86
7	heat shock protein Hsp70 [Gallus gallus]	7	100,00	100,00	553,45	135,71	gi|37590083	70097,88	5,66
8	Tubulin alpha-5 chain	5	100,00	100,00	385,27	115,86	gi|135423	50714,69	4,95
9	PREDICTED: hypothetical protein [Gallus gallus]	5	100,00	100,00	368,11	158,97	gi|118102310	50709,76	5,01
10	Tubulin beta-5 chain (Beta-tubulin class-V)	7	100,00	100,00	359,18	97,81	gi|135469	50395,24	4,79
11	PREDICTED: similar to dedicator of cytokinesis 7 [Gallus gallus]	6	100,00	100,00	272,12	71,50	gi|118094735	240282	6,36
12	PREDICTED: similar to alpha-tubulin 8 [Gallus gallus]	4	100,00	100,00	262,40	110,65	gi|50729032	50759,83	5,01
13	PREDICTED: similar to glutamine rich protein [Gallus gallus]	5	100,00	100,00	232,52	72,24	gi|118094814	147864,4	5,64
14	hypothetical protein [Gallus gallus] Proteasome activator complex subunit 3 (Proteasome activator 28-ga	3	100,00	100,00	210,24	112,81	gi|60098917	29519,63	5,85
15	Heat shock protein HSP 90-alpha	5	100,00	100,00	202,39	84,32	gi|123668	84405,69	5,01
16	PREDICTED: similar to Tubulin alpha-3 chain [Gallus gallus]	3	100,00	100,00	189,73	71,17	gi|118081928	28739,38	5,35
17	Tubulin alpha-2 chain (Testis-specific)	4	100,00	100,00	178,10	71,17	gi|135408	50450,43	4,86
18	solute carrier family 25 (mitochondrial carrier; adenine nucleotide translocator), member 6 [Gallus gallus	3	100,00	100,00	157,58	80,46	gi|54020693	32955,17	9,73
19	**PREDICTED: similar to activation-induced cytidine deaminase [Gallus gallus]**	2	100,00	100,00	152,35	92,27	gi|50729359	24271,34	9,52
20	PREDICTED: leucine-rich PPR-motif containing [Gallus gallus]	4	100,00	99,89	108,85	47,47	gi|118087977	157067,9	6,6
21	unnamed protein product [Gallus gallus] L-lactate dehydrogenase A chain (LDH-A)	1	100,00	100,00	101,66	101,66	gi|63566	36776,31	7,75
24	hypothetical protein [Gallus gallus] phosphofructokinase, platelet [Gallus gallus]	3	100,00	96,57	81,29	32,71	gi|53136740	61728,38	6,25
25	PREDICTED: similar to nuclear pore complex protein hnup153 [Gallus gallus]	2	100,00	99,70	76,12	43,29	gi|118086393	154357,8	9,19
26	nuclear calmodulin-binding protein [Gallus gallus]	2	100,00	97,96	65,59	34,96	gi|3822553	84697,49	4,68
27	pumilio 1 [Gallus gallus]	2	100,00	99,79	65,48	44,83	gi|82569972	127282,1	6,34
28	Elongation factor Tu, mitochondrial precursor (EF-Tu)	1	100,00	100,00	62,79	62,79	gi|88909611	38511,34	8,98
29	downstream of kinase 3 [Gallus gallus]	2	99,99	96,85	57,01	33,08	gi|124110115	47821,65	6,61
31	hypothetical protein [Gallus gallus] splicing factor, arginine/serine-rich 7 [Gallus gallus]	2	99,93	82,12	49,51	25,54	gi|53127360	26213,43	11,79
33	PREDICTED: hypothetical protein [Gallus gallus]	1	99,91	99,91	48,57	48,57	gi|118096811	123653,4	9,05
34	PREDICTED: similar to pDJA1 chaperone [Gallus gallus]	1	99,90	99,90	48,04	48,04	gi|118095620	45457,64	5,78
35	hypothetical protein [Gallus gallus] DnaJ (Hsp40) homolog, subfamily A, member 1 [Gallus gallus]	1	99,90	99,90	48,04	48,04	gi|53133322	45361,8	6,9
36	hypothetical protein [Gallus gallus] PREDICTED: centrosomal protein 170kDa isoform 1 [Gallus gallus]	1	99,83	99,83	45,64	45,64	gi|53133410	129183,2	7,94
37	hypothetical protein [Gallus gallus] Elongation factor 1-alpha 1 (EF-1-alpha-1) (Elongation factor Tu) (E	1	99,67	99,67	42,89	42,89	gi|53130784	50449,27	9,1
38	hypothetical protein [Gallus gallus] Stress-70 protein, mitochondrial precursor (75 kDa glucose-regulate	2	99,47	49,83	40,81	21,06	gi|53127632	73431,92	6,09
39	PREDICTED: dedicator of cytokinesis 10 [Gallus gallus]	1	99,20	99,20	39,03	39,03	gi|118095033	252058,7	6,54
40	heterogeneous nuclear ribonucleoprotein U, MARs binding protein p120, hnRNP U=matrix attachment r	1	96,75	96,75	32,94	32,94	gi|546484	1646,84	5,91
41	PREDICTED: similar to LOC443719 protein [Gallus gallus]	1	96,51	96,51	32,64	32,64	gi|118099808	54250,38	9,06
42	hypothetical protein [Gallus gallus] heterogeneous nuclear ribonucleoprotein H1 (H) [Gallus gallus]	1	95,25	95,25	31,30	31,30	gi|60098931	54691,77	5,49
43	PREDICTED: hypothetical protein [Gallus gallus]	1	94,37	94,37	30,56	30,56	gi|118107414	32041,84	9,7
44	PREDICTED: hypothetical protein [Gallus gallus]	1	91,97	91,97	29,02	29,02	gi|118104387	49153,13	9,18

1.2.2. TAPalone TAP10: pSK1-1A

Results with swissprot database: 15 significant proteins

Rank	Protein Name	Species	Peptide Count	Total Ion Score C.I. %	Best Ion Score C.I. %	Total Ion Score	Best Ion Score	Accession Number	Protein MW	Protein PI
5	(Q28065) C4b-binding protein alpha chain precursor (C4bp)	Bos taurus	3	100,00	99,99	148,60	55,67	C4BP_BOVIN	70951,26	5,99
6	(P07437) Tubulin beta-2 chain	Homo sapiens	3	100,00	99,94	101,02	48,90	TBB2_HUMA	50095,14	4,78
7	(P00340) L-lactate dehydrogenase A chain (EC 1.1.1.27) (LDH-A)	Gallus gallus	1	100,00	100,00	82,70	82,70	LDHA_CHIC	36645,27	7,74
8	(O35737) Heterogeneous nuclear ribonucleoprotein H (hnRNP H)	Mus musculus	2	100,00	99,99	76,07	58,19	HNRH1_MOU	49322,46	5,89
9	(Q00839) Heterogeneous nuclear ribonucleoprotein U (hnRNP U) (Scaffold attachment fa	Homo sapiens	1	100,00	100,00	76,02	76,02	HNRPU_HUM	91033,22	5,76
10	(Q9WV03) Protein FAM50A (XAP-5 protein)	Mus musculus	1	99,99	99,99	56,62	56,62	FA50A_MOU	40226,58	6,39
11	(P02552) Tubulin alpha-1 chain (Fragment)	Gallus gallus	2	99,99	99,31	56,14	38,51	TBA1_CHICK	46384,82	4,96
12	(P08108) Heat shock cognate 70 kDa protein (HSP70)	Oncorhynchus	1	99,99	99,99	56,07	56,07	HSP70_ONCM	71581,22	5,24
13	(P68371) Tubulin beta-2C chain (Tubulin beta-2 chain)	Homo sapiens	2	99,97	95,71	52,12	30,56	TBB2C_HUM	50255,17	4,79
14	(P68103) Elongation factor 1-alpha 1 (EF-1-alpha-1) (Elongation factor 1 A-1) (eEF1A-1	Bos taurus	1	99,95	99,95	50,06	50,06	EF1A1_BOVI	50451,24	9,1
15	(Q8K310) Matrin-3	Mus musculus	1	99,58	99,58	40,68	40,68	MATR3_MOU	95085,03	5,87
16	(Q5SW75) Protein phosphatase Slingshot homolog 2 (EC 3.1.3.48) (EC 3.1.3.16) (SSH-2	Mus musculus	1	99,52	99,52	40,06	40,06	SSH2_MOUS	160069,2	5,43
17	(Q7SIG6) Development and differentiation-enhancing factor 2 (Pyk2 C-terminus-associat	Mus musculus	1	98,14	98,14	34,18	34,18	DDEF2_MOU	107992,4	6,22
18	(Q14980) Nuclear mitotic apparatus protein 1 (NuMA protein) (SP-H antigen)	Homo sapiens	1	97,25	97,25	32,49	32,49	NUMA1_HUM	239213,6	5,63
19	(O97592) Dystrophin	Canis familiari	1	95,22	95,22	30,09	30,09	DMD_CANFA	427384,5	5,68

Results with NCBI-entire database: 17 significant proteins

Rank	Protein Name	Species	Peptide Count	Total Ion Score C.I. %	Best Ion Score C.I. %	Total Ion Score	Best Ion Score	Accession Number	Protein MW	Protein PI
2	PREDICTED: leucine-rich PPR-motif containing [Gallus gallus]	Gallus gallus	6	100,00	66,01	99,98	273,51	gi|118087977	157067,9	6,6
4	matrin 3 [Gallus gallus]	Gallus gallus	4	100,00	109,78	100,00	269,29	gi|45383822	101164,1	5,79
8	complement component 4 binding protein, alpha [Bos taurus]	Bos taurus	3	100,00	55,67	99,83	148,60	gi|27806291	70951,26	5,99
9	PREDICTED: similar to C4b-binding protein alpha chain [Bos taurus]	Bos taurus	3	100,00	64,55	99,98	134,53	gi|76677514	22393,34	6,34
10	lactate dehydrogenase A [Gallus gallus]	Gallus gallus	1	100,00	82,70	100,00	82,70	gi|45384208	36776,31	7,75
11	unnamed protein product [Mus musculus] **beta TUBULIN**	Mus musculus	2	100,00	48,90	99,21	79,46	gi|12846758	50064,14	4,78
12	scaffold attachment factor A [Homo sapiens]	Homo sapiens	1	100,00	76,02	100,00	76,02	gi|3202000	91164,26	5,76
14	PREDICTED: similar to eukaryotic translation elongation factor 1 alpha 2 isoform 1 [Car	Canis familiari	1	99,93	59,49	99,93	59,49	gi|74006680	13734,73	8,52
15	heterogeneous nuclear ribonucleoprotein H1 [Mus musculus]	Mus musculus	1	99,91	58,19	99,91	58,19	gi|10946928	49453,5	5,89
16	PREDICTED: similar to heterogeneous nuclear ribonucleoprotein H1-like protein [Danio	Danio rerio	1	99,91	58,19	99,91	58,19	gi|125833107	44245,05	8,88
17	Protein FAM50A (XAP-5 protein)	Mus musculus	1	99,87	56,62	99,87	56,62	gi|48474706	40226,58	6,39
18	Chain A, E175s Mutant Of Bovine 70 Kilodalton Heat Shock Protein	Bos taurus	1	99,85	56,07	99,85	56,07	gi|6137549	41525,37	6,16
19	splicing factor 4-like protein [Ictalurus punctatus]	Ictalurus punct	1	99,69	54,14	99,76	52,96	gi|87619629	17447,75	9,57
20	similar to elongation factor 1 alpha [Bos taurus]	Bos taurus	1	99,40	50,06	99,40	50,06	gi|28189733	17940,3	8,44
21	phosphofructokinase, platelet [Gallus gallus]	Gallus gallus	1	97,87	44,58	97,87	44,58	gi|71895711	61728,38	6,25
22	PREDICTED: hypothetical protein [Macaca mulatta]	Macaca mulatt	1	95,45	41,29	95,45	41,29	gi|109094473	9628,85	6,89

1.2.2. TAPalone TAP10: pSK1-1A

Results with NCBI Gallus database: 18 significant proteins

Rank	Protein Name	Peptide Count	Total Ion Score C.I. %	Best Ion Score C.I. %	Total Ion Score	Best Ion Score	Accession Number	Protein MW	Protein PI
1	PREDICTED: leucine-rich PPR-motif containing [Gallus gallus]	8	100,00	100,00	317,26	66,01	gi|118087977	157067,9	6,6
2	nuclear protein matrin 3 [Gallus gallus]	4	100,00	100,00	269,29	109,78	gi|17221616	101164,1	5,79
3	unnamed protein product [Gallus gallus]	3	100,00	99,96	101,02	48,90	gi|63167	50095,14	4,78
4	unnamed protein product [Gallus gallus] L-lactate dehydrogenase A chain (LDH-A)	1	100,00	100,00	82,70	82,70	gi|63566	36776,31	7,75
5	hypothetical protein [Gallus gallus] heterogeneous nuclear ribonucleoprotein H1-like protein [Gallus gall	2	100,00	100,00	76,07	58,19	gi|60098931	54691,77	5,49
6	heterogeneous nuclear ribonucleoprotein U, MARs binding protein p120, hnRNP U=matrix attachment r	1	100,00	100,00	76,02	76,02	gi|546484	1646,84	5,91
7	PREDICTED: similar to dedicator of cytokinesis 7 [Gallus gallus]	3	100,00	96,98	66,20	30,07	gi|118094735	240282	6,36
8	hypothetical protein [Gallus gallus] phosphofructokinase, platelet [Gallus gallus]	2	100,00	99,89	60,29	44,58	gi|53136740	61728,38	6,25
9	Tubulin alpha-1 chain	2	99,99	99,57	56,14	38,51	gi|135393	46384,82	4,96
10	heat shock protein Hsp70 [Gallus gallus]	1	99,99	99,99	56,07	56,07	gi|37590083	70097,88	5,66
11	PREDICTED: similar to RNA-binding protein splice [Gallus gallus]	1	99,98	99,99	52,96	54,14	gi|118103255	73606,93	6,11
12	c-beta-3 beta-tubulin	2	99,98	97,30	52,12	30,56	gi|212830	50285,15	4,78
13	hypothetical protein [Gallus gallus] Elongation factor 1-alpha 1 (EF-1-alpha-1) (Elongation factor Tu) (E	1	99,97	99,97	50,06	50,06	gi|53130784	50449,27	9,1
15	PREDICTED: similar to glutamine rich protein [Gallus gallus]	1	99,47	99,60	37,67	38,85	gi|118094814	147864,4	5,64
16	hypothetical protein [Gallus gallus] PREDICTED: centrosomal protein 170kDa isoform 1 [Gallus gallus]	1	98,89	98,89	34,41	34,41	gi|53133410	129183,2	7,94
17	PREDICTED: similar to KIAA0400 [Gallus gallus]	1	98,83	98,83	34,18	34,18	gi|118088999	112450	6,54
18	PREDICTED: hypothetical protein [Gallus gallus]	1	97,81	97,81	31,48	31,48	gi|118118493	13871,23	11,89
20	PREDICTED: hypothetical protein [Gallus gallus]	1	96,03	96,03	28,89	28,89	gi|118085635	65379,64	9,18

Appendix 2 - MASCOT analysis of TAP of Rad18 Fusions

2.1.1. Rad18-HA-CTAP fusion TAP8(12): Tf9/1-1
Results with NCBI Gallus database: 25 significant proteins

Rank	Protein Name	Peptide Count	Total Ion Score C.I. %	Best Ion Score C.I. %	Total Ion Score	Best Ion Score	Accession Number	Protein MW	Protein PI
1	**hypothetical protein [Gallus gallus] Rad18**	16	100,00	100,00	1228,31	158,84	gi|53135182	56241,34	8,54
2	heat shock cognate 70 [Gallus gallus]	6	100,00	100,00	269,70	122,84	gi|2996407	71011,37	5,47
3	nuclear protein matrin 3 [Gallus gallus]	5	100,00	99,98	205,20	55,68	gi|17221616	101164,1	5,79
4	PREDICTED: similar to glutamine rich protein [Gallus gallus]	5	100,00	100,00	168,36	67,45	gi|118094814	147864,4	5,64
5	PREDICTED: similar to dedicator of cytokinesis 7 [Gallus gallus]	5	100,00	99,67	152,41	43,03	gi|118094735	240282	6,36
6	PREDICTED: similar to Heterogeneous nuclear ribonucleoprotein U (scaffold attachment factor A) [Gal	3	100,00	100,00	141,81	79,57	gi|118088143	78452,08	9,56
9	PREDICTED: similar to ribosomal protein S8 [Gallus gallus]	2	100,00	99,99	88,88	56,88	gi|50751488	30838,53	10,42
10	**Jun-binding protein**	2	100,00	99,71	84,21	43,59	gi|387587	24427,68	10,14
11	PREDICTED: hypothetical protein [Gallus gallus] Ribosomal protein L27a	2	100,00	98,21	67,52	35,73	gi|118091246	16912,16	10,86
12	unnamed protein product [Gallus gallus] Tubulin beta-7 chain	2	100,00	96,91	63,87	33,36	gi|63167	50095,14	4,78
13	PREDICTED: similar to thyroid hormone receptor activator molecule [Gallus gallus]	1	99,98	99,98	55,64	55,64	gi|118100627	153644,7	7,83
14	**PREDICTED: similar to ribosomal protein L18a [Gallus gallus]**	2	99,97	91,68	54,23	29,06	gi|118082381	35199,53	11,5
15	hypothetical protein [Gallus gallus] ribosomal protein L4	2	99,89	77,10	47,65	24,66	gi|53135834	47005,83	11,11
16	PREDICTED: leucine-rich PPR-motif containing [Gallus gallus]	2	99,79	70,97	45,12	23,63	gi|118087977	157067,9	6,6
17	hypothetical protein [Gallus gallus] Elongation factor 1-alpha	2	99,79	80,33	45,06	25,32	gi|53130784	50449,27	9,1
18	hypothetical protein [Gallus gallus] 60S ribosonal protein L7	2	99,71	68,89	43,62	23,33	gi|53133816	28819,08	10,83
19	PREDICTED: similar to mKIAA0870 protein [Gallus gallus] DENN/MADD domain containing 3	2	99,66	64,61	42,93	22,77	gi|118087416	147388,2	7,37
20	**ubiquitin-conjugating enzyme [Gallus gallus] Rad6**	1	99,24	99,24	39,43	39,43	gi|4883773	17418,55	5,06
21	PREDICTED: similar to Ribosomal protein L8 [Gallus gallus]	1	99,22	99,22	39,36	39,36	gi|118083996	27165,86	11,12
22	PREDICTED: similar to DEAD (Asp-Glu-Ala-Asp) box polypeptide 17 [Gallus gallus]	1	99,11	99,32	38,74	39,92	gi|118082784	73679,55	8,85
23	**erythrocyte histone deacetylase [Gallus gallus]**	1	98,83	98,83	37,57	37,57	gi|2829214	55416,94	5,32
24	ribosomal protein L36 [Gallus gallus]	1	98,40	98,40	36,23	36,23	gi|12381879	12401,93	11,34
25	ribosomal protein L7a [Gallus gallus]	1	96,34	96,34	32,63	32,63	gi|52138653	30209	10,51
26	hypothetical protein [Gallus gallus] Pre-mRNA-slicing factor SLU7	1	95,16	95,16	31,41	31,41	gi|53136057	65779,56	6,77
27	hypothetical protein [Gallus gallus] small nuclear ribonucleoprotein D3 polypeptide 18kDa	1	94,91	94,91	31,19	31,19	gi|53130412	14021,35	10,33

2.1.2. NTAP-HA-Rad18 fusion TAP8(12): Tf9/3-3
Results with NCBI Gallus database: 17 significant proteins

Rank	Protein Name	Peptide Count	Total Ion Score C.I. %	Best Ion Score C.I. %	Total Ion Score	Best Ion Score	Accession Number	Protein MW	Protein PI
1	**hypothetical protein [Gallus gallus] Rad18**	23	100,00	100,00	1713,03	154,23	gi|53135182	56241,34	8,54
2	heat shock cognate 70 [Gallus gallus]	6	100,00	100,00	378,32	109,23	gi|2996407	71011,37	5,47
4	c-beta-3 beta-tubulin	7	100,00	100,00	229,40	70,08	gi|212830	50285,15	4,78
5	heat shock protein Hsp70 [Gallus gallus]	4	100,00	100,00	228,26	109,23	gi|37590083	70097,88	5,66
7	PREDICTED: similar to glutamine rich protein [Gallus gallus]	5	100,00	100,00	200,79	72,56	gi|118094814	147864,4	5,64
8	nuclear protein matrin 3 [Gallus gallus]	5	100,00	100,00	192,12	75,18	gi|17221616	101164,1	5,79
9	**Jun-binding protein**	3	100,00	100,00	155,35	85,40	gi|387587	24427,68	10,14
10	hypothetical protein [Gallus gallus] coatomer protein complex, subunit alpha [Gallus gallus]	5	100,00	99,73	148,07	43,97	gi|60099199	140060,4	7,53
12	PREDICTED: similar to beta prime cop [Gallus gallus]	3	100,00	100,00	142,21	65,30	gi|118094989	103935,2	5,11
14	hypothetical protein [Gallus gallus] Stress-70 protein, mitochondrial precursor (75 kDa glucose-regulatec	2	100,00	100,00	127,57	70,74	gi|53127632	73431,92	6,09
15	**PREDICTED: similar to ribosomal protein L18a [Gallus gallus]**	3	100,00	99,52	102,69	41,48	gi|118082381	35199,53	11,5
16	hypothetical protein [Gallus gallus] proteosome activator complex subunit 3	3	100,00	99,95	97,32	51,60	gi|60098917	29519,63	5,85
17	**ribosomal protein S3A [Gallus gallus]**	2	100,00	99,94	88,63	50,50	gi|129270064	30075,79	9,74
18	hypothetical protein [Gallus gallus] heterogeneous nuclear ribonucleoprotein H1 (H) [Gallus gallus]	2	100,00	99,97	85,18	53,15	gi|60098931	54691,77	5,49
19	PREDICTED: similar to Heterogeneous nuclear ribonucleoprotein U (scaffold attachment factor A) [Gal	2	100,00	99,98	80,34	55,95	gi|118088143	78452,08	9,56
20	60S ribosomal protein L15 (L10)	2	100,00	99,68	80,00	43,19	gi|1710491	19350,55	11,77
21	PREDICTED: similar to DNA strand-exchange protein SEP1 isoform 2 [Gallus gallus]	1	100,00	100,00	74,02	74,02	gi|118095037	194669,4	7,36
23	hypothetical protein [Gallus gallus] phosphofructokinase, platelet [Gallus gallus]	2	100,00	95,69	62,64	31,91	gi|53136740	61728,38	6,25
24	hypothetical protein [Gallus gallus] Enah/Vasp-like [Gallus gallus]	2	99,98	97,28	56,43	33,91	gi|53136370	44817,27	9,05
25	hypothetical protein [Gallus gallus] ribosomal protein L4 [Gallus gallus]	2	99,98	96,39	56,04	32,67	gi|53135834	47005,83	11,11
26	PREDICTED: similar to Rpl17 protein [Gallus gallus]	1	99,98	99,98	55,34	55,34	gi|50806588	21611,45	10,2
28	hypothetical protein [Gallus gallus] Elongation factor 1-alpha 1 (EF-1-alpha-1) (Elongation factor Tu) (E	2	99,95	94,79	51,28	31,08	gi|53130784	50449,27	9,1
29	**Rho GTPase activating protein 25 [Gallus gallus] hypothetical protein [Gallus gallus]**	1	99,93	99,93	50,01	50,01	gi|53133822	73601,97	6,54
30	unnamed protein product [Gallus gallus] 60S ribosomal protein L13 (Breast basic conserved protein 1)	1	99,90	99,90	48,36	48,36	gi|516684	24437,61	11,75
31	hypothetical protein [Gallus gallus] heterogeneous nuclear ribonucleoprotein M [Gallus gallus]	2	99,89	88,68	47,95	27,71	gi|53130368	76257,4	8,88
32	PREDICTED: similar to calcineurin A alpha [Gallus gallus]	2	99,84	68,88	46,16	23,32	gi|118090406	50625,3	5,6
33	ribosomal protein S8 [Gallus gallus]	1	99,79	99,79	44,94	44,94	gi|44968182	22112,91	10,18
34	PREDICTED: similar to MGC89673 protein [Gallus gallus]	1	99,70	99,70	43,42	43,42	gi|118095675	54347,38	8,59
35	ribosomal protein L18 [Gallus gallus]	1	99,61	99,61	42,36	42,36	gi|44968046	18894,64	11,84
36	PREDICTED: similar to Leucine-rich repeats and calponin homology (CH) domain containing 3 [Gallus	1	99,19	99,19	39,14	39,14	gi|118095156	88073,43	6,41
37	60S acidic ribosomal protein P0 (L10E)	1	99,13	99,13	38,84	38,84	gi|1350778	34434,84	5,72
38	hypothetical protein [Gallus gallus] small nuclear ribonucleoprotein D3 polypeptide 18kDa [Gallus gallu	1	98,89	98,89	37,79	37,79	gi|53130412	14021,35	10,33
39	PREDICTED: dedicator of cytokinesis 10 [Gallus gallus]	1	98,56	98,56	36,67	36,67	gi|118095033	252058,7	6,54
40	actin, gamma 1 propeptide [Gallus gallus]	1	98,37	98,37	36,13	36,13	gi|56119084	42150,93	5,3
41	kinesin family member C1 [Gallus gallus]	1	97,70	97,70	34,63	34,63	gi|126165270	72073,42	9,23
42	ribosomal protein L14 [Gallus gallus]	1	96,87	96,87	33,30	33,30	gi|12381873	15639,43	10,55
44	PREDICTED: similar to 40S ribosomal protein S2 [Gallus gallus]	1	96,22	96,22	32,48	32,48	gi|118097914	32528,2	10,21
45	**retinoblastoma binding protein 4 [Gallus gallus]**	1	96,13	96,13	32,37	32,37	gi|45382339	47862,16	4,74
46	PREDICTED: hypothetical protein [Gallus gallus]	1	95,94	95,94	32,16	32,16	gi|118096811	123653,4	9,05
43	**PREDICTED: similar to Rpl10a-prov protein [Gallus gallus]**	1	95,82	96,81	32,03	33,21	gi|50760435	24863,65	9,88
47	PREDICTED: hypothetical protein [Gallus gallus] ribosomal protein L27a	1	95,42	95,42	31,64	31,64	gi|118091246	16912,16	10,86

2.1.3. TAPalone control TAP8(12): Tf7/1-16

Results with NCBI Gallus database: 22 significant proteins

Rank	Protein Name	Peptide Count	Total Ion Score C.I. %	Best Ion Score C.I. %	Total Ion Score	Best Ion Score	Accession Number	Protein MW	Protein PI
1	PREDICTED: similar to dedicator of cytokinesis 7 [Gallus gallus]	6	100,00	100,00	307,94	84,98	gi|118094735	240282	6,36
2	heat shock cognate 70 [Gallus gallus]	6	100,00	100,00	284,20	84,27	gi|2996407	71011,37	5,47
3	PREDICTED: similar to glutamine rich protein [Gallus gallus]	6	100,00	99,96	227,55	51,76	gi|118094814	147864,4	5,64
4	heat shock protein Hsp70 [Gallus gallus]	4	100,00	100,00	194,19	64,06	gi|37590083	70097,88	5,66
5	nuclear protein matrin 3 [Gallus gallus]	3	100,00	100,00	140,90	65,81	gi|17221616	101164,1	5,79
6	PREDICTED: similar to thyroid hormone receptor activator molecule [Gallus gallus]	5	100,00	97,32	122,78	33,86	gi|118100627	153644,7	7,83
7	protein p120 - chicken (fragments)	2	100,00	100,00	122,74	89,17	gi|631021	15920,97	3,88
8	hypothetical protein [Gallus gallus] Elongation factor 1-alpha 1 (EF-1-alpha-1) (Elongation factor Tu) (E	3	100,00	99,74	112,51	44,06	gi|53130784	50449,27	9,1
9	PREDICTED: similar to triple functional domain (PTPRF interacting) [Gallus gallus]	3	100,00	99,94	109,56	50,22	gi|118086576	350191,1	6,07
10	hypothetical protein [Gallus gallus] Enah/Vasp-like [Gallus gallus]	2	100,00	100,00	82,33	61,62	gi|53136370	44817,27	9,05
11	unnamed protein product [Gallus gallus] tubulin	2	100,00	99,55	81,13	41,58	gi|63070	46384,82	4,96
13	unnamed protein product [Gallus gallus] tubulin	3	100,00	96,06	76,26	32,19	gi|63167	50095,14	4,78
14	PREDICTED: similar to calcineurin A alpha [Gallus gallus]	2	100,00	98,44	66,98	36,21	gi|118090406	50625,3	5,6
15	hypothetical protein [Gallus gallus] Calcium/calmodulin-dependent protein kinase type II delta chain (Ca	2	100,00	98,37	65,29	36,02	gi|53130868	54738,69	6,66
16	PREDICTED: similar to actin binding protein anillin [Gallus gallus]	1	100,00	100,00	61,89	61,89	gi|118086193	124953	8,69
17	PREDICTED: leucine-rich PPR-motif containing [Gallus gallus]	2	99,99	99,10	60,18	38,61	gi|118087977	157067,9	6,6
18	PREDICTED: similar to mKIAA0870 protein [Gallus gallus]	2	99,99	93,06	59,34	29,73	gi|118087416	147388,2	7,37
20	PREDICTED: similar to Leucine-rich repeats and calponin homology (CH) domain containing 3 [Gallus	2	99,95	96,24	51,38	32,39	gi|118095156	88073,43	6,41
21	PREDICTED: similar to DNA strand-exchange protein SEP1 isoform 2 [Gallus gallus]	1	99,89	99,89	47,61	47,61	gi|118095037	194669,4	7,36
23	downstream of kinase 3 [Gallus gallus]	2	99,27	34,05	39,51	19,95	gi|124110115	47821,65	6,61
24	PREDICTED: similar to putative chromatin structure regulator [Gallus gallus]	1	98,09	98,09	35,33	35,33	gi|118100214	190283	4,79
10	PREDICTED: similar to progestin induced protein, partial [Gallus gallus]	1	98,60	98,60	37,13	37,13	gi|118107387	14308,29	6,51

2.2.1. Rad18-HA-CTAP fusion TAP10: Tf9/1-1

Results with NCBI Gallus database: 58 significant proteins

Rank	Protein Name	Peptide Count	Total Ion Score C.I. %	Best Ion Score C.I. %	Total Ion Score	Best Ion Score	Accession Number	Protein MW	Protein PI
1	**hypothetical protein [Gallus gallus] Rad18**	20	100,00	100,00	2220,55	246,55	gi|53135182	56241,34	8,54
2	tubulin alpha chain - chicken (fragment)	10	100,00	100,00	777,17	176,41	gi|71575	46255,78	5
3	unnamed protein product [Gallus gallus] Tubulin	11	100,00	100,00	722,08	118,26	gi|63167	50095,14	4,78
4	nuclear protein matrin 3 [Gallus gallus]	11	100,00	100,00	675,64	157,24	gi|17221616	101164,1	5,79
5	heat shock cognate 70 [Gallus gallus]	9	100,00	100,00	632,70	154,65	gi|2996407	71011,37	5,47
6	PREDICTED: leucine-rich PPR-motif containing [Gallus gallus]	15	100,00	100,00	616,43	70,24	gi|118087977	157067,9	6,6
7	c-beta-3 beta-tubulin	9	100,00	100,00	551,48	118,26	gi|212830	50285,15	4,78
8	hypothetical protein [Gallus gallus] phosphofructokinase, platelet [Gallus gallus]	9	100,00	100,00	537,27	110,62	gi|53136740	61728,38	6,25
9	Tubulin alpha-5 chain	5	100,00	100,00	371,25	106,79	gi|135423	50714,69	4,95
10	PREDICTED: similar to dedicator of cytokinesis 7 [Gallus gallus]	6	100,00	100,00	327,53	112,44	gi|118094735	240282	6,36
11	hypothetical protein [Gallus gallus] Proteasome activator complex subunit 3 (Proteasome activator 28-ga	6	100,00	100,00	299,66	106,55	gi|60098917	29519,63	5,85
12	heat shock protein Hsp70 [Gallus gallus]	5	100,00	100,00	288,32	124,21	gi|37590083	70097,88	5,66
13	PREDICTED: similar to Heterogeneous nuclear ribonucleoprotein U (scaffold attachment factor A) [Gal	4	100,00	100,00	285,12	115,65	gi|118088143	78452,08	9,56
14	PREDICTED: similar to MGC97820 protein [Gallus gallus] Tubulin	5	100,00	100,00	276,73	94,20	gi|50756041	51955,39	4,96
15	PREDICTED: similar to glutamine rich protein [Gallus gallus]	4	100,00	100,00	222,35	93,01	gi|118094814	147864,4	5,64
16	hypothetical protein [Gallus gallus] Enah/Vasp-like [Gallus gallus]	5	100,00	100,00	212,87	64,64	gi|53136370	44817,27	9,05
17	Tubulin alpha-2 chain (Testis-specific)	3	100,00	100,00	183,53	94,20	gi|135408	50450,43	4,86
18	hypothetical protein [Gallus gallus] Calcium/calmodulin-dependent protein kinase type II delta chain (Ca	4	100,00	100,00	170,24	63,81	gi|53130868	54738,69	6,66
19	hypothetical protein [Gallus gallus] Stress-70 protein, mitochondrial precursor (75 kDa glucose-regulatec	3	100,00	100,00	157,07	76,88	gi|53127632	73431,92	6,09
20	hypothetical protein [Gallus gallus] Elongation factor 1-alpha 1 (EF-1-alpha-1) (Elongation factor Tu) (E	4	100,00	99,96	139,28	52,27	gi|53130784	50449,27	9,1
21	hypothetical protein [Gallus gallus] heterogeneous nuclear ribonucleoprotein M [Gallus gallus]	4	100,00	99,99	119,05	58,93	gi|53130368	76257,4	8,88
22	downstream of kinase 3 [Gallus gallus]	3	100,00	99,99	115,45	59,46	gi|124110115	47821,65	6,61
23	cThy28 [Gallus gallus]	2	100,00	100,00	108,15	81,61	gi|20302922	28136,15	8,32
24	ATP/ADP antiporter [Gallus gallus]	2	100,00	99,99	102,44	57,77	gi|22775582	33054,25	9,78
25	hypothetical protein [Gallus gallus] splicing factor, arginine/serine-rich 7 [Gallus gallus]	3	100,00	99,98	101,48	55,31	gi|53127360	26213,43	11,79
26	hypothetical protein [Gallus gallus] heterogeneous nuclear ribonucleoprotein H1 (H) [Gallus gallus]	2	100,00	99,93	97,31	50,18	gi|60098931	54691,77	5,49
27	actin, gamma 1 propeptide [Gallus gallus]	3	100,00	99,61	94,03	42,47	gi|56119084	42150,93	5,3
28	PREDICTED: dedicator of cytokinesis 10 [Gallus gallus]	4	100,00	80,06	90,06	25,42	gi|118095033	252058,7	6,54
29	**Rho GTPase activating protein 25 hypothetical protein [Gallus gallus]**	1	100,00	100,00	86,51	86,51	gi|53133822	73601,97	6,54
30	**ribosomal protein S3A [Gallus gallus]**	3	100,00	99,23	86,46	39,58	gi|129270064	30075,79	9,74
31	unnamed protein product [Gallus gallus] Nucleophosmin (NPM) (Nucleolar phosphoprotein B23) (Numa	2	100,00	99,73	82,56	44,09	gi|63705	32840,1	4,66
32	PREDICTED: similar to RNA-binding protein splice [Gallus gallus]	2	100,00	99,58	79,03	42,22	gi|118103255	73606,93	6,11
33	PREDICTED: similar to CTP synthase [Gallus gallus]	2	100,00	99,70	70,28	43,71	gi|118101517	52126,26	5,55
34	PREDICTED: similar to dedicator of cytokinesis 8 [Gallus gallus]	2	100,00	99,96	69,68	52,66	gi|118103958	233501,2	6,27
36	DEAD-box RNA helicase [Gallus gallus]	3	100,00	65,43	62,80	23,03	gi|5114446	67150,74	8,93
37	hypothetical protein [Gallus gallus] Bifunctional methylenetetrahydrofolate dehydrogenase/cyclohydrola	1	99,99	99,99	61,23	61,23	gi|53131685	36559,66	9,51
38	unnamed protein product [Gallus gallus] Nucleolin (Protein C23)	2	99,99	99,16	58,41	39,15	gi|63711	75651,41	4,9
39	PREDICTED: similar to 40S ribosomal protein S2 [Gallus gallus]	1	99,99	99,99	58,26	58,26	gi|118097914	32528,2	10,21
40	PREDICTED: similar to KIAA0310 protein [Gallus gallus]	2	99,98	98,62	56,30	37,03	gi|118099405	264805,7	5,65
41	nuclear calmodulin-binding protein [Gallus gallus]	2	99,98	94,14	55,09	30,74	gi|3822553	84697,49	4,68

42	kinesin family member 20A [Gallus gallus]	2	99,98	90,48	54,46	28,63	gi|61098268	100160,9	6,15
43	PREDICTED: similar to splicing factor 3b, subunit 1 [Gallus gallus]	1	99,97	99,97	54,04	54,04	gi|118093397	155552,3	8,4
44	PREDICTED: similar to thyroid hormone receptor activator molecule [Gallus gallus]	1	99,97	99,97	53,68	53,68	gi|118100627	153644,7	7,83
46	PREDICTED: similar to Rnps1 protein [Gallus gallus]	1	99,91	99,91	49,00	49,00	gi|118098270	34514,92	11,9
47	PREDICTED: hypothetical protein [Gallus gallus]	1	99,76	99,76	44,57	44,57	gi|118096811	123653,4	9,05
48	ubiquitin and ribosomal protein L40 [Gallus gallus]	1	99,74	99,74	44,34	44,34	gi|47604954	15015,08	9,87
49	PREDICTED: similar to activating signal cointegrator 1 complex subunit 3-like 1, partial [Gallus gallus]	1	99,68	99,68	43,31	43,31	gi|118126471	93213,52	5,31
50	hypothetical protein [Gallus gallus] progesterone receptor membrane component 2 [Gallus gallus]	1	99,64	99,64	42,80	42,80	gi|53128122	21684,85	5,26
51	hypothetical protein [Gallus gallus] small nuclear ribonucleoprotein D3 polypeptide 18kDa [Gallus gallu	1	99,48	99,48	41,24	41,24	gi|53130412	14021,35	10,33
52	PREDICTED: similar to nuclear receptor co-repressor 1 [Gallus gallus]	1	99,03	99,03	38,54	38,54	gi|118100324	271868,3	7,19
53	**Jun-binding protein**	1	99,02	99,25	38,50	39,68	gi|387587	24427,68	10,14
54	PREDICTED: similar to putative chromatin structure regulator [Gallus gallus]	1	99,00	99,00	38,42	38,42	gi|118100214	190283	4,79
55	PREDICTED: similar to Leucine-rich repeats and calponin homology (CH) domain containing 3 [Gallus	1	98,38	98,38	36,33	36,33	gi|118095156	88073,43	6,41
56	PREDICTED: hypothetical protein [Gallus gallus]	1	98,07	98,07	35,55	35,55	gi|118090816	95381,44	5,56
57	Ferrochelatase, mitochondrial precursor (Protoheme ferro-lyase) (Heme synthetase)	1	97,25	97,25	34,03	34,03	gi|3913810	45970,6	9,1
58	pumilio 1 [Gallus gallus]	1	96,13	96,13	32,54	32,54	gi|61098182	116881	6,25
59	PREDICTED: hypothetical protein [Gallus gallus]	1	94,72	94,72	31,19	31,19	gi|118099168	59037,65	7,28
60	BASH [Gallus gallus] B cell linker protein BLNK [Gallus gallus]	1	94,71	94,71	31,18	31,18	gi|4063823	62070,13	7,27

2.2.2. NTAP-HA-Rad18 fusion TAP10: Tf9/3-3
Results with NCBI Gallus database: 31 significant proteins

Rank	Protein Name	Peptide Count	Total Ion Score C.I. %	Best Ion Score C.I. %	Total Ion Score	Best Ion Score	Accession Number	Protein MW	Protein PI
1	**hypothetical protein [Gallus gallus] Rad18**	13	100,00	100,00	1073,81	153,03	gi|53135182	56241,34	8,54
2	unnamed protein product [Gallus gallus] tubulin	8	100,00	100,00	282,32	61,32	gi|63167	50095,14	4,78
3	tubulin alpha	4	100,00	100,00	281,06	87,44	gi|223280	46258,81	5
4	heat shock cognate 70 [Gallus gallus]	7	100,00	100,00	275,34	73,01	gi|2996407	71011,37	5,47
5	nuclear protein matrin 3 [Gallus gallus]	7	100,00	99,98	249,96	54,09	gi|17221616	101164,1	5,79
6	c-beta-3 beta-tubulin	8	100,00	99,50	249,59	40,17	gi|212830	50285,15	4,78
7	PREDICTED: leucine-rich PPR-motif containing [Gallus gallus]	8	100,00	99,40	240,18	39,39	gi|118087977	157067,9	6,6
8	PREDICTED: similar to Heterogeneous nuclear ribonucleoprotein U (scaffold attachment factor A) [Gal	5	100,00	100,00	184,07	68,22	gi|118088143	78452,08	9,56
9	heat shock protein Hsp70 [Gallus gallus]	4	100,00	100,00	158,38	69,89	gi|37590083	70097,88	5,66
11	PREDICTED: similar to glutamine rich protein [Gallus gallus]	5	100,00	99,60	142,04	41,14	gi|118094814	147864,4	5,64
12	Tubulin alpha-5 chain	3	100,00	100,00	135,66	78,53	gi|135423	50714,69	4,95
13	hypothetical protein [Gallus gallus] Phosphofructokinase platelet	5	100,00	88,88	120,68	26,71	gi|53136740	61728,38	6,25
14	hypothetical protein [Gallus gallus] Elongation factor 1-alpha	3	100,00	99,94	112,49	49,63	gi|53130784	50449,27	9,1
15	hypothetical protein [Gallus gallus] Stress 10 protein, mitochondrial precursor	3	100,00	99,87	98,76	46,14	gi|53127632	73431,92	6,09
16	pumilio 1 [Gallus gallus]	3	100,00	99,32	81,62	38,87	gi|82569972	127282,1	6,34
17	PREDICTED: similar to dedicator of cytokinesis 7 [Gallus gallus]	3	100,00	87,61	66,48	26,24	gi|118094735	240282	6,36
18	PREDICTED: similar to nuclear receptor co-repressor 1 [Gallus gallus]	2	99,99	99,08	58,83	37,53	gi|118100324	271868,3	7,19
19	DEAD-box RNA helicase [Gallus gallus]	2	99,99	98,87	58,14	36,64	gi|5114446	67150,74	8,93
20	PREDICTED: similar to CTP synthase [Gallus gallus]	2	99,96	97,61	51,46	33,39	gi|118101517	52126,26	5,55
21	PREDICTED: similar to DNA strand-exchange protein SEP1 isoform 2 [Gallus gallus]	1	99,96	99,96	51,43	51,43	gi|118095037	194669,4	7,36
22	**ribosomal protein S3A [Gallus gallus]**	2	99,93	95,23	48,57	30,38	gi|129270064	30075,79	9,74
23	PREDICTED: similar to beta prime cop [Gallus gallus]	1	99,86	99,86	45,63	45,63	gi|118094989	103935,2	5,11
25	hypothetical protein [Gallus gallus] coatmer protein complex subunit alpha	2	99,80	91,80	44,11	28,03	gi|60099199	140060,4	7,53
26	PREDICTED: hypothetical protein [Gallus gallus]	2	99,44	47,28	39,71	19,95	gi|118085583	134059,7	6,11
27	PREDICTED: similar to 40S ribosomal protein S2 [Gallus gallus]	1	99,23	99,23	38,28	38,28	gi|118097914	32528,2	10,21
28	**erythrocyte histone deacetylase [Gallus gallus]**	1	99,09	99,09	37,56	37,56	gi|2829214	55416,94	5,32
29	SUS2 (ABNORMAL SUSPENSOR 2) [Arabidopsis thaliana]	1	98,66	98,66	35,91	35,91	gi|15220049	279262,2	8,93
30	PREDICTED: similar to melanoma ubiquitous mutated protein [Gallus gallus]	1	98,65	98,65	35,87	35,87	gi|118103238	53658,19	5,45
31	PREDICTED: hypothetical protein [Gallus gallus] RNA binding motif protein 33	1	98,63	98,63	35,79	35,79	gi|118096811	123653,4	9,05
32	**Jun-binding protein**	1	97,89	97,89	33,93	33,93	gi|387587	24427,68	10,14
33	unnamed protein product [Gallus gallus] similar to dbpB/YB-1 of mouse	1	97,38	97,38	32,99	32,99	gi|516701	36296,97	9,85

2.2.3. TAPalone control TAP10: Tf7/1-16
Results with NCBI Gallus database: 29 significant proteins

Rank	Protein Name	Peptide Count	Total Ion Score C.I. %	Best Ion Score C.I. %	Total Ion Score	Best Ion Score	Accession Number	Protein MW	Protein PI
1	tubulin alpha	7	100,00	100,00	480,62	116,01	gi|223280	46258,81	5
3	PREDICTED: leucine-rich PPR-motif containing [Gallus gallus]	11	100,00	100,00	404,49	78,97	gi|118087977	157067,9	6,6
4	nuclear protein matrin 3 [Gallus gallus]	8	100,00	100,00	333,23	68,66	gi|17221616	101164,1	5,79
5	c-beta-3 beta-tubulin	7	100,00	100,00	303,40	102,37	gi|212830	50285,15	4,78
6	heat shock cognate 70 [Gallus gallus]	4	100,00	100,00	236,96	108,13	gi|2996407	71011,37	5,47
8	PREDICTED: similar to glutamine rich protein [Gallus gallus]	4	100,00	100,00	170,76	75,54	gi|118094814	147864,4	5,64
10	heat shock protein Hsp70 [Gallus gallus]	3	100,00	100,00	138,18	73,00	gi|37590083	70097,88	5,66
12	PREDICTED: similar to dedicator of cytokinesis 7 [Gallus gallus]	4	100,00	98,26	110,75	35,82	gi|118094735	240282	6,36
13	hypothetical protein [Gallus gallus] TPX2, microtubule-associated protein homolog [Gallus gallus]	3	100,00	99,88	101,41	47,41	gi|53136376	86081,12	9,56
14	hypothetical protein [Gallus gallus] heterogeneous nuclear ribonucleoprotein H1 (H) [Gallus gallus]	1	100,00	100,00	99,42	99,42	gi|60098931	54691,77	5,49
16	hypothetical protein [Gallus gallus] Elongation factor 1-alpha 1 (EF-1-alpha-1) (Elongation factor Tu) (E	2	100,00	100,00	93,13	70,98	gi|53130784	50449,27	9,1
17	PREDICTED: similar to NADH dehydrogenase (ubiquinone) 1 alpha subcomplex, assembly factor 1 [Ga	1	100,00	100,00	81,72	81,72	gi|50748169	35437,67	8,59
18	PREDICTED: similar to triple functional domain (PTPRF interacting) [Gallus gallus]	2	100,00	99,98	78,76	56,15	gi|118086576	350191,1	6,07
19	PREDICTED: similar to Heterogeneous nuclear ribonucleoprotein U (scaffold attachment factor A) [Gal	2	100,00	99,99	78,30	57,30	gi|118088143	78452,08	9,56
21	unnamed protein product [Gallus gallus] Nucleophosmin (NPM) (Nucleolar phosphoprotein B23) (Numa	2	100,00	99,85	76,35	46,45	gi|63705	32840,1	4,66
22	hypothetical protein [Gallus gallus] Calcium/calmodulin-dependent protein kinase type II delta chain (Ca	2	100,00	99,93	70,49	49,72	gi|53130868	54738,69	6,66
23	PREDICTED: dedicator of cytokinesis 10 [Gallus gallus]	2	100,00	99,93	70,40	49,74	gi|118095033	252058,7	6,54
24	downstream of kinase 3 [Gallus gallus]	2	100,00	98,40	69,55	36,18	gi|124110115	47821,65	6,61
25	hypothetical protein [Gallus gallus] Stress-70 protein, mitochondrial precursor (75 kDa glucose-regulatec	1	99,96	99,96	52,48	52,48	gi|53127632	73431,92	6,09
26	PREDICTED: hypothetical protein [Gallus gallus]	1	99,96	99,96	51,98	51,98	gi|118096811	123653,4	9,05
28	hypothetical protein [Gallus gallus] Enah/Vasp-like [Gallus gallus]	1	99,85	99,85	46,40	46,40	gi|53136370	44817,27	9,05
29	hypothetical protein [Gallus gallus] small nuclear ribonucleoprotein D3 polypeptide 18kDa [Gallus gallu	1	99,67	99,67	43,01	43,01	gi|53130412	14021,35	10,33
30	hypothetical protein [Gallus gallus] Bifunctional methylenetetrahydrofolate dehydrogenase/cyclohydrola	1	99,25	99,25	39,45	39,45	gi|53131685	36559,66	9,51
31	PREDICTED: similar to 40S ribosomal protein S2 [Gallus gallus]	1	98,16	98,16	35,57	35,57	gi|118097914	32528,2	10,21
32	PREDICTED: similar to thyroid hormone receptor activator molecule [Gallus gallus]	1	97,53	97,53	34,29	34,29	gi|118100627	153644,7	7,83
33	hypothetical protein [Gallus gallus] heterogeneous nuclear ribonucleoprotein M [Gallus gallus]	1	97,34	97,34	33,97	33,97	gi|53130368	76257,4	8,88
34	Pax-5 [Gallus gallus]	1	96,16	96,16	32,38	32,38	gi|4630779	42174,26	9,08
35	PREDICTED: similar to activating signal cointegrator 1 complex subunit 3-like 1, partial [Gallus gallus]	1	95,64	95,64	31,82	31,82	gi|118126471	93213,52	5,31
36	PREDICTED: hypothetical protein [Gallus gallus]	1	95,09	95,09	31,31	31,31	gi|118085635	65379,64	9,18

Abbreviations

A	adenine
AID	Activation induced cytidine deaminase
ampR	ampicillin resistance
AP	apurinic/apyrimidinic
APOBEC	Apolipoprotein B mRNA editing enzyme, catalytic polypetide
APS	Ammonium peroxodisulfate
BCR	B cell receptor
BER	base excision repair
Bp	base pair
C	cytosine
CB-B	calmodulin binding beads
CBP	calmodulin binding peptide
cDNA	complementary deoxyribonucleic acid
C-Region	constant region
CSB	Cockayne syndrome protein B
CSR	class switch recombination
dA	deoxyadenine
dC	deoxycytidine
DDR	DNA damage response
dG	deoxyguanidine
dT	deoxythimidine
dU	deoxyuridine
DMSO	Dimethyl sulfoxide
DNA	Deoxyribonucleic acid
DNA-PKcs	DNA dependent protein kinase catalytic subunit
dNTP	Deoxyribonucleotide triphosphate
DSB	double strand break
DSBR	double strand break repair
dsDNA	double stranded DNA
D-Segment	diversity segment of the V-Genes
DTT	Dithiothreitol
ECL	enhanced chemiluminescence
EBV	Epstein-barr virus
EBNA	EBV-encoded nuclear antigen
EDTA	Ethylene diamine tetraacetate
et al.	‘et alterae’
FCS	fetal calf serum
g	gram
G	guanine
GC	germinal centre
GOI	gene of interest
$GOI^{-/-}$	gene of interest knockout
GST	Glutathion-S-transferase
H	hour
HA	Heamagglutinin
hCMVieE	human cytomegalovirus intronic early enhancer
HEPES	4-(2-Hydroxyethyl)-1-piperazinethane sulfonic acid
HPRT	Hypoxanthine-phosphoribosyl-transferase
HR	homologous recombination
Ig	immunglobulin

IP	immunoprecipitation
IRES	Internal ribosomal entry site
J-Segment	joining segment of the V-Genes
K	Lysine
Kb	kilobase
kDa	kilo Dalton
l	Litre
LC	liquid chromatography
LTR	long terminal repeats
M	molar (Mol/Litre)
MALDI	Matrix Assisted Laser Desorption/Ionisation
mg	milligram
MgCl2	Magnesium chloride
min	minute
ml	milliliter
mM	millimolar
MMR	mismatch repair
MOPS	3-(N-Morpholino) propane-sulphonate
mRNA	messenger ribonucleic acid
MS	mass spectrometry
mV	millivolt
µg	microgram
µl	microlitre
µM	micromolar
nano-LC	nano-Liquid Chromatography
NES	nuclear export signal
V-gene	gene of the variable region
Ng	nanogram
NHEJ	non-homologous end-joining
nm	nanometer
NLS	nuclear loacalisation signal
PAGE	polyacrylamide gel electrophoresis
PBS	phosphate buffered saline
PCR	polymerase chain reaction
PCNA	Proliferating cell nuclear antigen
$PCNA^{Ubi}$	Monoubiquitinated PCNA
$PCNA^{(Ubi)n}$	Polyubiquitinated PCNA
pH	negative logarithm of the hydrogen ion concentration
POI	protein of interest
Pol	polymerase
PVDF	Polyvinylidene difluoride
Py ori	polyoma origin of replication
ψV	pseudo-V gene
qRT-PCR	quantitative real time polymerase chain reaction
R	Arginine
RNA	Ribonucleic acid
RNase	Ribonuclease
RPA	Replication protein A
rpm	rotations per minute
RT	room temperature
RT-PCR	reverse transcription – polymerase chain reaction
Sec	seconds

SDS	Sodium dodecyl sulphate
SHM	somatic hypermutation
S-Region	switch region
SSB	single strand break
SV40	Simian virus 40
T	thymine
TAP	tandem affinitiy purification
TAPalone	the cell clone expressing the TAP tag alone
TEMED	N,N,N',N'- Tetramethylendiamine
TEV	Tobacco etch virus
TEV E	eluate obtained after TEV protease cleavage
TLS	translesion synthesis
TOF	time of flight
Tris	Tris hydroxyl methyl aminomethane
U	Unit (of enzyme activity)
U	uracil
UNG	Uracil N-glycosylase
UV	ultraviolet radiation
V	volt
VH Gene	gene of the variable region heavy chain
V Region	variable Region
Vs	versus
wt	wildtype
w/v	weight per volume

Index of Figures

FIGURE#	*FIGURE TITLE*	*Page #*
Figure 1	*Coordination of the cell cycle checkpoints with DNA damage processing*	*3*
Figure 2	*Adaptive genetic alterations in the Ig heavy chain locus*	*7*
Figure 3	*Model for repair of AID-induced lesions by Somatic Hypermutation, Class Switch recombination and Gene conversion (Rada et.al. 2004)*	*10*
Figure 4	*Targeting of Somatic Hypermutation by locus-specific differential processing of AID-induced lesions*	*11*
Figure 5	*The Rad6 Pathway in yeast*	*13*
Figure 6	*Schematic representation of the functional domains and ligand-interacting regions of human Rad18 Source: Notenboom et al. 2007.*	*18*
Figure 7A	*A schematic representation of the TAP Tag*	*20*
Figure 7B	*An overview of Tandem Affinity Purification (TAP)*	*20*
Figure 8	*An overview of the approach to study protein interaction networks in DT40 cells*	*24*
Figure 9	*A Schematic depiction of the exogenous expression vectors tested*	*25*
Figure 10	*Expression levels of AID-TAP fusions in DT40 cells*	*27*
Figure 11	*Analysis of tandem affinity purification of AID-TAP fusions*	*29*
Figure 12	*The chromatogram of the nano-LC separation of AID-TAP fusion peptides*	*31*
Figure 13	*Expression levels of Rad18-HA-TAP fusions*	*35*
Figure 14A	*Native PAGE of Rad18 fusions and TAPalone*	*37*
Figure 14B	*Nuclear/cytoplasmic localisation of Rad18-HA-TAP fusions and TAPalone control*	*37*
Figure 15	*Survival curves of the methylcellulose colony survival assay with increasing doses of cisplatin (in μM)*	*38*
Figure 16	*Western blot analysis of tandem affinity purification of Rad18-HA-TAP fusions*	*39*
Figure 17	*Silver stain analysis of TAP method of Rad18-HA-TAP fusions*	*40*
Figure 18	*The chromatogram of the nano-LC separation of peptides of Rad18-HA-TAP fusions and TAP-alone.*	*41*
Figure 19	*Co-immunoprecipitation experiments for interesting potential Rad18 interaction partners*	*45*
Figure 20	*MMS induced activation of the JNK pathway upon stalled replication in Rad18 proficient and deficient DT40 cells*	*47*
Figure 21A	*The activation of JNK pathway upon DNA damage in the ψ⁻ parental and ψ⁻ PCNA K164R mutant DT40 cells*	*49*
Figure 21B	*DNA damage induced activation of PI3K/Akt pathway in ψ⁻ wild type vs. ψ⁻ Rad18-/- and the ψ⁻ parental and ψ⁻ PCNA K164R mutant DT40 cells*	*49*

Index of Tables

TABLE#	*TABLE TITLE*	*Page #*
Table 1	*An overview of exogenous and endogenous expression levels determined by qRT-PCR*	*26*
Table 2	*A compilation of some of the potential interactions identified for AID-TAP fusions when using the NCBI Gallus database for MASCOT search analysis*	*34*
Table 3	*An example of the primary list of the potential interactions identified for Rad18-TAP fusions*	*42*
Table 4	*An overview of the known and interesting potential interaction partners identified for the Rad18-HA-TAP fusions*	*43*
Table 5	*List of Enzymes used*	*65*
Table 6	*List of primary antibodies*	*66*
Table 7	*List of secondary antibodies*	*66*
Table 8	*Primers for qRT-PCR*	*67*
Table 9	*Oligonucleotides used for cloning the Rad18-HA-TAP fusions*	*67*
Table 10	*Oligonucleotides used for cloning the Rad18-HA construct*	*68*
Table 11	*Source and particulars of the cell lines used*	*68*
Table 12	*Chicken Media for the DT40 culture*	*78*

Acknowledgements

I would like to offer my sincere thanks to all the people who have been instrumental in helping me complete this endeavor. This work would have been impossible without the active support of all these people mentioned here (in no particular order).

I thank my advisor, Berit Jungnickel for giving me the opportunity to pursue my doctoral studies in her able guidance and supervision. I thank her for the support she provided throughout the period of my study and especially for helping me see my mistakes and learn from them.

I would like to thank Stephanie Tobollik for teaching me the major technical approach of this study, besides all the other help in the lab. I am grateful for her patience with my annoying questions and for being a good teacher.

I thank André Kutzera and Sandra Windberg for the valuable technical support they have provided for this work. I also owe them a big thank you for helping me improve my spoken German language skills.

I am very thankful to Maren Mierau for the help at the time I landed in Germany and it was such a gesture of warm welcome that I will ever remember. I also thank her for the troubleshooting we have done together in the lab and for the encouraging words when sometimes it did not get us anywhere ☺

Many thanks to Hanna Scheller and Isin Ertongur, for the enlightening discussions we had on both professional and social aspects. I thank them both for helping me understand and adjust to the nuances of living in Germany, besides teaching me to bake delicious cakes and cookies. I am thankful for the friendship that has developed among us over this period of time bridging the cultural and language differences.

I would like to thank Ines Pfeil for the insightful discussions that I was privileged to have with her and for the hand on my shoulder when I was feeling low. (I must mention that I am also thankful to Ines for the recipe of my most favorite apple-walnut cake that I still bake over and over again).

I would like to thank Samantha Pill for her co-operation to perform the last experiments we did together. I also thank Kerstin, Jutta, Lourdes, Julia, David and Nils. It was wonderful to work with them.

I thank Hakan Sarioglu, Andrea Hartmann, Janine Griese and Ludwig Wiesent for their immense support on working with the LC/MALDI devices and MASCOT software.

I thank my official PhD supervisor Prof. Dr. Friederike Eckardt-Schupp for her support and suggestions. I would like to thank Prof. Dr. Georg Bornkamm, Prof. Dr. Dirk Eick, Dr Ulla-Zimber Strobl and Dr. Bettina Kempkes for their valuable suggestions and constructive criticisms on the work.

Special thanks to Frau Schrezenmeir and Frau Manglkammer who helped me get through with all administrative procedures.

I extend my thanks to all the members of the KMOLBI for the wonderful and friendly working atmosphere. I am grateful to all the friends in Munich and in other parts of Germany for making life enjoyable and adventurous during my entire stay. A special thanks to Cristina Rico Garcia for being such a wonderful friend and the time we spent together while staying with her during the final months of my tenure.

I would like to acknowledge Rajesh, my "soul" reason to come to Germany, for the discussions, suggestions and troubleshooting he offered throughout the period of this study and for the life, dreams, friendship and love that we share. I am grateful to him for being there for me and helping me bounce back on track whenever I felt down and assuring me always "things will fall into place" during difficult times.

I offer my gratitude to my parents for their huge support and motivation. I thank my father for the constant support and guidance he offered and for his gentle reminder that he believes that I could succeed in whatever I undertake. I am grateful to my mom, my best friend and mentor for teaching me everything I need, to face all challenges in life. I thank her for being here in Germany in the grueling final months of my PhD providing me immense moral support and help with mundane day to day tasks. I thank my brother and sister for their enormous support and for giving me the encouragement to never give up. Finally I am grateful to God, whose Grace, has lead me to where I stand today.

Ehrenwörtliche Erklärung

Ich versichere hiermit ehrenwörtlich, dass die Dissertation von mir selbstständig, ohne unerlaubte Beihilfe angefertigt worden ist. Diese Arbeit hat in gleicher oder ähnlicher Form noch keiner anderen Prüfungsbehörde vorgelegen.

München, den 15. Januar 2009

Sushmita Gowri Sreekumar

Declaration

I hereby declare that this thesis is the result of independent work done by me without any unauthorised source of assistance. This work, in the same or a similar form, has not been submitted to any other board of examination.

Munich, 15th January, 2009

Sushmita Gowri Sreekumar

Curriculum vitae

Personal Profile:

Name	Sushmita Gowri Sreekumar
Date of Birth	4th of February, 1978
Place of Birth:	Chennai, India
Citizenship:	Indian

****

Academic Profile:

Schooling (1984-1994)

Rosary Matriculation Higher Secondary School, Chennai, India

Matriculation Examination (1994)

Board of Matriculation Examination, Tamil Nadu, India

Higher Secondary School Leaving Certificate in science (1994-1996)

Tamil Nadu State Board of Examinations, India

Bachelor of Science (1996-1999)

Guru Nanak College, University of Madras, India

Master of Science (2000-2002)

Department of Life Sciences, University of Madras, India

Junior Research Fellow (2003-2004)

National Center for Biological Sciences, Bangalore, India

Doctoral studies (2005 – 2009)

Faculty of Biology, Ludwig-Maximilians University,

Helmhotz Zentrum, Munich, Germany